Universiteit Gent
Faculteit van de Toegepaste Wetenschappen
Vakgroep ELIS

Introductie van kleur in reflectieve PDLC en PNLC microdisplays

Introduction of color in reflective PDLC and PNLC microdisplays

Filip Bruyneel

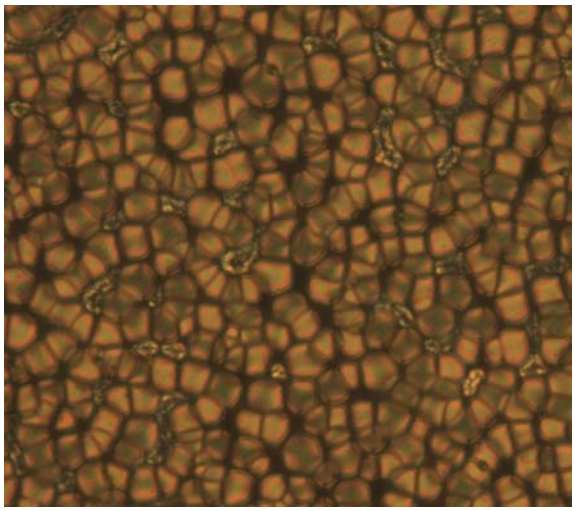

Proefschrift tot het verkrijgen van de graad van
doctor in de toegepaste wetenschappen
richting elektrotechniek
Academiejaar 2001-2002

promotor:

Prof. Herbert De Smet
TFCG-IMEC
vakgroep ELIS
Sint-Pietersnieuwstraat 41
9000 Gent

voor dit doctoraatsonderzoek werd een beurs verleend door het IWT-Vlaanderen (Instituut voor de aanmoediging van Innovatie door Wetenschap en Technologie in Vlaanderen)

illustration on the cover: pictures of PDLC using crossed polarizers showing the LC droplets. This PDLC was cured at very low UV intensities (ambient light). The droplets' diameter is about 15μm.

Dankwoord

Deze doctoraatsscriptie is een bundeling van de resultaten van een goede 3 jaar in de TFCG\IMEC groep aan de Universiteit Gent. Dit werk is niet alleen een bekroning van de geleverde inspanningen van mezelf maar ook van een heleboel andere mensen. Sta me toe om deze hier expliciet te vermelden en mijn dank voor hun medewerking uit te drukken.

Vooreerst wens ik mijn promotor, Prof. Dr. Ir. Herbert De Smet, te bedanken voor de begeleiding, voor de vele technische discussies en voor richting te geven aan mijn onderzoek.

Daarnaast wens ik ook Prof. Dr. Ir. André Van Calster te bedanken die voor de nodige omkadering heeft gezorgd om dit doctoraatsonderzoek te laten doorgaan binnen zijn onderzoeksgroep.

Ik wens ook Dr. Ir. Jan Vanfleteren te bedanken die me tijdens het eerste jaar van mijn doctoraatsonderzoek wegwijs heeft gemaakt in de assemblage van displays en het interpreteren van de experimenten.

I would like to thank Toru Fujisawa and Masao Aizawa of Dainippon Ink & Chemicals (Japan) for supplying me the Polymer Network Liquid Crystal material and for the many interesting discussions we have had via e-mail, on conferences and during my visits to Japan.

Voor de experimenten werden veelal testdisplays gebruikt. Hoewel de assemblage van de displays door mezelf gebeurde, werden de basiscomponenten voor de assemblage van de displays veelal door andere mensen gemaakt. Hiervoor zou ik dan ook Ir. Nadine Carchon en Ir. Dieter Cuypers willen bedanken. Jullie hebben steeds voor een voldoende voorraad

testmateriaal gezorgd dat de ene keer al wat meer exotisch was dan de andere keer.

Om het principe van veldgeorienteerd adresseren aan te tonen en beter te begrijpen, dienden er een heleboel metingen te gebeuren. Ik wil Ir. Wim Hendrix bedanken die in het kader van zijn eindwerk een groot deel van deze metingen voor zijn rekening heeft genomen. Hieromtrent wens ik Geert Van Steenberge en Tom Bert te bedanken die ook enkele metingen hebben uitgevoerd.

Bij studies kan de familie voor een belangrijke stimulans zorgen. Bij mij was dat niet anders. Ik wens in het bijzonder mijn ouders en mijn grootmoeder te bedanken. Ik was steeds vrij om te studeren wat ik wilde en op de momenten dat ik ze nodig had, waren ze er voor mij. Hierbij denk ik dan aan de kans die zij mij gegeven hebben om na Industrieel Ingenieur verder te studeren voor Burgerlijk Ingenieur en de steun die ik gekregen heb tijdens de laatste maanden van mijn doctoraatsstudie. Mijn vader (die zelf ook gedoctoreerd is) wens ik ook te bedanken voor de vele gespreken die we gehad hebben over publiceren en doctoreren in het algemeen. Dit heeft ongetwijfeld zijn invloed gehad op het eindresultaat van deze doctoraatsstudie.

Tot slot wens ik ook het IWT te bedanken voor het verlenen van een doctoraatsbeurs.

Filip Bruyneel
Gent
29 maart 2002

CHRONOLOGICAL LIST OF PUBLICATIONS

journals:

1. Filip Bruyneel, Herbert De Smet, Jan Vanfleteren, André Van Calster, “Method for measuring the cell gap in liquid crystal displays”, in ***Optical Engineering***, Vol. 40, No. 2, pp. 259-267, February 2001

2. Filip Bruyneel, Herbert De Smet, Jan Vanfleteren, André Van Calster, “Cell gap optimization and alignment effects in reflective PDLC microdisplays”, in ***Liquid Crystals***, Vol. 28, No. 8, pp. 1245-1252, August 2001

3. Filip Bruyneel, Herbert De Smet, André Van Calster, Jan Egelhaaf, “Comparison of reflective PNLCDs and reflective single polarizer Heilmeier Guest Host displays”, in ***Journal of the Society of Information Displays***, Vol. 9, No. 4, pp. 313-318, December 2001

4. Filip Bruyneel, Herbert De Smet, André Van Calster, ”Reduction of the Switching Time of Polymer Dispersed Liquid Crystal Using Field Oriented Addressing”, in ***IEEE Electron Device Letters***, Vol. 23, Issue 7, pp. 401-404, July 2002

international conferences:

1. Filip Bruyneel, Herbert De Smet, Jan Vanfleteren, André Van Calster, Toru Fujisawa, Masao Aizawa, "Characteristics of PNLC in reflective displays," in *Proceedings of the 20th International Display Research Conference (IDRC)*, (Palm Beach, USA), pp. 217-220, September 2000

2. Filip Bruyneel, Herbert De Smet, André Van Calster, Jan Egelhaaf, ‘Measurement and evaluation of the applicability of reflective displays for direct view applications’, in *Proceedings of The Seventh International Display Workshops (IDW)*, (Kobe, Japan), pp.45-48, November 2000

3. Filip Bruyneel, Herbert De Smet, Jan Vanfleteren, André Van Calster, "Assembly of Reflective PDLC Microdisplays," SID’01, (San Jose, USA), pp. 442-445, June 2001

4. Filip Bruyneel, Wim Hendrix, Herbert De Smet, André Van Calster, “Fast PDLC using Field Oriented Addressing”, Asia Display/IDW ’01, (Nagoya, Japan), pp. 45-48, October 2001

5. Filip Bruyneel, Dieter Cuypers, Herbert De Smet, André Van Calster, "Reflective color PDLC displays using color filters," SID’02, (Boston, USA), pp. 534-537, May 2002

national conferences:

1. Filip Bruyneel, Herbert De Smet, André Van Calster, “Introduction of color in reflective microdisplays”, RUG-FTW - 2nd PhD Symposium – December 12, 2001 – paper 9

co-author:

1. André Van Calster, Filip Bruyneel, Dieter Cuypers, Nadine Carchon, Geert Van Doorselaer, Jean Van den Steen, Herbert De Smet, ‘Miniature reflective displays’, in *Proceedings of The Seventh International Display Workshops (IDW)*, (Kobe, Japan), pp. 179-182, November 2000

2. T. Bert, G. Van Steenberge, H. De Smet, F. Bruyneel, J. Doutreloigne, E. Schroten, A.A.J. Ketelaars, G. Hadziioannou, “Passive matrix addressing of electrophoretic image display”, Eurodisplay 2002

impact of the publications on other work:

The principle for the measurement and evaluation of the applicability of reflective displays for direct view applications, as described in chapter 2 paragraph 4 “Analysis of the applicability of reflective displays for direct view applications”, has been implemented in commercial measurement set-ups and has contributed to an international standard on the measurement of reflective displays:

Michael E. Becker, “Standards and Metrology for Reflective LCDs”, SID’02, (Boston, USA), pp. 136-139, May 2002

Inhoudsopgave - Content

Lijst met veelgebruikte symbolen en afkortingen - List of symbols and abbreviations _____ xi

NEDERLANDSE SAMENVATTING

1 Situering van het doctoraat _____ NE-1

1.1 Inleiding _____ NE-1

1.2 Polymer Dispersed Liquid Crystal en Polymer Network Liquid Crystal _____ NE-2

1.3 Reflectieve vloeibaar kristal beeldschermen _____ NE-3

1.4 Microdisplays _____ NE-4

1.5 Reflectieve kleurenbeeldschermen _____ NE-5

1.6 Doelstellingen van dit doctoraat _____ NE-6

2 Meetopstellingen _____ NE-8

2.1 Inleiding _____ NE-8

2.2 Meting van de elektro-optische eigenschappen van PDLC en PNLC _____ NE-8

2.3 Meting van de cell gap in vloeibaar kristal beeldschermen __ NE-9

2.3.1 Inleiding _____ NE-9

2.3.2 Principe van meetmethode _____ NE-10

2.3.3 Omzetting van het principe in de praktijk_____ NE-11

2.4 Meetopstelling voor de analyse van reflectieve beeldschermen voor 'direct view'-toepassingen *NE-12*

2.4.1 Inleiding NE-12

2.4.2 Principe van de meetopstelling NE-13

2.4.3 Realisatie van de meetopstelling NE-13

2.5 Conclusie *NE-14*

3 Karakterisatie van PDLC en PNLC voor reflectieve beeldschermen NE-15

3.1 Inleiding *NE-15*

3.2 Karakterisatie van PDLC *NE-16*

3.2.1 Optimalisatie van het PDLC mengsel NE-16

3.2.2 Invloed van de UV-parameters NE-16

3.2.3 Invloed van de cell gap NE-18

3.2.4 Besluit bij de karakterisatie van PDLC NE-19

3.3 Karakterisatie van PNLC *NE-19*

3.4 DC-spanning in reflectieve PDLC en PNLC beeldschermen *NE-20*

3.5 Toepasbaarheid van reflectieve PDLC en PNLC beeldschermen voor 'direct view'-toepassingen *NE-20*

3.6 Conclusie bij de karakterisatie van PDLC en PNLC voor reflectieve beeldschermen *NE-21*

4 Assemblage en vullen van microdisplays NE-22

4.1 Inleiding *NE-22*

4.2 Beschrijving van de assemblage en vulmethodes *NE-23*

4.2.1 Druppelvulmethode NE-23

4.2.2 Aangepaste vacuumvulmethode NE-23

4.2.3 Capillaire vulmethode NE-24

4.3 Problemen bij het vullen en assembleren van PDLC en PNLC microdisplays NE-24

4.3.1 Vullen van vias NE-24

4.3.2 Stabiliteit van de cell gap NE-25

4.4 Conclusie NE-26

5 Veldgeorienteerde adressering voor kleurensequentiële beelschermen NE-27

5.1 Inleiding NE-27

5.2 Principe van veldgeorienteerd adresseren NE-27

5.2.1 Inleiding NE-27

5.2.2 Werkingsprincipe van veldgeorienteerd adresseren NE-28

5.2.3 Implementatie van het principe NE-29

5.3 Resultaten van de experimenten NE-30

5.4 Besluit NE-31

6 Kleurenbeeldschermen met behulp van kleurenfilters NE-32

6.1 Inleiding NE-32

6.2 Optimalisatie van de kleurenfilters NE-33

6.3 Resultaten van de experimenten NE-34

6.4 Besluit NE-35

7 Personal viewer NE-36

8 Innovatieve aspecten van dit doctoraat _____ NE-37

9 Nieuwe uitdagingen _____ NE-39

ENGLISH TEXT

CHAPTER 1: Relevance of this Ph.D. research

1 Introduction _____ 1-1

2 Liquid crystals _____ 1-2

2.1 Principle _____ 1-2

2.2 Polymer Dispersed Liquid Crystal and Polymer Network Liquid Crystal _____ 1-4

2.2.1 Introduction _____ 1-4

2.2.2 Electro-optical properties _____ 1-6

2.2.3 Display configurations _____ 1-7

2.3 Goals of this Ph.D. research _____ 1-8

3 Reflective liquid crystal displays _____ 1-9

3.1 Introduction _____ 1-9

3.2 Reflective liquid crystal displays using polarizers _____ 1-10

3.3 Polarizer-free reflective displays _____ 1-13

3.4 Goals of this Ph.D. research _____ 1-15

4 Microdisplays _____ 1-16

4.1 Introduction _____ 1-16

4.2 Challenges of LCOS _____ 1-18

4.2.1 Technological challenges _____ 1-18

4.2.2 Electro-optical challenges _____ 1-20

4.3 Goals of this Ph.D. research _____ 1-23

5 Reflective color displays _____ 1-24

5.1 Introduction _____ 1-24

5.2 Color filters 1-24
5.3 Color displays using diffraction of light 1-25
5.3.1 Principle 1-25
5.3.2 Holographic Optical Elements 1-27
5.3.3 Holographic PDLC and PNLC 1-28
5.3.4 Dielectric mirrors 1-30
5.3.5 Diffractive mirrors 1-31
5.4 Color sequential addressing 1-31
5.5 Goals of this Ph.D. research 1-32

6 Conclusion 1-33

References 1-34

CHAPTER 2: Measurement set-ups

1 Introduction 2-1

2 Measurement of the opto-electrical characteristics of PDLC and PNLC 2-2

3 Measurement of the cell gap in liquid crystal displays 2-7
3.1 Introduction 2-7
3.2 Concept of the measurement method 2-8
3.2.1 Basic theory 2-8
3.2.2 Empirical model for LCD measurements 2-12
3.2.3 Principle of measurement of the cell gap of filled LCDs 2-14
3.3 Measurements 2-14
3.3.1 Measurement set-up 2-14
3.3.2 Cell gap based on the interference spectrum 2-16
3.3.3 Method based on the Fourier Transform 2-18
3.3.4 Method based on the Inverse Fourier Transform 2-20
3.3.5 Method based on an empirical model 2-21

3.3.6 Cell gap measurement of a filled LCD 2-22
3.3.7 Error margin of the measurement set-up 2-24
3.4 Discussion 2-26
3.5 Conclusion 2-28

4 Analysis of the applicability of reflective displays for direct view applications 2-29
4.1 Introduction 2-29
4.2 Principle of the measurement set-up 2-29
4.3 Discussion 2-33
4.4 Conclusion 2-33

5 Conclusion 2-34

References 2-35

CHAPTER 3: Characterization of PDLC and PNLC for reflective displays

1 Introduction 3-1

2 Characterization of PDLC for reflective displays 3-3
2.1 Preparation of the PDLC mixture 3-3
2.2 Influence of the UV parameters 3-4
2.2.1 Spectrum of the UV light sources 3-4
2.2.2 UV intensity 3-7
2.2.3 UV cure time 3-11
2.3 Influence of the cell gap 3-17
2.3.1 Results of the experiments 3-17
2.3.2 Discussion 3-19
2.3.3 Conclusion 3-22
2.4 Conclusion 3-22

3 Characterization of PNLC for reflective displays 3-24

3.1 Influence of the cell gap 3-24
3.2 Influence of the UV cure time 3-27
3.3 Conclusion 3-29

4 DC effect in reflective PDLC and PNLC displays 3-30
4.1 Introduction 3-30
4.2 Measurement of the DC voltage 3-31
4.3 Discussion 3-31
4.4 Conclusion 3-32

5 Applicability of reflective PDLC and PNLC displays for direct view applications 3-33
5.1 Introduction 3-33
5.2 Results 3-33
5.3 Discussion 3-36
5.4 Conclusion 3-39

6 Conclusion on the characterization of PDLC and PNLC for reflective displays 3-40

References 3-41

CHAPTER 4: Assembly and filling of PDLC and PNLC microdisplays

1 Introduction 4-1

2 Description of the assembly and filling methods 4-2
2.1 Droplet filling method 4-2
2.2 Vacuum filling method 4-3
2.3 Capillary filling method 4-5

3 Typical problems during the filling and the assembly of PDLC and PNLC microdisplays 4-6

3.1 Filling of vias 4-6
3.2 Cell gap stability 4-8

4 Conclusion 4-15

References 4-16

CHAPTER 5: Field oriented addressing for color sequential displays

1 Introduction 5-1

2 Principle of field oriented addressing 5-2
2.1 Introduction 5-2
2.2 Operating principle of field oriented addressing 5-3
2.3 Implementation of the principle 5-4

3 Characteristics of PDLC using field oriented addressing 5-7

4 Conclusion 5-12

References 5-13

CHAPTER 6: Color displays using color filters

1 Introduction 6-1

2 Optimizing the color filters 6-2

3 Results 6-6

4 Discussion 6-8

5 Conclusion 6-10

References 6-11

CHAPTER 7: Personal viewer

1 Introduction _____ *7-1*

2 Design rules _____ *7-1*

3 Design of the personal viewer _____ *7-2*

4 Prototype _____ *7-3*

5 Conclusion _____ *7-4*

References _____ **7-5**

CHAPTER 8: Conclusions concerning the innovative aspects of this Ph.D.

CHAPTER 9: What's next?

APPENDIX A: Color pictures

Lijst met veelgebruikte symbolen en afkortingen

List of symbols and abbreviations

n_o	ordinary refractive index
n_e	extra oridinary refractive index
n_p	refractive index of the polymer
ε_o	oridinary dielectric constant
ε_e	extra oridinary dielectric constant
PIPS	Photoinitiated Polymerization-Induced Phase Separation
TIPS	Thermally-Induced Phase Separation
SIPS	Solvent-Induced Phase Separation
LCOS	Liquid Crystal On Silicon
CMOS	Complementary Metal Oxide Semiconductor
mW	milli Watt
Ag	silver
Ni	nickel
Al	aluminum
Cu	copper
CMP	Chemical Mechanical Polishing
TiN	Titanium Nitride
V_{dc}	Direct Current Voltage
V_{BP}	Back Plane Voltage
HOE	Holographic Optical Element
PDLC	Polymer Dispersed Liquid Crystal
HPDLC	Holographic Polymer Dispersed Liquid Crystal
PNLC	Polymer Network Liquid Crystal
LC	Liquid Crystal
LCD	Liquid Crystal Display

FLC	Ferro-electric Liquid Crystal
VAN	Vertically Aligned Nematic
TN	Twisted Nematic
STN	Super Twisted Nematic
V_{90}	voltage to switch PDLC or PNLC to 90% transparent
V_{th}	threshold voltage
ΔV_{hyst}	difference in switching voltage due to hysteresis
I_{th}	detected light intensity at V_{th}
I_{90}	detected light intensity at V_{90}
I_{noise}	noise in the detected light intensity
$I_{white\_standard}$	detected light intensity of a white standard
I_{max}	maximum detected light intensity
I_{min}	minimum detected light intensity
UV	Ultra Violet
IR	Infra Red
Xe	Xenon
DC	Direct Current
Hz	Hertz
μm	micro meter
nm	nano meter
rms	root mean square
T_{rise}	rise time
T_{decay}	decay time
$\lvert R(\lambda) \rvert^2$	reflected spectrum
$\lvert R(f) \rvert^2$	Fourier transform of the reflected spectrum
λ	wavelength
f	spatial frequency
d_{gap}	cell gap
n_{gap}	refractive index of the material in the cell gap
FT	Fourier Transform

FFT	Fast Fourier Transform
IFFT	Inverse Fast Fourier Transform
$\delta(f)$	Dirac pulse
ARC	Anti Reflective Coating
ITO	Indium Tin Oxide
PC	Personal Computer
TPM	Twin Peaks Method
MPM	Multi Peaks Method
Δ	99% error margin
n	number of values
t_{995}	Student variable for 99% error margin
d_{avg}	average cell gap
Re	real part
Im	imaginary part
F_0	spatial frequency resolution of the FFT
H_2O	water
SiON	Silicon Oxynitride
PECVD	Plasma Enhanced Chemical Vapour Deposition
RIE	Reactive Ion Etching
BRDF	Bidirectional Reflactance Distribution Function
%wt	weight concentration
Hg	mercury
HgXe	mercury xenon
E	reorientation field
E_{th}	threshold electric field
E_{appl}	applied electric field
°C	degrees Celsius
HGH	Heilmeier Guest Host
ω	dark area
φ	angle of contrast inversion

θ	angular position of the observer
DFM	Droplet Filling Method
VFM	Vacuum Filling Method
CFM	Capillary Filling Method
FOA	Field Oriented Addressing
IPS	In Plane Switching
FFS	Fringe Field Switching
V_{ptp}	Volts peak to peak
rpm	rounds per minute

Introductie van kleur in reflectieve PDLC en PNLC microdisplays

Nederlandse samenvatting van de Engelse tekst
Dutch summary of the English text

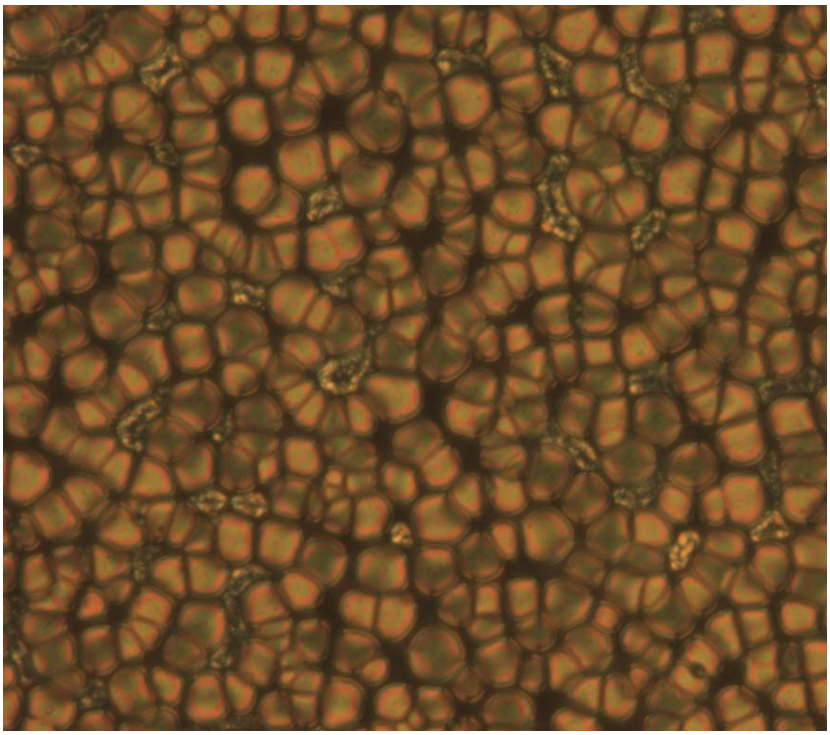

1 Situering van het doctoraat

1.1 Inleiding

Op microdisplays wordt er tegenwoordig veel onderzoek verricht. De achterzijde van deze beeldschermen bestaat uit een CMOS-chip waarop reflecterende elektrodes worden aangebracht. In dit doctoraatsonderzoek wordt er tussen het tegenglas aan de voorzijde van het microdisplay en de achterzijde een vloeibaar kristal aangebracht. Het vloeibaar kristal dat gebruikt wordt is ofwel Polymer Dispersed Liquid Crystal (PDLC) of Polymer Network Liquid Crystal (PNLC). PDLC en PNLC zijn gelijkaardig wat samenstelling en elektro-optisch principe betreft. Het optisch principe is gebaseerd op de verstrooiing van licht. Hierbij worden er geen polarisatoren gebruikt waardoor PDLC en PNLC beeldschermen een veel hogere helderheid hebben dan de meeste andere vloeibaar kristal beeldschermen. De bedoeling van dit onderzoeksproject is een volledig kleuren PDLC of PNLC microdisplay te onwikkelen dat geschikt is voor ‘personal viewer’-toepassingen. ‘Personal viewer’-toepassingen maken gebruik van een lenzensysteem dat een vergroot virtueel beeld creëert van het microdisplay. Het lenzensysteem moet compact zijn om het te kunnen integreren in draagbare toepassingen (view finder in een camcorder, beeldscherm in een GSM, palm top PC,…).

Dit doctoraatsonderzoek kan men in 4 domeinen situeren: vloeibare kristallen, reflectieve beeldschermen, microdisplays en reflectieve kleurenbeeldschermen. In de volgende paragrafen wordt er een stand van zaken gegeven van deze 4 domeinen. Aan het einde van dit hoofdstuk worden de doelstellingen van dit doctoraat behandeld.

1.2 Polymer Dispersed Liquid Crystal en Polymer Network Liquid Crystal

Polymer Dispersed Liquid Crystal (PDLC) en Polymer Network Liquid Crystal (PNLC) zijn gelijkaardig. Ze zijn beiden op hetzelfde elektro-optische principe gebaseerd, namelijk de verstrooiing van licht. Beiden zijn een mengsel van vloeibaar kristal, monomeer en photo-initiator. Door deze mengsels met UV te belichten start een polymerisatieproces waardoor er een stabiele film ontstaat. De polymerisatie zorgt voor een fasescheiding van het polymeer en het vloeibaar kristal. De polymeerstructuur is verschillend voor PDLC en PNLC. PDLC bestaat uit een polymeermatrix die het vloeibaar kristal omsluit in druppels (Fig. 1.2). In PNLC vormt het vloeibaar kristal een continue laag (Fig. 1.3). De polymeermatrix is als een netwerk dat is ondergedompeld in het vloeibaar kristal. In dit doctoraat bestaat het PDLC uit het prepolymeer PN393 en het vloeibaar kristal TL213. Beide componenten kunnen afzonderlijk bekomen worden bij Merck (Duitsland en VK). PNLC wordt als 1 component geleverd door Dainippon Ink & Chemicals (Japan).

Wanneer er geen elektrisch veld over het PDLC of het PNLC staat, zijn de vloeibaar kristal molekulen willekeurig georienteerd. In dit geval onstaat er lichtverstrooiing door een verschil in brekingsindex aan de interface tussen het polymeer en het vloeibaar kristal en aan de interface tussen de vloeibaar kristallen onderling. Wanneer er een spanning over het PDLC of PNLC wordt aangelegd, zal het vloeibaar kristal zich parallel met het elektrisch veld orienteren. Invallend licht ervaart geen verschil in brekingsindex aan de verschillende interfaces waardoor het PDLC of PNLC transparant wordt.

De elektro-optische eigenschappen van het PDLC en PNLC (lichtverstrooiing, contrast, schakeltijden, schakelspanning, hysteresis) worden bepaald door de manier waarop het PDLC en PNLC worden bereid. Hierbij denken we aan de samenstelling van het mengsel, UV-

belichtingstijd, UV-intensiteit en temperatuur tijdens belichting. Daarnaast speelt ook de dikte van de PDLC- of PNLC-film een rol.

1.3 Reflectieve vloeibaar kristal beeldschermen

De meeste vloeibaar kristal beeldschermen die in toepassingen zoals laptops geïntegreerd worden zijn transmissief. Het nadeel van deze beeldschermen is dat ze een lichtbron nodig hebben aan de achterzijde van het beeldscherm (backlight). Voor mobiele toepassingen is het belangrijk dat men deze lichtbron kan elimineren. Zo kan het energieverbruik van het beeldscherm teruggebracht worden van enkele Watt to minder dan 100mW. Bovendien neemt het gewicht van het beeldscherm af. Het ideale beeldscherm voor mobiele toepassingen heeft genoeg aan het omgevingslicht als lichtbron. Dit is de doelstelling van reflectieve beeldschermen. De uitdaging voor deze beeldschermen is een hoge helderheid en een groot contrast te bekomen voor een ruim bereik aan kijkhoeken en bij verschillende types van belichting. Het is dan ook belangrijk dat deze beeldschermen al het invallend licht zo efficient mogelijk gebruiken. Onderzoek hieromtrent concentreert zich vooral op verschillende vloeibaar kristal technologiën en op de reflector-elektrodes. Reflectieve beeldschermen kunnen geklassificieerd worden op basis van het aantal polarisatoren die er in het beeldscherm gebruikt worden (0, 1 of 2) en of kleurenbeeldschermen kunnen bekomen worden met of zonder kleurfilters. De algemene tendens is dat beeldschermen met 2 polarisatoren het hoogste contrast hebben maar de laagste helderheid. Beeldschermen zonder polarisatoren hebben dan weer een hoge helderheid maar een laag contrast. De karakteristieken van beeldschermen met 1 polarisator bevinden zich ergens tussenin.

1.4 Microdisplays

Microdisplays combineren technologie uit de beeldschermindustrie met technologie uit de halfgeleiderindustrie. Deze combinatie zorgt voor een aantal voordelen. Microdisplays maken gebruik van CMOS-technologie voor de actieve matrix (pixeltransistoren) op de achterzijde van het beeldscherm. Hierdoor kunnen de afmetingen van de pixels beperkt worden tot minder dan 15μm. Dit laat kleine beeldschermen (typisch 5X5mm^2 tot 20X15mm^2) met hoge resoluties toe (120X160 pixels tot 2560X2048 pixels). Een ander voordeel is dat met CMOS hogere schakelsnelheden kunnen bekomen worden in vergelijking met Thin Film Transistor (TFT) technology die gebruikt wordt bij transmissieve vloeibaar kristal beeldschermen. Microdisplays gebruiken reflectieve elektroden waardoor de apertuurverhouding (>95%) groter is dan die van de transmissieve elektroden bij transmissieve vloeibaar kristal beeldschermen (70% tot 80%). De apertuurverhouding is de verhouding van het oppervlak van een pixel dat gebruikt wordt voor het weergeven van informatie tot de totale fysische oppervlakte van een pixel. Hoe hoger de apertuurverhouding is hoe hoger het optisch rendement van het beeldscherm. Verder is het energieverbruik van microdisplays laag (10mW~250mW).

De kleine afmetingen van de pixels zorgen er voor dat een waarnemer met het blote oog niet alle informatie op het microdisplay kan waarnemen. Daarom wordt er gebruik gemaakt van een optisch systeem om de informatie op het microdisplay te vergroten. Deze optische systemen zijn ofwel ‘personal viewer’-systemen ofwel projectoren. In het geval van een ‘personal viewer’-systeem genereert het optisch systeem een virtueel vergroot beeld. Deze systemen zijn gericht op mobiele toepassingen. Het is dan ook belangrijk dat het ‘personal viewer’-systeem compact is en weinig weegt. In het geval van een projector wordt een reëel vergroot beeld gegenereerd. Het beeld wordt dan geprojecteed op een scherm.

1.5 Reflectieve kleurenbeeldschermen

Er zijn verschillende manieren om reflectieve kleurenbeeldschermen te bekomen. De gebruikte technologie voor het bekomen van kleur is in grote mate afhankelijk van het vloeibaar kristal. De reden hiervoor is dat de aanpak om het optisch rendement op te drijven verschilt van vloeibaar kristal tot vloeibaar kristal.

Voor transmissieve vloeibaar kristal beeldschermen worden kleurenfilters gebruikt voor het bekomen van kleur. Het nadeel van deze methode is het lage rendement. Een eerste reden is dat de pixels moeten opgesplitst worden in 3 subpixels. Ieder subpixel heeft de informatie weer van 1 van de 3 basiskleuren (bv. rood, groen en blauw). Bovendien absorbeert ieder kleurenfilter ongeveer 2/3 van het kleurenspectrum. Het gevolg hiervan is dat de helderheid van het beeldscherm sterk afneemt. Bij transmissieve beeldschermen wordt dit opgevangen door de lichtbron aan de achterzijde van het beeldscherm. Bij reflectieve beeldschermen is dit niet mogelijk. Vandaar dat er voor reflectieve beeldschermen naar andere oplossingen wordt gezocht.

Een eerste mogelijk alternatief is kleur bekomen met diffractie van licht. Dit principe wordt aangewend onder verschillende vormen. Holographic Optical Elements (HOE) van Dupont zijn op dit principe gebaseerd. HOEs bestaan uit een photopolymeer dat bij de aanmaak belicht wordt met 2 laserbundels. De eerste lichtbundel bepaalt de richting van het invallend licht en de tweede bundel bepaalt de kijkrichting van de waarnemer. Bij het belichten zal er constructieve en destructieve interferentie ontstaan in het photopolymeer. Dit resulteert in materiaal met verschillende brekingsindex waardoor er diffractie kan plaatsvinden. HOEs kunnen zowel reflectief als transmissief gebruikt worden. Ze werden reeds in draagbare toepassingen en projectoren gedemonstreerd. Ook Holographic PDLC (HPDLC) maakt gebruik van diffractie van licht. Om HPDLC te bekomen wordt PDLC met 2 laserbundels uitgehard. Op plaatsen met constructieve interferentie van de laserbundels

wordt er polymeer gevormd. Het vloeibaar kristal migreert naar de plaatsen met destructieve inteferentie. Diffractie van licht treedt op wanneer er geen spanning over het HPDLC voorkomt. In dit geval heeft men immers periodieke lagen met verschillende brekingsindex. Legt men wel een spanning over het HPDLC aan, dan wordt het HPDLC transparant. Een nadeel van HPDLC zijn de hoge schakelspanningen (50V en hoger). Bovendien kunnen kleurenbeeldschermen slechts bekomen worden door 3 beeldschermen (voor iedere basiskleur 1) op elkaar te plaatsen. Het voordeel is wel dat er geen licht verloren gaat bij de kleurenscheiding. PDLC kleurenbeeldschermen gebaseerd op de diffractie van licht werden ook gedemonstreerd met behulp van dielektrische spiegels en diffractieve spiegels.

Dit doctoraat is ook gericht op 'personal viewer'-toepassingen. Vanuit dit oogpunt kan men ook kleursequentiële adressering als een optie onderzoeken voor het bekomen van kleurenbeeldschermen. Bij kleurensequentiële adressering wordt de informatie van de 3 basiskleuren kort na elkaar op het beeldscherm afgebeeld. Dit gebeurt zo snel dat de kleurindruk die op het oog wordt achtergelaten een menging is van de 3 basiskleuren. Het probleem hierbij is dat het vloeibaar kristal voldoende snel moet kunnen schakelen. Dit principe werd reeds gedemonstreerd voor PDLC. Het nadeel hierbij is dat de PDLC mengsels die hiervoor gebruikt worden niet commercieel beschikbaar zijn en dat de schakelspanningen veel te hoog zijn voor microdisplays.

1.6 Doelstellingen van dit doctoraat

In een eerste fase zullen de elektro-optische eigenschappen van PDLC en PNLC geanalyseerd worden op testcellen. De bedoeling hiervan is het verband vast te leggen tussen de beeldschermparameters (zoals de cell gap, UV parameters bij het belichten, de assemblage, gebruikte vulmethode, DC spanning) en de beeldschermcriteria (zoals contrast, schakeltijd, schakelspanning, hysteresis en reflectie). Zo kunnen de beeldschermcriteria

geoptimaliseerd worden. Hiervoor moeten er 3 meetopstellingen ontworpen en gerealiseerd worden. Dit zijn een meetopstelling voor het opmeten van de elektro-optische eigenschappen van PDLC en PNLC, een meetopstelling voor het meten van de cell gap in vloeibaar kristal beeldschermen en een meetopstelling voor de analyse van reflectieve beeldschermen in draagbare 'direct view'-toepassingen. Eens het verband tussen de beeldschermparameters en de beeldschermcriteria gekend is, kan deze kennis gebruikt worden voor het optimaliseren van de assemblage van monochrome microdisplays. Verder moet er een lenzensysteem ontworpen en gebouwd worden om de toepasbaarheid van PDLC en PNLC microdisplays in 'personal viewer'-toepassingen aan te tonen. In een laatste fase van het onderzoeksproject ligt de nadruk op de introductie van kleur in reflectieve PDLC en PNLC microdisplays. Een eerste piste die hierbij onderzocht wordt is het gebruik van kleurenfilters. Een andere piste onderzoekt de mogelijkheden om met veldgeoriënteerd adresseren de schakeltijden van PDLC en PNLC terug te brengen tot niveaus die compatibel zijn met kleurensequentiële adressering.

2 Meetopstellingen

2.1 Inleiding

Een eerste doelstelling van het doctoraatsonderzoek is het optimaliseren van de karakteristieken van reflectieve PDLC en PNLC beeldschermen. Hierbij zijn meetopstellingen onontbeerlijk. Voor dit doctoraatsonderzoek zijn er 3 meetopstellingen gerealiseerd. Een eerste meetopstelling laat toe om de elektro-optische eigenschappen van reflectieve PDLC en PNLC beeldschermen op te meten. Onder elektro-optische eigenschappen verstaat men de schakelspanningen, de schakeltijden, de reflectie, het contrast en de hysteresis. Een tweede opstelling wordt gebruikt voor het meten van de cell gap van het vloeibaar kristal beeldscherm. Met een derde meetopstelling wordt de toepasbaarheid van reflectieve beeldschermen geanalyseerd. Deze meetopstelling is bedoeld om de leesbaarheid van een reflectief beeldscherm na te gaan in verschillende omgevingen. Dit moet toelaten om het gebruiksgemak van beeldschermtechnologiën te evalueren en met elkaar te vergelijken.

2.2 Meting van de elektro-optische eigenschappen van PDLC en PNLC

Voor het opmeten van de elektro-optische eigenschappen van PDLC en PNLC (schakeltijd, schakelspanning, hysteresis, contrast en reflectie) wordt er gebruik gemaakt van een meetopstelling waarbij het reflectief beeldscherm met een gecollimeerde lichtbundel wordt belicht (Fig. 2.1-2.2). De lichtbron zelf is een Xe-lichtbron. Deze lichtbron heeft een stabiel en vlak spectrum in het zichtbare gebied. Met behulp van een lens en 2 diafragmas wordt het gegeneerde licht omgezet in een gecollimeerde lichtbundel. Een UV-filter en een IR-filter moeten er voor zorgen dat het beeldscherm enkel met zichtbaar licht wordt belicht. Het gereflecteerde licht

wordt gedetecteerd met een Avalanche Photodiode. Voor de detector bevindt er zich een lens die toelaat om het beeldscherm scherp te stellen op de detector. De opening van het diafragma voor deze lens bepaalt de detectiehoek.

2.3 Meting van de cell gap in vloeibaar kristal beeldschermen

2.3.1 Inleiding

De cell gap van een vloeibaar kristal beeldscherm bepaalt in grote mate de elektro-optische eigenschappen van het beeldscherm. Bij de karkaterisatie van een vloeibaar kristal is het nodig om nauwkeurig te weten wat de waarde van de cell gap is. Bij de assemblage van de beeldschermen wordt de cell gap onder controle gehouden met behulp van spacers. De spacers zijn bol- of cilindervormig en zijn gemaakt van glas of een kunststof. Het is de bedoeling dat de diameter van de spacers overeenkomt met de gewenste cell gap. In de praktijk kan er een verschil optreden tussen de gewenste en werkelijke cell gap. Dit kan te wijten zijn aan de druk die gebruikt werd bij de assemblage, capillaire krachten tijdens het vullen van de beeldschermen met vloeibaar kristal, uitharden van de afdichtingslijmnaad rond het beeldscherm, stofdeeltjes, concentratie spacers,… Vandaar dat een nauwkeurige cell gap meetmethode een interessant instrument is voor de optimalisatie van beeldschermassemblage en voor de karakterisatie van het vloeibaar kristal.

Er bestaan reeds meetmethodes voor het meten van de cell gap. Deze zijn echter alleen toepasbaar op beeldschermen die reeds gevuld zijn met vloeibaar kristal. Bovendien zijn deze methodes niet toepasbaar op vloeibare kristallen waarvan het optisch principe niet gebaseerd is op de polarisatie van licht (zoals PDLC en PNLC). Vandaar dat er een nieuwe meetmethode is ontwikkeld.

De meetmethode voor het meten van de cell gap is gebaseerd op de interferentie van licht. 2-golflengten-interferentie van licht wordt reeds gebruikt voor het meten van de afstand tussen twee reflecterende oppervlaktes. De uitrusting die in dergelijke meetopstelling wordt gebruikt, komt niet voor in andere meetopstellingen voor beeldschermen. Vandaar dat er een methode op basis van wit-licht-interferometrie op punt werd gesteld. Het voordeel van deze methode is dat ze toelaat de cell gap te meten zowel vóór het vullen van de beeldschermen als na het vullen. Bovendien laat deze meetmethode toe de cell gap te meten bij zowel beeldschermen die gebaseerd zijn op de polarisatie van licht als beeldschermen die gebaseerd zijn op lichtverstrooiing (zoals PDLC en PNLC).

2.3.2 Principe van meetmethode

Het lichtspectrum dat gereflecteerd wordt door 2 parallelle oppervlakken vertoont een interferentiepatroon van de vorm:

$$|R(\lambda)|^2 = A + B\cos(4\pi n_{gap} d_{gap}/\lambda) \qquad \text{Verg. (2.1)},$$

waarbij λ=golflengte van het licht; d_{gap}=dikte van de cell gap; n_{gap}=brekingsindex van het materiaal in de cell gap. A en B zijn afhankelijk van de reflectiecoëfficient van beide oppervlakken. Uit Verg. (2.1) volgt dat er een eenduidig verband bestaat tussen de periode van het gereflecteerd spectrum en $n_{gap}d_{gap}$. Om de cell gap te bepalen dient men alleen nog de brekingsindex van het materiaal te kennen. Wanneer het beeldscherm nog niet met vloeibaar kristal is gevuld, bevat de cell gap lucht. In dit geval is $n_{gap} \approx 1$. Wanneer de cell gap reeds gevuld is met vloeibaar kristal kan men de cell gap bepalen door de vloeibaar kristal molekulen parallel met het invallend licht te oriënteren. In dit geval is $n_{gap}=n_o$ waarbij n_o=ordinaire brekingsindex van het vloeibaar kristal. Bij sommige vloeibare kristallen met een $\Delta\varepsilon<0$ (bv. Vertically Aligned Nematic) zijn de molekulen parallel met het licht georiënteerd zonder dat er een spanning moet aangelegd worden. Bij andere vloeibaar kristallen met een $\Delta\varepsilon>0$ (zoals PDLC, PNLC, Twisted

Nematic,…) moet er wel een spanning aangelegd worden om tijdens de meting van het spectrum de molekulen parallel met het licht te oriënteren.

2.3.3 Omzetting van het principe in de praktijk

Voor het opmeten van het interferentiespectrum wordt het beeldscherm onder een microscoop geplaatst (Fig. 2.7). Het gedetecteerde spectrum wordt met een PC uitgelezen. Er zijn verschillende manieren om de periodiciteit van Verg. (2.1), en dus de waarde van de cell gap, te bepalen. In principe volstaat het om 1 maximum en 1 minimum te kennen van het gereflecteerde spectrum. Het meetbereik van de spectrumanalyser (465nm tot 1650nm) en de waarde van de gemeten cell gap (van 3μm tot 10μm) leiden er toe dat het gemeten spectrum meerdere maximima en minima bevat. Een eerste manier is dat men de maxima en minima in het gemeten spectrum bepaalt. Hieruit kan men dan de periodiciteit en de cell gap bepalen. Een tweede mogelijkheid is een model op te stellen van het gereflecteerd spectrum en dit aan het gemeten spectrum te fitten. Men kan ook eerst het gemeten spectrum bewerken vooraleer men de cell gap bepaalt. Een derde mogelijkheid bestaat er dan ook in om het gemeten spectrum $|R(\lambda)|^2$ om te zetten naar een spectrum $|R(1/\lambda)|^2$, dit analoog te filteren en daarna hierop een Fouriertransformatie uit te voeren. Met het analoog filteren probeert men component A uit Verg. (2.1) te elimineren. Deze is immers geen constante en kan vooral bij het bepalen van kleine waarden van de cell gap voor problemen zorgen (Fig. 2.9-2.11). De Fouriergetransformeerde van $|R(1/\lambda)|^2$ moet een duidelijke piek vertonen bij de frequentie die bepaald wordt door de cell gap (zie Verg. (2.1)). Omdat de twee reflecteerde oppervlakken die de cell gap bepalen nooit perfect evenwijdig zijn, het gebied waarin gemeten wordt niet oneindig klein is en in de praktijk geen Fouriertransformatie wordt uitgevoerd maar een Fast Fouriertransfomatie (waardoor er enkel discrete punten van het Fourierspectrum worden berekend), is de piek geen Dirac-puls zoals de theorie voorspelt. De piek

wordt hierdoor meer gespreid. Om de nauwkeurigheid van de cell gap bepaling nog op te drijven, kan men de Fast Fouriertransformatie digitaal filteren. Met dit digitaal filter elimineert men alle frequenties die niets te maken hebben met de cell gap. Na de Fouriergetransformeerde digitaal te filteren voert men een Inverse Fast Fouriertransformatie uit. Hierdoor bekomt men opnieuw een analoog signaal waarvan men de periode (en dus de cell gap) kan bepalen (Fig. 2.12). De kalibratie van deze meetopstelling toont aan dat deze methodes toelaten de cell gap te bepalen met een foutmarge van 2% en minder.

2.4 Meetopstelling voor de analyse van reflectieve beeldschermen voor ‘direct view’-toepassingen

2.4.1 Inleiding

Tot op heden zijn er geen standaarden voor het meten van reflectieve beeldschermen voor ‘direct view’-toepassingen. Een dergelijke standaard, die wel al bestaat voor emissieve en transmissieve beeldschermen, zou toelaten de verschillende technologiën met elkaar te vergelijken. De moeilijkheid bij het ontwerpen van een meetopstelling die een dergelijke analyse toelaat is dat de aard van de lichtbron (het licht uit de omgeving) sterk uiteenlopend kan zijn. Dit is niet het geval bij emissieve en transmissieve beeldschermen. De meetopstelling moet dan ook in staat zijn resultaten te genereren die representatief zijn voor de omstandigheden waarin het beeldscherm gebruikt zal worden. Alle belichtingsomstandigheden kunnen niet gesimuleerd worden (er zijn er oneindig veel). Het komt er dus op neer het aantal lichtbronnen te beperken. Door een goede selectie van deze lichtbronnen moet het op basis van de

metingen mogelijk zijn voorspellingen te maken over de bruikbaarheid van het beeldscherm in alle belichtingsomstandigheden.

2.4.2 Principe van de meetopstelling

Het omgevingslicht kan men opsplitsen in 2 componenten: een direkte lichtcomponent en een diffuse lichtcomponent. Daarnaast speelt ook de positie van de waarnemer een belangrijke rol in de belichting van het beeldscherm. In tegenstelling tot transmissieve en emissieve beeldschermen bevindt de waarnemer bij reflectieve beeldschermen zich aan dezelfde zijde van het beeldscherm als de lichtbron. Dit betekent dat de waarnemer de belichting van het beeldscherm volledig of gedeeltelijk kan verhinderen. Vooral bij draagbare 'direct view'-beeldschermen komt dit vaak voor omdat de waarnemer zich dicht bij het beeldscherm bevindt. Het is dus belangrijk om de waarnemer in de meetopstelling te integreren.

2.4.3 Realisatie van de meetopstelling

De meetopstelling is opgesplitst in een meetopstelling voor diffuse belichting (Fig. 2.17-2.18) en een meetopstelling voor direkte belichting (Fig. 2.19). Bij direkte belichting verhindert de waarnemer de belichting volledig of niet. Vandaar dat dezelfde meetopstelling als voor het meten van de elektro-optische eigenschappen wordt gebruikt. Voor het simuleren van diffuse belichting wordt een integrerende sfeer gebruikt. Het te meten beeldscherm wordt in 1 opening van de integrerende sfeert geplaatst. Diametraal ertegenover bevindt zich de detectoropening waarachter de detector zich bevindt. Deze detectoropening zorgt er voor dat er over een bepaalde ruimtehoek geen diffuse belichting van het beeldscherm voorkomt, net zoals bij een waarnemer. Hoe dichter de waarnemer zich bij het beeldscherm bevindt, hoe groter de ruimtehoek waarover er geen diffuse belichting van het beeldscherm optreedt. In de meetopstelling kan men deze ruimtehoek aanpassen door de detectoropening te vergroten en door een buis

in de detectoropening te schuiven. Op deze manier is het mogelijk de afstand van de waarnemer tot het beeldscherm te simuleren. De hoek waaronder de waarnemer naar het beeldscherm kijkt, wordt gesimuleerd door het beeldscherm te roteren.

2.5 Conclusie

Er worden meetopstellingen beschreven die in het kader van dit doctoraatsonderzoek gebruikt werden voor het meten van 3 verschillende aspecten van reflectieve PDLC en PNLC beeldschermen. Met de eerste worden de elektro-optische karakteristieken van PDLC en PNLC opgemeten. Met een tweede kan de cell gap van de beeldschermen gemeten worden. De derde laat toe een analyse te maken van de toepasbaarheid van reflectieve beeldschermen voor ‘direct view’-toepassingen.

3 Karakterisatie van PDLC en PNLC voor reflectieve beeldschermen

3.1 Inleiding

PDLC (Polymer Dispersed Liquid Crystal) en PNLC (Polymer Network Liquid Crystal) hebben het zelfde elektro-optisch effekt. Het zijn echter twee verschillende materialen. Na het curen bekomt men dan ook lagen met een verschillende morfologie. De PDLC-laag bestaat uit een polymeerlaag met daarin druppels vloeibaar kristal. De druppels vloeibaar kristal worden tijdens het polymeriseren van het PDLC gevormd. De PNLC-laag daarentegen kan men eerder beschouwen als een polymeernetwerk dat ondergedompeld is in een vloeibaar-kristal-laag. Het vloeibaar kristal zit dus niet geconcentreerd in druppels maar vormt een continuë laag die verspreid zit in de ruimtes van het polymeernetwerk.

PDLC is een verzamelnaam voor verschillende mengsels bestaande uit een prepolymeer en een vloeibaar kristal. In dit doctoraat worden produkten van Merck gebruikt. Het prepolymeer is PN393 en het vloeibaar kristal is TL213. Beide componenten worden afzonderlijk geleverd. PNLC wordt door Dainippon Ink & Chemicals geleverd. Het vloeibaar kristal en het prepolymeer van PNLC kunnen niet afzonderlijk bekomen worden.

In dit doctoraat worden de invloed van enkele parameters op de elektro-optische eigenschappen van PDLC en PNLC voor reflectieve beeldschermen onderzocht. Een eerste parameter is de UV belichting. De polymerisatie van het prepolymeer in zowel PDLC als PNLC gebeurt met UV. De invloed van de UV intensiteit en de belichtingstijd op het PDLC en PNLC zijn beschreven. Een tweede parameter is de dikte (de cell gap) van de PDLC- en PNLC-laag.

Tot op heden werd er vooral onderzoek uitgevoerd op PDLC en PNLC voor transmissieve beeldschermen en reflectieve beeldschermen met een

absorberende laag. In dit doctoraat ligt de nadruk op PDLC en PNLC voor reflectieve beeldschermen met een reflector. Deze combinatie heeft echter een aantal belangrijke voordelen wat betreft contrast en reflectie voor 'direct view'–toepassingen in vergelijking met reflectieve beeldschermen die gebruik maken van een ander vloeibaar kristal. Dit blijkt ook uit een analyse die de toepasbaarheid voor 'direct view'-toepassingen van reflectieve beeldschermen met PNLC vergelijkt met die van 1-polarisator Guest Host Heilmeier reflectieve beeldschermen.

3.2 Karakterisatie van PDLC

3.2.1 Optimalisatie van het PDLC mengsel

Bij de aanmaak van het PDLC-mengsel kan de mengverhouding van het prepolymeer (PN393) tot het vloeibaar kristal (TL213) vrij gekozen worden. Metingen tonen aan dat PDLC met een mengverhouding van 20%wt PN393 en 80%wt TL213 tot een goed compromis leidt wat de elektro-optische eigenschappen betreft. Een hogere concentratie PN393 leidt tot een hoger contrast, een hogere reflectie en lagere schakelspanningen. Een lagere concentratie PN393 leidt tot kleinere schakeltijden.

3.2.2 Invloed van de UV-parameters

3.2.2.1 UV spectrum van de belichtingsbronnen

Bij de karakterisatie van PDLC is het niet alleen belangrijk de UV-intensiteit en belichtingstijd op te geven. Metingen tonen aan dat er aanzienlijke verschillen in de elektro-optische eigenschappen optreden afhankelijk van de gebruikte belichtingsbron. De reden hiervoor is dat de UV-intensiteit slechts over een klein deel van het UV wordt gemeten (rond 360nm).

3.2.2.2 UV-intensiteit

De metingen op reflectieve PDLC beeldschermen met een reflector bevestigen vroegere publicaties over transmissieve beeldschermen en reflectieve beeldschermen met een absorberende laag. Uiteindelijk komt het er op neer dat de diameter van de druppels vloeibaar kristal in het PDLC afneemt naarmate de UV-intensiteit bij het belichten toeneemt. Toegepast op de elektro-optische eigenschappen betekent dit dat een hogere UV-intensiteit resulteert in een hogere reflectie, contrast en schakelspanning. De schakeltijden daarentegen nemen af.

3.2.2.3 Belichtingstijd

Om een stabiele PDLC-film te bekomen is het belangrijk dat het belichten pas wordt gestopt wanneer het polymerisatie-proces afgelopen is. Een analyse van de stabiliteit van de elektro-optische eigenschappen in de tijd toont aan dat vooral de schakelspanning en schakeltijden gevoelig zijn aan een te korte belichting. Aan de andere kant zorgt overbelichting voor een abrupte en drastische verandering in de elektro-optische eigenschappen (Fig. 3.6). Bij een te lange UV-belichting wordt het vloeibaar kristal aangetast. Fotos van het overbelichte PDLC tonen gebieden waar er geen lichtverstrooiing optreedt (Fig. 3.7-3.8). Metingen van de capaciteit en de reflectie als funktie van de temperatuur (Fig. 3.9) tonen duidelijk een verschillende relatie aan voor niet-overbelicht en overbelicht PDLC. Hierdoor nemen het contrast, de reflectie en de schakelspanningen drastisch af. De schakeltijden nemen dan weer spectaculair toe. Dit werd nog niet eerder in de litteratuur beschreven. Dit is vooral van belang wanneer men snelschakelend PDLC wil bekomen. Snelschakelend PDLC kan men bekomen door te belichten met een hoge UV-intensiteit. Hierdoor komen de belichtingstijd voor stabiel PDLC en het punt van overbelichting steeds dichter bij elkaar te liggen.

3.2.3 Invloed van de cell gap

De invloed van de cell gap op de elektro-optische eigenschappen van PDLC in reflectieve beeldschermen met een reflector komen overeen met wat in vroegere publicaties werd beschreven. Bij toenemende cell gap neemt de reflectie toe en het contrast af terwijl de schakeltijden en het reorientatieveld (het elektrisch veld dat overeen komt met de schakelspanning) ongeveer contstant blijven. Een afwijking van dit theoretisch gedrag wordt vastgesteld bij beeldschermen met een cell gap kleiner dan 4μm. Is de cell gap kleiner dan 4μm dan neemt de lichtverstrooiing en het reorientieveld sterk af en de schakeltijden spectaculair toe in vergelijking met beeldschermen met een cell gap groter dan 4μm (Fig. 3.10). Deze spectaculaire wijziging in opto-elektrische eigenschappen heeft zijn oorsprong in het verschil in alignering van het vloeibaar kristal. Vloeibaar kristal dat zich in druppels in de bulk (volledig omsloten door PDLC) bevindt, aligneert zich parallel met de interface met de polymeerstructuur (Fig. 3.14). Vloeibaar kristal dat zich in druppels bevindt die een interface hebben met de ITO-elektrode op het tegenglas of de Al reflector elektrode zal zich loodrecht op de interface met de polymeerstructuur aligneren. Bij een cell gap kleiner dan 4μm komt er bijna geen bulk meer voor in de PDLC-laag. Het vloeibaar kristal zal dan ook enkel loodrecht op de interface met het polymeer gealigneerd zijn. Dit verklaart de spectaculaire wijziging in elektro-optische eigenschappen. Het verschil in alignering kan ook vastgesteld worden aan de hand van een aantal experimenten. Vooreerst is er een duidelijk verschil in reflectie zichtbaar wanneer men de PDLC-laag van 3μm vergelijkt met die van 4μm onder een microscoop met gepolariseerd licht (Fig. 3.11). Het verschil in alignering kan ook vastgesteld worden door de reflectie en de capaciteit in funktie van de temperatuur op te meten (Fig. 3.12-3.13).

3.2.4 Besluit bij de karakterisatie van PDLC

In deze paragraaf staan de resultaten van de analyse naar het verband tussen de cell gap en de UV-parameters enerzijds en de elektro-optische eigenschappen anderzijds. Deze analyse is gebaseerd op experimenten met PDLC mengsels die uit 20%wt PN393 en 80%wt TL213 bestaan. Over het algemeen komen de resultaten overeen met eerder gepubliceerd werk. Uitzonderingen hierop zijn de karakteristieken van PDLC bij overbelichten en van PDLC beeldschermen met een 3μm cell gap. De oorzaak van deze afwijkingen werd achterhaald en staat in dit hoofdstuk beschreven. Aan de hand van deze karakterisatie is het mogelijk de optimale UV-belichtingsparameters en cell gap te kiezen.

3.3 Karakterisatie van PNLC

De karakterisatie van PNLC gebeurt op dezelfde manier als die van PDLC. Er is een gelijkaardig verband voor PNLC en PDLC tussen de elektro-optische eigenschappen enerzijds en de cell gap en belichtingstijd anderzijds. De elektro-optische eigenschappen van PNLC wijken bovendien op dezelfde manier af van het theoretisch model als bij PDLC. Dit betekent dat een te kleine cell gap (<4μm) en een overbelichting bij het polymeriseren een drastische verandering in de elektro-optische eigenschappen veroorzaken.
Hoewel het verband gelijkaardig is, zijn er toch grote verschillen in de absolute waarde van de elektro-optische eigenschappen van PDLC en PNLC. De schakeltijden en de hysteresis zijn het laagst en de reflectie en het contrast zijn het hoogst voor PNLC. De schakelspanning is het laagst voor PDLC.

3.4 DC-spanning in reflectieve PDLC en PNLC beeldschermen

Bij het aanleggen van een spanning fluctueert de intensiteit van het licht gereflecteerd door het beeldscherm met dezelfde frequentie als de aangelegde spanning. In dit doctoraatsonderzoek werd aangetoond dat de fluctuaties , ook wel 'flicker' genoemd, veroorzaakt worden door een DC-spanning. Deze DC spanning is te wijten aan de asymmetrie in gebruikte materialen voor de elektrode op het tegenglas (ITO of Indium Tin Oxide) en de elektrodes op de achterzijde van het beeldscherm (Al). Door het verschil in werkfunkties die deze materialen hebben, ontstaat er een DC spanning wanneer het ITO en Al met elkaar worden kortgesloten.

Deze DC-spanning ligt tussen de 0.25V en 1.1V. Er is geen verband tussen de DC-spanning enerzijds en de belichtingsparameters, de cell gap en vloeibaar kristal (PDLC of PNLC) anderzijds. De DC-spanning moet gecompenseerd worden om een goede werking van het beeldscherm toe te laten. Dit kan gebeuren op een technologische manier (bv. ITO-laag op Al reflector-elektroden aanbrengen) of op een elektronische manier.

3.5 Toepasbaarheid van reflectieve PDLC en PNLC beeldschermen voor 'direct view'-toepassingen

De toepasbaarheid van reflectieve PDLC en PNLC beeldschermen voor direct view toepassingen wordt geanalyseerd met behulp van de meetopstelling die beschreven staat in het hoofdstuk "Meetopstellingen". Hierbij wordt de analyse van een reflectief PNLC beeldscherm vergeleken met de analyse van een 1-polarisator Heilmeier Guest Host beeldscherm.

De analyses tonen aan dat de reflectie, het contrast en de hoek met contrast inversie sterk afhankelijk zijn van het type belichting (diffuus of direkt) en

de positie van de waarnemer. De analyses tonen ook aan dat de ‘best case’-situaties voor één beeldschermtechnologie evengoed de ‘worst case’-situaties kunnen zijn voor een andere. Voor een goede analyse is het dus belangrijk om bij de evaluatie van de beeldschermen metingen uit te voeren bij verschillende vormen van belichting en relatieve posities van de waarnemer, belichtingsbron en beeldscherm.
Reflectieve PNLC beeldschermen hebben een goed contrast en reflectie voor mobiele direct view toepassingen. De 1-polarisator-Heilmeier Guest Host beeldschermen hebben onder bepaalde voorwaarden een aanvaardbare waarde voor de reflectie. Het contrast blijft echter aan de lage kant.

3.6 Conclusie bij de karakterisatie van PDLC en PNLC voor reflectieve beeldschermen

De invloed van de UV-parameters en de cell gap op de elektro-optische eigenschappen van PDLC en PNLC voor reflectieve beeldschermen is onderzocht. De resultaten volgen theoretische voorspellingen die gelden voor transmissieve beeldschermen en reflectieve beeldschermen met een absorberende laag. Uitzonderingen hierop vormen PDLC en PNLC beeldschermen die werden overbelicht of die een cell gap hebben van minder dan 4μm. De oorzaak van dit afwijkend gedrag kon worden achterhaald.
De DC-spanning is te wijten aan het gebruik van verschillende materialen voor de elektrode op het tegenglas (ITO) en voor de pixel-elektrodes (Al).
De reflectie en het contrast hangen sterk af van het type belichting en de positie van de waarnemer. De metingen tonen aan dat wat voor één technologie de ‘best case’ situatie is voor een andere de ‘worst case’ situatie kan zijn en omgekeerd.

4 Assemblage en vullen van microdisplays

4.1 Inleiding

Bij de assemblage van de beeldschermen is het belangrijk een uniforme PDLC- of PNLC-laag te bekomen. Het probleem bij PDLC en PNLC is dat het prepolymeer in het PDLC- en PNLC-mengsel componenten bevatten die kunnen verdampen bij blootstelling aan vacuum. Dit betekent dat klassieke vulmethodes die bijvoorbeeld gebruikt worden voor het vullen van vloeibaar kristal beeldschermen met Twisted Nematic niet kunnen gebruikt worden voor PDLC en PNLC.

In dit doctoraatswerk worden er 3 alternatieve methodes voor de assemblage en het vullen van PDLC en PNLC beeldschermen geanalyseerd en geoptimaliseerd. Deze omvatten een druppelvulmethode, een capillaire vulmethode en een aangepaste vacuumvulmethode. Metingen op testbeeldschermen geven aan dat de elektro-optische eigenschappen van PDLC en PNLC niet worden beïnvloed door de gebruikte vulmethode. Hieruit kan men afleiden dat de vluchtige component in het prepolymeer niet verdampt bij het vullen. Bij de assemblage komen er wel 2 andere problemen voor die zich vooral demonstreren bij het assembleren van microdisplays. Een eerste probleem is dat de vias die de reflector-elektrode met de onderliggende transistoren verbinden niet worden gevuld met PDLC of PNLC. Een ander probleem wordt veroorzaakt door de stabiliteit van de cell gap na het UV-belichten van PDLC en PNLC.

4.2 Beschrijving van de assemblage en vulmethodes

4.2.1 Druppelvulmethode

Bij de druppelvulmethode (Fig. 4.1) wordt er een druppel PDLC of PNLC op de achterzijde van het beeldscherm, die uit de CMOS chip bestaat, aangebracht. Het tegenglas wordt dan tegen de achterzijde aangedrukt waardoor de druppel over gans het tegenglas wordt uitgesmeerd. De spacers die zich op het tegenglas bevinden zorgen er voor dat de afstand tussen het tegenglas en de achterzijde van het beeldscherm overeenkomt met de gewenste cell gap. De laag PDLC of PNLC wordt met UV belicht. Na de polymerisatie van het PDLC of het PNLC zijn het tegenglas en de achterzijde aan elkaar gehecht door het PDLC of PNLC. Het prepolymeer in het PDLC of PNLC is immers een acrylaat dat naast zijn optische funktie bij de werking van PDLC of PNLC ook als lijm kan gebruikt worden. Uiteindelijk wordt de rand van het beeldscherm nog afgedicht met een UV lijm.

4.2.2 Aangepaste vacuumvulmethode

Zoals reeds gezegd in de inleiding bevatten PDLC en PNLC vluchtige componenten in het prepolymeer die kunnen verdampen bij blootstelling aan vacuum. Vandaar dat bij het vullen de blootstelling aan vacuum tot een minimum moet herleid worden. Vacuumvullen heeft echter het voordeel dat er tijdens het vullen geen luchtinsluitsels kunnen voorkomen in het beeldscherm. De bedoeling van de aangepaste vulmethode is om van dit voordeel gebruik te maken terwijl de blootstelling van het vloeibaar kristal aan vacuum tot een minimum wordt beperkt.

De blootstelling aan vacuum wordt tot een minimum beperkt met 2 maatregelen. Bij klassieke vulmethodes bevindt het vloeibaar kristal zich in

een open reservoir voor het vullen. Wanneer vacuum wordt bereikt, wordt de vulopening van het beeldscherm in dit reservoir ondergedompeld. Bij de aangepaste vulmethode bevindt het vloeibaar kristal zich in een spuit (Fig. 4.2). Wanneer vacuum wordt bereikt, wordt het vloeibaar kristal voor de vulopening aangebracht. Eens het vloeibaar kristal zich voor de vulopening bevindt, vult de cell gap van het beeldscherm zich door capillaire krachten. Op deze manier wordt het vloeibaar kristal niet aan lage druk blootgesteld in de periode dat de vulklok vacuum wordt gezogen. Een tweede maatregel is dat bij de aangepaste vacuumvulmethode het vacuum direkt weer wordt verbroken wanneer het vloeibaar kristal de volledige vulopening bedekt. Bij de klassieke vacuumvulmethodes kan de druk geleidelijk opgevoerd worden.

4.2.3 Capillaire vulmethode

Bij de capillaire vulmethode wordt de cell gap met vloeibaar kristal gevuld door het optreden van capillaire krachten. Naast een vulopening moet er bij het vullen nog een tweede opening in de lijmafdichtingsnaad van het beeldscherm zitten. Deze bevindt zich aan de zijde tegenover de vulopening en laat toe dat de lucht in de cell gap kan ontsnappen.

4.3 Problemen bij het vullen en assembleren van PDLC en PNLC microdisplays

4.3.1 Vullen van vias

Een eerste probleem betreft het vullen van vias in de Al reflector-elektrodes van het microdisplay (Fig. 4.3-4.5). Deze vias verbinden de reflector-elektrodes met de onderliggende pixeltransistoren (Fig. 1.9). Deze vias zijn 2μm diep. Dit zorgt lokaal voor een sterke toename van de cell gap die nominaal 4μm bedraagt. Deze problemen treden vooral op bij de aangepaste

vacuumvulmethode en de capillaire vulmethode. Bij de aangepaste vacuumvulmethode kan dit probleem opgelost worden door het verbreken van het vacuum meer geleidelijk te laten gebeuren en door het beeldscherm op te warmen. Bij de capillaire vulmethode wordt dit probleem opgelost door het beeldscherm op te warmen.

4.3.2 Stabiliteit van de cell gap

De lichtverstrooiende eigenschappen van PDLC zijn niet altijd stabiel in tijd. Soms komt het voor dat PDLC dat vlak na de UV-belichting nog lichtverstrooiend is na verloop van tijd transparant wordt. Deze overgang van lichtverstrooiende toestand naar transparante toestand treedt meestal binnen de 24u na het UV-belichten op en spreidt zich geleidelijk over een deel van het beeldscherm uit. Deze overgang is onomkeerbaar bij kamertemperatuur en komt vooral voor bij de aangepaste vacuumvulmethode (Fig. 4.7) en de druppelvulmethode (Fig. 4.6). De gebieden waar deze overgang zich heeft voorgedaan zijn dan ook niet bruikbaar voor het weergeven van informatie wat de kwaliteit van het beeldscherm sterk naar beneden haalt. De plaats waar de transparante gebieden optreden zijn typisch voor de gebruikte vulmethode.

Door de beeldschermen te verwarmen tot boven 40°C worden de transparante gebieden opnieuw lichtverstrooiend. Dit wijst er op dat het vloeibaar kristal nog intact is. Waarnemingen met een microscoop met gepolariseerd licht tonen aan dat de vloeibaar kristal molekulen vertikaal (Fig. 4.8) gealigneerd zijn. Deze vertikale alignatie is te wijten aan een expansie van de cell gap nadat het PDLC met UV werd belicht. Metingen op testbeeldschermen (Table 4.1) met behulp van de meetopstelling voor het meten van de cell gap tonen aan dat de overgang naar de transparante toestand enkel optreedt in de gebieden waar de cell gap toeneemt na het UV-belichten. De metingen van de cell gap tonen aan dat kort na het vullen de cell gap tot 3.3µm kan samengedrukt zijn terwijl de spacerdiameter 4µm bedraagt. Deze sterke compressie van de cell gap worden toegeschreven aan

de grote capillaire krachten die optreden bij het vullen van het beeldscherm. De samengedrukte spacers expanderen wat tot een toename van de cell gap leidt na het UV-belichten van het PDLC.
Om een overgang van lichtverstrooiend PDLC naar transparant PDLC te voorkomen moet de cell gap stabiel blijven na het belichten van het PDLC. Dit kan gebeuren door de spacerconcentratie op te drijven. Een andere mogelijkheid is te wachten met het UV-belichten van het PDLC tot de cell gap zijn nominale waarde heeft bereikt.

4.4 Conclusie

Er werden 3 alternatieve vul- en assemblagemethodes voor de klassieke vacuumvulmethode onderzocht. De methodes zijn de druppelvulmethode, de aangepaste vacuumvulmethode en de capillaire vulmethode. Deze vulmethodes voorkomen de verdamping van de vluchtige componenten in het prepolymeer van het PDLC en PNLC. Bij het vullen van microdisplays kunnen er problemen optreden bij het vullen van vias of ten gevolge van de stabiliteit van de cell gap na het UV-belichten. Deze problemen werden opgelost voor alle vulmethodes. Uiteindelijk blijkt de capillaire vulmethode het meest betrouwbaar te zijn voor het vullen van microdisplays.

5 Veldgeorienteerde adressering voor kleurensequentiële beelschermen

5.1 Inleiding

In één van de voorgaande paragrafen werd aangetoond dat de elektro-optische eigenschappen van PDLC en PNLC afhankelijk zijn van het gebruikte type polymeer en vloeibaar kristal, de cell gap en de UV-parameters bij het belichten. Het is echter moeilijk om één van de elektro-optische eigenschappen te veranderen zonder de andere te beïnvloeden. Zo heeft PDLC met lage schakelspanning steeds hoge schakeltijden en vice versa. Het zou dan ook interessant zijn een parameter te vinden die enkel de schakeltijden verlaagt zonder de schakelspanning te verhogen. Dit kan met behulp van veldgeorienteerd adresseren. In de meeste vloeibaar kristal beeldschermen wordt de optische respons van het vloeibaar kristal enkel bepaald door de amplitude van het elektrisch veld. Bij veldgeorienteerd adresseren beïnvloedt naast de amplitude ook de orientatie van het elektrisch veld de optische respons van het vloeibaar kristal. Metingen tonen aan dat met behulp van veldgeorienteerd adresseren de schakeltijden kunnen gereduceerd worden tot niveaus voor kleurensequentiële PDLC beeldschermen .

5.2 Principe van veldgeorienteerd adresseren

5.2.1 Inleiding

PDLC is pas geschikt voor kleurensequentiële beeldschermen als de schakeltijden T_{stijg} en T_{relax} voldoende klein zijn ($T_{stijg} + T_{relax} \leq 10$ms). De

schakeltijden kunnen worden gereduceerd door een optimalisatie van de UV parameters en het PDLC mengsel (zie paragraaf "Karakterisatie van PDLC en PNLC voor reflectieve beeldschermen"). Het nadeel van deze werkwijze is echter dat een optimalisatie van de schakeltijden leidt tot een verhoging van de schakelspanning. Andere elektro-optische eigenschappen zoals het contrast en de reflectie worden er ook door beïnvloed. Door bij het schakelen van het vloeibaar kristal een groter elektrisch veld $E_{aangelegd}$ aan te leggen kan men de stijgtijd T_{stijg} reduceren daar $T_{stijg} \cong \frac{\gamma}{\varepsilon_0 \Delta\varepsilon\left(E_{aangelegd}^2 - E_{th}^2\right)}$ (Verg. (3.1)). Hierin is γ = rationele viscociteitscoëfficient, ε_0 = diëlektrische constante in de vrije ruimte, $\Delta\varepsilon$ = diëlektrische anisotropie van het vloeibaar kristal en $E_{aangelegd}$ = aangelegd elektrisch veld en E_{th} = threshold elektrisch veld. Dit principe kan niet toegepast worden voor de relaxatietijd T_{relax} aangezien $T_{relax} \cong \frac{2\gamma}{\varepsilon_0 \Delta\varepsilon E_{th}^2}$ (Verg. (3.2)). Het is echter belangrijk om ook T_{relax} te reduceren om PDLC geschikt te maken voor kleursequentiële beeldschermen. In dit hoofdstuk wordt een methode besproken om T_{relax} te reduceren met behulp van een nieuwe adresseringsmethode. Bij deze methode wordt niet alleen de amplitude van het aangelegd elektrisch veld gewijzigd maar ook de orientatie. Vandaar dat deze methode veldgeorienteerd adresseren wordt genoemd.

5.2.2 Werkingsprincipe van veldgeorienteerd adresseren

De lichtverstrooiende toestand van het PDLC wordt bij de klassieke adresseringsmethode bekomen bij een willekeurige orientatie van de vloeibaar kristal molekulen. In dit geval staat er geen elektrisch veld over de PDLC film (Fig. 5.1). Licht dat op de PDLC film invalt, ervaart een verschil in brekingsindex op de interface tussen de polymeermatrix en de vloeibaar

kristal molekulen. Hierdoor treedt er lichtverstrooiing op. Wanneer er een vertikaal elektrisch veld wordt aangelegd zullen de vloeibaar kristal molekulen zich parallel met het elektrisch veld oriënteren. Licht dat nu op het PDLC invalt zal geen verschil in brekingsindex ervaren. Hierdoor is het PDLC transparant. Bij de klassieke adressering is er dus enkel een elektrisch veld nodig bij de overgang van de lichtverstrooiende naar de transparante toestand. Dit verklaart waarom enkel de stijgtijd T_{stijg} afhankelijk is van het aangelegde elektrisch veld en niet de relaxatietijd T_{relax}.

Bij de klassieke adresseringsmethode wordt de orientatie van de vloeibaar kristal molekulen enkel bepaald door de amplitude van het elektrisch veld. Bij veldgeorienteerd adresseren wordt de orientatie van de vloeibaar kristal molekulen ook bepaald door de orientatie van het elektrisch veld. Het elektrisch veld kan immers geschakeld worden tussen de vertikale en de horizontale orientatie. Wanneer het elektrisch veld horizontaal georienteerd is, zullen de vloeibaar kristal molekulen zich ook horizontaal oriënteren (Fig. 5.1). In dit geval zal invallend licht een verschil in brekingsindex ervaren tussen de polymeermatrix en de vloeibaar kristal molekulen. Omdat nu zowel de transparante als de lichtverstrooiende toestand van het PDLC bepaald wordt door een elektrisch veld zal niet alleen de stijgtijd T_{stijg} maar ook de relaxatietijd T_{relax} bepaald worden door het aangelegd elektrisch veld $E_{aangelegd}$. Bijgevolg kan ook de relaxatietijd T_{relax} gereduceerd worden door het elektrisch veld aan te passen.

5.2.3 Implementatie van het principe

Een belangrijke uitdaging bij de implemenantie van het principe van veldgeorienteerd adresseren is het bekomen van een vertikaal en een horizontaal elektrisch veld in de cell gap van het beeldscherm. Om een perfekt vertikaal en horizontaal elektrisch veld te bekomen, zijn er vier elektrodes nodig: twee horizontale elektrodes voor het bekomen van het vertikaal elektrisch veld en twee vertikale elektrodes voor het bekomen van het horizontaal elektrisch veld. Dit is een vrij complexe structuur voor een

pixel-elektrode en het is niet voor de hand liggend om deze structuur te implementeren vanuit technologisch oogpunt.
Daarom wordt er een alternatieve layout voor de pixel-elektrode gebruikt. Hierbij heeft iedere pixel drie elektrodes (Fig. 5.2). Iedere pixel-elektrode bestaat uit 2 vingerelektrodes op de achterzijde van het beeldscherm en 1 transparante ITO (Indium Tin Oxide) elektrode op het tegenglas. Deze laatste elektrode is gemeenschappelijk voor alle pixels van het beeldscherm. Vingerelektrodes worden ook gebruikt bij In Plane Switching (IPS) en bij Fringe Field Switching (FFS) om een horizontaal elektrisch veld te bekomen. In tegenstelling to IPS en FFS wordt er bij veldgeorienteerd adresseren nog altijd een ITO elektrode gebruikt. Deze is nodig voor het bekomen van een vertikaal elektrisch veld.
Het horizontaal elektrisch veld wordt bekomen door beide vingerelektrodes een tegengestelde elektrische potentiaal te geven die symmetrisch is ten opzichte van de potentiaal van de ITO-elektrode. Het vertikaal elektrisch veld wordt bekomen door aan vingerelektrode A en B dezelfde elektrisch potentiaal aan te bieden verschillend van de potentiaal van de ITO-elektrode.
Door het aantal elektrodes in de pixel-elektrode te reduceren van vier naar drie neemt de uniformiteit van het vertikaal en het horizontaal elektrisch veld af. Simulaties (Fig. 5.3) tonen aan dat het horizontale elektrisch veld sterk zal zijn tussen de vingerelektrodes en zwak nabij de ITO-elektrode. Het vertikaal elektrisch veld is vrij uniform. Tussen de ITO-elektrode en de vingerelektrodes zal er altijd een vertikaal elektrisch veld aanwezig zijn.

5.3 Resultaten van de experimenten

Metingen op testbeeldschermen tonen duidelijk aan dat de relaxatietijd aanzienlijk kan verminderd worden door gebruik te maken van veldgeorienteerd adresseren (Fig. 5.6). Behalve de relaxatietijd neemt ook het contrast af. De mate van reductie van de relaxatietijd en contrast hangt niet alleen af van de amplitude van de aangelegde spanning (en dus van de

grootte van het horizontaal en vertikaal elektrisch veld). De afmetingen van de pixel-elektrode spelen ook een belangrijke rol (Table 5.1 en 5.2). Hiermee wordt de afstand tussen de vingerelektrodes *a*, de breedte van de vingerelektrodes *b* en de cell gap *d* bedoelt. De reductie van de schakeltijden tot niveaus die compatibel zijn met kleurensequentiële beeldschermen is mogelijk met een pixel-configuratie waarbij *a*=3µm, *b*=1µm en *d*=3µm. Met deze pixel-configuratie bekomt men een T_{stijg}=2.56ms en een T_{relax}=0.64ms bij een schakelspanning van $8.5V_{rms}$. Deze schakelspanning is aanzienlijk lager dan de $100V_{rms}$ die nodig is voor het aansturen van andere kleurensequentiële beeldschermen. Het contrast bedraagt 2.7 wat van dezelfde grootte-orde is als andere kleurensequentiële PDLC beeldschermen.

5.4 Besluit

Er werd aangetoond dat het mogelijk is om met veldgeorienteerd adresseren tussen een transparante toestand en een lichtverstrooiende toestand te schakelen. Zowel de stijgtijd als de relaxatietijd hangen af van de amplitude van de aangelegde spanning en de pixelconfiguratie. Met deze methode kunnen er schakeltijden bekomen worden die compatibel zijn met kleurensequentiële beeldschermen en dit bij relatief lage spanningen.

6 Kleurenbeeldschermen met behulp van kleurenfilters

6.1 Inleiding

De standaardtechnologie voor het bekomen van kleur in transmissieve vloeibaar kristal beeldschermen is met behulp van kleurfilters. Het is echter niet voor de hand liggend om deze technologie over te dragen op reflectieve PDLC en PNLC beeldschermen. Een belangrijk probleem bij reflectieve beeldschermen is de helderheid van het beeldscherm. De helderheid moet voldoende hoog blijven bij verschillende vormen van belichting. Daarom worden reflectieve beeldschermen zo ontworpen dat het invallend licht zo efficiënt mogelijk wordt gebruikt. Kleurenfilters halen dit rendement aanzienlijk naar beneden. Het principe van kleurenfilters is immers gebaseerd op de absorptie van licht. Bij transmissieve beeldschermen wordt dit opgelost door een lichtbron achter het beeldscherm te plaatsen. Bij reflectieve beeldschermen voor 'direct view'-toepassingen is dit geen oplossing. Een alternatief is de helderheid van de kleurfilters te verhogen door de kleurzuiverheid te verminderen. Voor een deel kan dit gebeuren door de dikte van de kleurfilters aan te passen. De kleurselectiviteit ligt echter in grote mate reeds vast door de samenstelling van het kleurfiltermateriaal.
Een ander probleem is dat er UV nodig is bij het belichten van het PDLC en het PNLC. De kleurenfilters absorberen niet alleen een deel van het kleurenspectrum maar ook UV. In het geval de kleurenfilters aan de glaszijde is aangebracht, wordt het belichten van het PDLC en PNLC met UV belemmerd. De totale UV transmissie van de kleurenfilters kan zo laag zijn dat een goede polymerisatie van PDLC enkel mogelijk is met een lichtbron met hoge UV intensiteit. Door de hoge UV absorptie zal bij het belichten een groot deel van het geabsorbeerde UV omgezet worden in warmte. Hierdoor zal echter ook het PDLC of PNLC tijdens het

polymeriseren een temperatuursstijging ondervinden wat zijn weerslag kan hebben op de eigenschappen van het PDLC of PNLC [1]. Het is ook belangrijk dat de UV transmissie van de rode, groene en blauwe kleurfilters dezelfde is. Zo heeft het PDLC onder de verschillende kleurfilters dezelfde elektro-optische eigenschappen.

6.2 Optimalisatie van de kleurenfilters

De optimalisatie van de kleurenfilters moet leiden tot beeldschermen met een hoge helderheid en groot kleurenspectrum. Belangrijk hierbij is dat de kleurenfilters een hoge UV-transmissie hebben en dit voor zowel de rode, groene als blauwe kleurenfilters. Bij de eerste evaluatie van de kleurenfiltermaterialen wordt er vooral gekeken naar de UV-transmissie. Er werden kleurenfiltermaterialen getest die gebruikt worden voor transmissieve beeldschermen. Deze produkten werden geproduceerd door Brewer Science. Ze vertonen een sterke kleurselectiviteit (Fig. 6.1). De UV transmissie van deze kleurenfiltermaterialen is echter laag en verschilt sterk van kleur tot kleur (Table 6.1).

Kleurenfiltermaterialen van Arch Chemicals vertonen een hogere UV transmissie. Deze materialen werden specifiek voor reflectieve beeldschermen ontwikkeld. De kleurselectiviteit is lager dan bij de produkten van Brewer Science. Dit leidt tot een hogere helderheid van de beeldschermen. Door een optimalisatie van de filterdikte kan de UV transmissie van de rode, groene en blauwe kleurfilters op elkaar afgestemd worden. Op deze manier werden er monopixel kleurendisplays geassembleerd die een karakterisatie van het PDLC toelaten (Fig. 6.3). De kleurenfilters worden op het tegenglas aangebracht. Er wordt geen planarisatielaag op de kleurfilters aangebracht omdat het verschil in filterdiktes tussen de 3 basiskleuren (grootte-orde 250nm) niet van die aard is dat de elektro-optische eigenschappen van het PDLC er sterk door

beïnvloed worden. Op de kleurenfilters wordt de transparante ITO-elektrode aangebracht.

6.3 Resultaten van de experimenten

De karakterisatie van het PDLC toont dat er verschillen zijn in de elektro-optische eigenschappen van het PDLC onder de rode, groene en blauwe kleurenfilters. Deze verschillen kunnen niet verklaard worden door het kleine verschil in UV transmissie tussen de verschillende kleuren. De filterdikte werd echter enkel geoptimaliseerd voor UV met een golflengte van 365nm. Een breder deel van het UV spectrum moet wellicht in rekening gebracht worden voor de optimalisatie van de kleurfilters. Een gelijkaardig fenomeen kon echter worden vastgesteld bij het curen van PDLC met verschillende types van UV bronnen. Hoewel het PDLC bij dezelfde UV intensiteit bij 365nm werd gepolymeriseerd, verschillen de elektro-optische eigenschappen aanzienlijk.

De materialen van Arch Chemicals werden gebruikt voor de assemblage van een kleurenmicrodisplay. De kleurenfilters zijn aangebracht op het tegenglas. De kleurenfilters zijn niet voorzien van een planarisatielaag. De kleurenfilters zijn in strepen aangebracht. De breedte van de strepen is ongeveer 65μm (Fig. 6.5). De ruimte tussen de kleurenfilters (ongeveer 15μm breed) wordt open gelaten en is dan ook transparant. Bij transmissieve beeldschermen wordt deze ruimte veelal opgevuld met een lichtabsorberend materiaal (black matrix). Bij transmissieve beeldschermen is dit nodig omdat de krachtige lichtbron die zich achter het beeldscherm bevindt het contrast sterk naar beneden zou halen indien een deel van het licht ongehinderd de voorzijde van het beeldscherm zou bereiken. Bij reflectieve beeldschermen is dit niet nodig. In tegendeel. Door de black matrix weg te laten, zal er een groter percentage van het invallend licht terug naar de waarnemer worden gereflecteerd. Hierdoor stijgt de helderheid van het beeldscherm. Dit is wel ten koste van de kleurselectiviteit van het beeldscherm. Door een opening

tussen de verschillende kleurstrepen te laten, is er ook een grotere aligneringsfout toegelaten bij het assembleren van het kleurenbeeldscherm.
Voor het assembleren van de kleurenmicrodisplays wordt dezelfde apparatuur gebruikt als bij de assemblage van de zwart-wit-microdisplays. Wanneer men de geassembleerde kleurenfilters onder een microscoop worden bekeken blijken deze goed gealigneerd te zijn ten opzichte van de pixel-elektrodes (Fig. 6.6). De helderheid van het PDLC kleurenmicrodisplay bedraagt 22,5% (Fig. 6.7) wat hoger is in vergelijking met andere reflectieve kleurenbeeldschermen.

6.4 Besluit

Er werd kleurenfiltermateriaal geoptimaliseerd voor PDLC kleurenbeeldschermen. Hierbij wordt de dikte aangepast zodat de UV-transmissie voor de 3 kleuren op elkaar is afgestemd. De UV-belichtingstijd wordt zo gekozen dat de elktro-optische eigenschappen van het PDLC onder de drie verschillende kleuren (rood, groen en blauw) gelijkaardig zijn. Met behulp van deze parameters wordt een kleurenfilterpatroon ontwikkeld dat gebruikt wordt voor de assemblage van microdisplays. Speciale aandacht gaat hierbij uit naar de helderheid van het beeldscherm en de marge voor de aligneringsfout bij assemblage van het tegenglas op de microdisplaychip. Uiteindelijk heeft dit geleidt tot een assemblage van microdisplays met een helderheid van 22,5% wat hoger is in vergelijking met andere reflectieve kleurenbeeldschermen.

7 Personal viewer

De pixels in microdisplays zijn zo klein dat het blote oog niet alle afgebeelde informatie kan waarnemen. Daarom worden er lenzensystemen gebruikt die de afgebeelde informatie moeten vergroten. Voor draagbare toepassingen heet zo'n lenzensysteem een 'pesonal viewer'. De 'pesonal viewer' genereert een virtueel vergroot beeld.

Om de mogelijkheden van PDLC en PNLC microdisplays te demonstreren werd een personal viewer gerealiseerd. Deze bestaat uit 1 standaardlens en 2 spiegels. Voor de analyse en de optimalisatie van de personal viewer wordt gebruik gemaakt van het softwarepakket ZEMAX. De resultaten van de simulaties worden geverifieerd in een tijdelijk opstelling. Dit heeft dan uiteindelijk geleid tot de realisatie van een 'personal viewer'.

8 Innovatieve aspecten van dit doctoraat

Een belangrijk onderdeel van dit doctoraat is de karakterisatie van PDLC en PNLC voor reflectieve beeldschermen met een reflector. Hiervoor werden er 3 meetopstellingen ontworpen en gerealiseerd. Eén meetopstelling wordt gebruikt voor het meten van de elektro-optische eigenschappen van PDLC en PNLC in reflectieve beeldschermen. Met een tweede meetopstelling is het mogelijk de cell gap van het beeldscherm te bepalen met een foutmarge kleiner dan 2%. Voor het meten van de cell gap met deze meetopstelling worden er weinig eisen gesteld aan het vloeibaar kristal beeldscherm. Zo kan de cell gap gemeten worden vóór en na het vullen van het vloeibaar kristal beeldscherm. Het vloeibaar kristal beeldscherm mag transmissief of reflectief zijn. Het elektro-optisch principe van het vloeibaar kristal mag zowel gebaseerd zijn op de polarisatie van licht als op de verstrooiing van licht. Een derde meetopstelling wordt gebruikt om de bruikbaarheid van verschillende types reflectieve beeldschermen te analyseren voor 'direct view'-toepassingen. Deze meetopstelling gebruikt een totaal verschillende benadering in vergelijking met andere gelijkaardige meetopstelling voor transmissieve of emissieve beeldschermen. Dit principe werd reeds overgenomen in commerciële meetopstellingen en in standaarden voor het meten van reflectieve beeldschermen.

Er werd een uitvoerige karakterisatie van PDLC en PNLC voor reflectieve beeldschermen met een reflector gemaakt. Tot op heden wordt PDLC en PNLC vooral gebruikt in transmissieve beeldschermen of reflectieve beeldschermen met een absorberende laag. Over het algemeen kan het elektro-optisch gedrag van het PDLC en PNLC verklaard worden aan de hand van eerder gepubliceerde theoriën. Er zijn echter twee uitzonderingen. Een eerste zijn de karakteristieken ten gevolge van overbelichting en een tweede zijn de karakteristieken bij een cell gap kleiner dan 4μm.

Drie alternatieve PDLC- en PNLC-vulmethodes werden geoptimaliseerd. Behalve de problemen in verband met de blootstelling van PDLC en PNLC aan vacuum zijn er ook problemen met het vullen van de vias en de stabiliteit van de cell gap na het belichten. Men moet hierbij rekening houden dat de cell gap van het beeldscherm slechts 4μm bedraagt. Dit is weinig in vergelijking met de cell gap van andere PDLC en PNLC beeldschermen. Uiteindelijk werden alle problemen opgelost voor alle 3 de vulmethodes.

Er werd een nieuw prinicipe uitgedokterd voor de aansturing van vloeibare kristallen. Met de klassieke aansturing worden de elektro-optische eigenschappen van het vloeibaar kristal beeldscherm gewijzigd door de amplitude van elektrisch veld aan te passen. Met behulp van dit nieuwe principe wordt niet alleen de amplitude maar ook de orientatie van het vloeibaar kristal gewijzigd. Dit principe wordt veldgeorienteerd adresseren genoemd. Met behulp van veldgeorienteerd adresseren is het mogelijk de schakeltijden te reduceren tot niveaus die vereist zijn voor kleurensequentieel adresseren. De schakelspanningen die hiervoor gebruikt moeten worden zijn aanzienlijk lager dan die voor andere kleurensequentiële PDLC beeldschermen.

Kleuren PDLC beeldschermen werden bekomen met behulp van kleurfilters. De UV transmissie voor de 3 basiskleuren werd op elkaar afgesteld. Hierbij is het belangrijk het juiste filtermateriaal te kiezen en filterdikte aan te passen. De parameters voor het belichten met UV worden ook geoptimaliseerd om de electro-optische eigenschappen van het PDLC onder de drie basiskleuren beter op elkaar af te stemmen.

9 Nieuwe uitdagingen

In het kader van dit doctoraat werden er enkele problemen met betrekking tot "Introductie van kleur in reflectieve PDLC en PNLC microdisplays" opgelost. Natuurlijk konden niet alle problemen opgelost worden en zijn er een aantal nieuwe opgedoken. Hier volgt een kort overzicht van enkele van die problemen.

Hoewel reeds een groot deel van de karakterisatie van het PDLC en PNLC is gebeurd, is dit werk nog steeds niet af. Zo kan er nog verder onderzoek gebeuren op het vlak van de hysteresis in PDLC en PNLC en op de DC-spanning die optreedt in reflectieve beeldschermen.

Er werd aangetoond dat veldgeorienteerd adresseren de schakeltijden van PDLC aanzienlijk kan verminderen, zelfs met lage schakelspanningen. Het contrast is voorlopig nog aan de lage kant. Mogelijke pistes voor de verbetering van het contrast zijn reflectieve beeldschermen, optimalisatie van de UV belichtingsparameters, nieuwe PDLC mengsels,… Daar het enkel de bedoeling was na te gaan of veldgeoriënteerd adresseren de schakeltijden kan reduceren, werd er enkel tussen een vertikaal en een horizontaal veld geschakeld. Men kan het elektrisch veld echter ook een oriëntatie geven die tussen de horizontale en de vertikale ligt. Op deze manier zou men grijswaarden kunnen selecteren.

Er werd aangetoond dat met kleurenfilters een reflectief PDLC kleurenbeeldscherm haalbaar is. Het zou echter interessant zijn om kleurenfilters te hebben met een betere UV-transmissie. Op deze manier zou men de karakteristieken van het PDLC onder de verschillende kleurenfilters nog beter op elkaar kunnen afstemmen. Bovendien zou men voor de polymerisatie van PDLC geen lichtbronnen meer moeten gebruiken met een hoge UV-intensiteit.

Tot op heden werd er maar weinig onderzoek verricht naar personal viewers voor PDLC en PNLC beeldschermen. Een groot deel van de patenten met betrekking tot personal viewers heeft te maken met de loodrechte belichting

van het beeldscherm. Dit is belangrijk bij beeldscherm met polarisatoren. Er werd echter aangetoond dat met PDLC en PNLC een goed contrast en hoge helderheid kan bereikt worden bij een niet-loodrechte belichting. Dit kan het ontwerp van de personal viewer sterk vereenvoudigen.

Introduction of color in reflective PDLC and PNLC microdisplays

English text

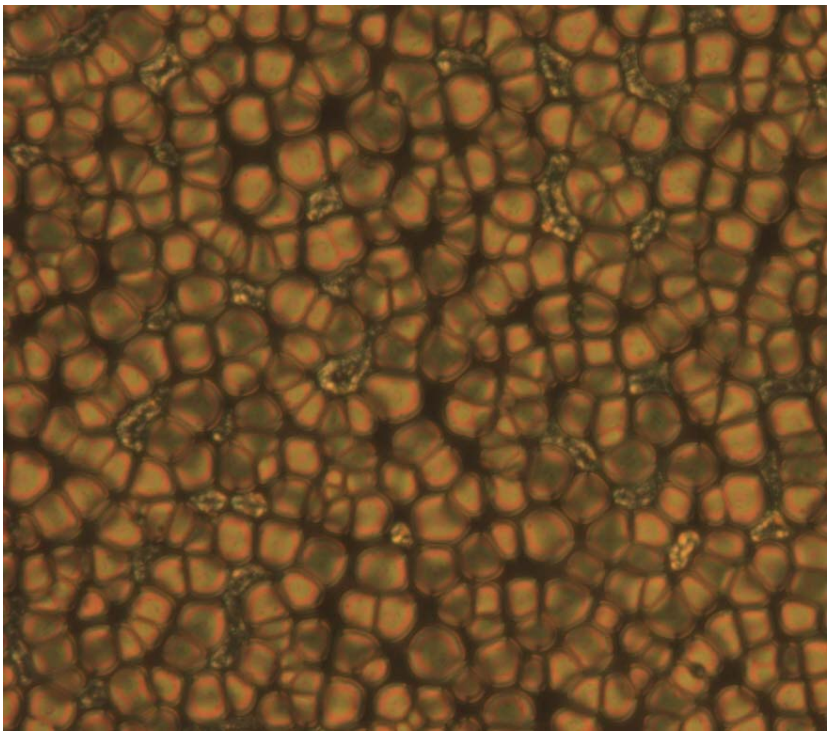

CHAPTER 1:
Relevance of this Ph.D. research

1 Introduction

Microdisplays play an important role in today's display research. These tiny displays are based on a CMOS chip. On top of this chip there is an internal reflector and a liquid crystal layer. The liquid crystals used in this project are Polymer Dispersed Liquid Crystal (PDLC) and Polymer Network Liquid Crystal (PNLC). Displays using PDLC or PNLC don't require polarizers. Therefore, these displays are much brighter compared to displays using polarizers. Unfortunately they also have less greyscales and a lower contrast ratio. The goal of this research project is to develop a full color PDLC or PNLC microdisplay for personal viewer applications. Personal viewers use a lens system to generate an enlarged virtual image. The whole personal viewer has to be small so it can be integrated in small and/or portable applications (view finder in a camcorder, display in a cellular phone, palm top PC, enhanced reality glasses and many more).

The goal of this chapter is to demonstrate the relevance of this Ph.D. research. This Ph.D. is involved in 4 main areas of research. Each paragraph deals with one of these. These include liquid crystals, reflective displays, microdisplays and reflective color displays. The status of these 4 topics is given as it was at the beginning of the research. A present day status is given on topics that do not interfere with the results of this Ph.D. At the end of each paragraph the specific goals of this Ph.D. are briefly discussed.

2 Liquid crystals

2.1 Principle

Liquid crystal (LC) molecules are elongated organic molecules. Their refractive index n and their dielectric constant ε are anisotropic. Because of the anisotropy of n and ε the refractive index experienced by light passing through a LC layer can be controlled by an electric field. To express this anisotropy the refractive index n is represented by a tensor with 3 components (Fig. 1.1). The two components perpendicular to the long axis of the LC molecule have a magnitude n_o. The component parallel to the long axis of the LC molecule has a magnitude n_e. The polarization components of light passing through a LC layer will experience a different refractive index n depending on the orientation of the LC molecules relative to the propagation direction of the incoming light. The orientation of the LC molecules can be controlled in an electronic way due to the anisotropy in ε. ε_o and ε_e are the dielectric constants experienced by an electric field perpendicular and parallel to the long axis of the LC molecules respectively.

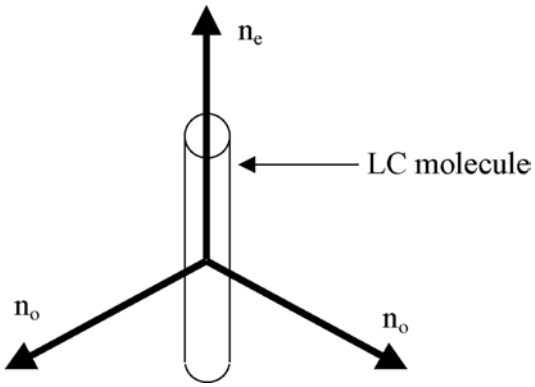

Fig. 1.1: Definition of the refractive indexes of a LC molecule.

When an electric field is applied across the liquid crystal molecules the liquid crystal molecules will align so the free energy density becomes

minimal [1]. In the case the dielectric anisotropy $\Delta\varepsilon=\varepsilon_e-\varepsilon_o > 0$, the liquid crystal molecules will align parallel to the electric field. In the case the dielectric anisotropy $\Delta\varepsilon < 0$, the liquid crystal molecules will align perpendicular to the electric field. In the case there is no electric field across the liquid crystal molecules the liquid crystal molecules will align so the elastic free energy density and anchoring free energy becomes minimal [1]. The elastic free energy describes the deformation of the LC. These include splay, twist and bend. The elastic free energy is determined by the interaction between the liquid crystal and a surface. To control the alignment of the LC in the absence of an electric field alignment layers are used.

The liquid crystal alignment can be controlled by the applied electric field. This means also that the refractive index experienced by incoming light can be controlled by an electric field. Over the years many different liquid crystal materials have been developed. Often each liquid crystal has more than one way of exploiting the electronically switchable refractive index for display applications. A list with all the different liquid crystal and display technologies is beyond the scope of this introduction. One often used technique takes advantage of the difference in polarization between incoming light and light exiting the liquid crystal layer. By putting linear optical polarizers in front and behind the display the light passing the display can be blocked or transmitted depending on the liquid crystal orientation. This technique is often used in transmissive LCDs. Another technique is to switch the liquid crystal between a scattering state and a transparent state. This technique is used in Polymer Dispersed Liquid Crystal (PDLC) and Polymer Network Liquid Crystal (PNLC).

2.2 Polymer Dispersed Liquid Crystal and Polymer Network Liquid Crystal

2.2.1 Introduction

Polymer Dispersed Liquid Crystal (PDLC) and Polymer Network Liquid Crystal (PNLC) have some similarities and differences (Table 1.1). Both LCs are based on the same optical principle: switching the PDLC or PNLC between a transparent and a scattering state. The relationship between the applied electric voltage across the LC layer and the optical properties (scattering / transmission) is similar. Both PDLC and PNLC are a mixture of

differences	similarities
supplier of the materials	optical principle based on scattering
materials	relationship between electric field and optical properties
polymer structure after curing	PIPS

Table 1.1: Differences and similarities between PDLC and PNLC.

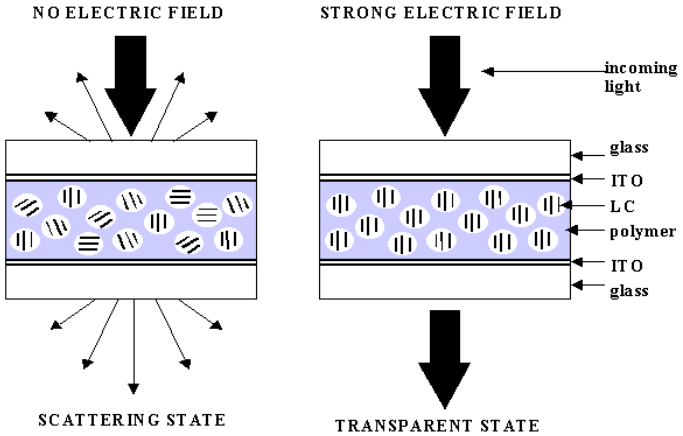

Fig. 1.2: Cross section of PDLC structure demonstrating the optical principle.

LC molecules, monomers and photo-initiators. These mixtures have to be cured with UV to obtain a stable film. During the UV curing the polymerization process starts. This results in a separation between the polymer and the LC molecules. Film formation based on UV curing is known in literature as Photoinitiated Polymerization-Induced Phase Separation (PIPS) [2]. Other film formation processes are Thermally-Induced Phase Separation (TIPS) and Solvent-Induced Phase Separation (SIPS) [2]. In this Ph.D. research the film formation processs is PIPS. The materials for PDLC and PNLC are supplied by two different manufacturers. PDLC is a mixture of the prepolymer PN393 and the LC TL213. The prepolymer and the LC are supplied separately by Merck (Germany and UK). PNLC is supplied as one component by Dainippon Ink and Chemicals (Japan). The polymer structure of the PNLC and PDLC film is different. PDLC consists of a polymer matrix and dispersed in this matrix are droplets of LC (Fig. 1.2). PNLC can be compared with a polymer matrix submerged

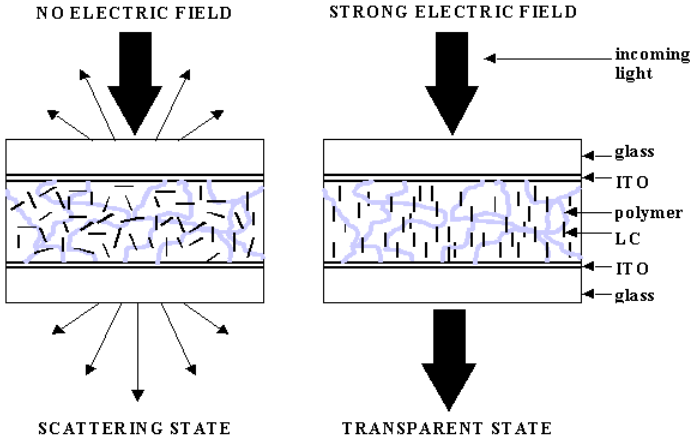

Fig. 1.3: Cross section of PNLC structure demonstrating the optical principle.

in LC molecules. Contrary to the PDLC the LC molecules are a continuous layer (Fig. 1.3). Scattering effects occur at the interface between the LC

molecules and at the interface between the LC molecules and the polymer matrix. Due to the scattering the PDLC and the PNLC have a paper white appearance (Fig. 1.4).

Fig. 1.4: Due to the light scattering this reflective PNLC display has the same appearance as white paper.

2.2.2 Electro-optical properties

The optical principle of PDLC and PNLC is based on the scattering of light. When there is no voltage applied across the PDLC/PNLC film the LC molecules will be randomly aligned in the polymer matrix. This alignment corresponds with the state of minimal elastic free energy density and anchoring free energy [1]. Incoming light will experience a difference in refractive index at the interface between the LC molecules and the polymer matrix and at the interface between neighbouring LC molecules. This results in scattering of light at these interfaces. When an electric field is applied across the PDLC/PNLC film the LC molecules will align parallel to the electric field so the free energy density is minimal [1]. The dielectric anisotropy of the LC molecules in PDLC and PNLC $\Delta\varepsilon$ is positive. Incoming light will experience no difference in refractive index at the different interfaces. In this case the PDLC film or PNLC film is transparent. To have a

good transparent state for the PDLC or PNLC it is important that $n_o=n_p$ with n_o = ordinary refractive index of the LC and n_p=refractive index of the polymer.

The electro-optical properties of the PDLC / PNLC (scattering, contrast ratio, switching time, switching voltage and hysteresis) are determined by the way the PDLC / PNLC film is prepared. First of all there are the materials that are used and the ratio they are mixed in to obtain the PDLC mixture [3-9]. In this Ph.D. study the materials for PDLC are the LC TL213 and the prepolymer is PN393. Parameters that control the way the PIPS takes place are the temperature, the UV intensity and the UV cure time [6-10]. This determines the polymer structure in the PDLC / PNLC and the electro-optical properties of the PDLC / PNLC. The result is a wide window for the PDLC and PNLC process parameters resulting in PDLC / PNLC with different properties.

The cell gap of the display also plays an important role in the electro-optical properties of the PDLC and PNLC [6,8,9]. The cell gap is the thickness of the PDLC or PNLC layer. The bigger the cell gap is the higher the voltage will have to be to obtain an electric field with a certain magnitude between the electrode on the cover glass and the electrode on the backplane. This influences for instance the magnitude of the switching voltages. The bigger the cell gap is the thicker the scattering PDLC or PNLC layer will be. This has an influence on the reflectance of the display.

2.2.3 Display configurations

In general PDLC and PNLC are used in 3 different display configurations: transmissive display, reflective display with an absorber and reflective display with a reflector. These display configurations are discussed in the next paragraph on “Reflective liquid crystal displays”.

2.3 Goals of this Ph.D. research

The first aim of this Ph.D. is to analyze and optimize the PDLC and PNLC for reflective displays with a reflector. So far research has been focussed on transmissive and reflective displays with an absorber. The parameters that will be analyzed are the cell gap of the display and the UV curing parameters (cure time and UV intensity). The optimization of PDLC and PNLC for reflective displays is a first step towards the optimization of reflective PDLC and PNLC microdisplays. By using a reflector electrode the scattering of the PDLC and PNLC will be high for small cell gaps. This will allow a reduction of the switching voltage to levels compatible with microdisplays.

3 Reflective liquid crystal displays

3.1 Introduction

Transmissive LCDs are not ideally suited for low power mobile applications because they require a backlight. Eliminating this backlight reduces the power consumption from a few watts to less than 100mW and reduces the size and weight of the display. The ideal display for mobile applications would require only environmental light as light source. This is the ultimate goal of reflective displays. The challenge for these displays is to have a high brightness and contrast ratio for a wide range of viewing angles and for different types of illumination. A general definition of the contrast ratio is the ratio of the luminance of the bright state of the display to the luminance of the dark state of the display. The definition used in this Ph.D. will be discussed in more detail in paragraph 2.2: "Measurement of the opto-electrical characteristics of PDLC and PNLC". To reach these objectives the display must use incoming light in the most efficient way. Research focuses on different LC technologies and reflector types to improve the reflectance, the contrast ratio and the viewing angle of the display. In the rest of this paragraph some of these technologies will be discussed. The reflective displays can be classified [11,12] based on the number of polarizers the display has (0, 1 or 2) and whether color displays have color filters or not. The general idea is that displays using 2 polarizers have the highest contrast ratio but lowest brightness. Displays without polarizers (zero polarizer displays) have the highest brightness but the lowest contrast ratio. The characteristics of displays with only 1 polarizer are somewhere inbetween the zero polarizer and 2 polarizer displays [13].

3.2 Reflective liquid crystal displays using polarizers

When moving from transmissive to reflective LCDs the most straightforward solution is to use a reflective electrode instead of a transmissive electrode on the backplane of the LCD. In this case only small adaptations have to be made to make the conventional Twisted Nematic (TN) and Super TN (STN) technology with 2 polarizers for transmissive LCDs compatible with reflective LCDs (Fig. 1.5). However a disadvantage of this approach is the low display brightness. The polarizers alone absorb at least 55% of the light [14].

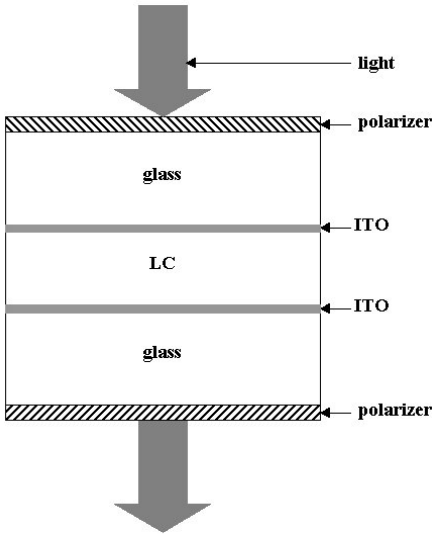

Fig. 1.5: Cross section showing the position of the polarizers in a transmissive LCD.

Another problem is that full color reflective LCDs using this technology require color filters. This will reduce the brightness of the display even further. An alternative method has been proposed for reflective color STN displays [15] without using color filters. In this case the birefringence Δn of a STN with a high retardation Δn * d (d is the cell gap of the display) is

electrically controlled (Electronically Controlled Birefringence or ECB mode). The disadvantage of the ECB mode is that the color capability is limited to about 4 colors [12] and color purity is not satisfactory [11].

In the case of a 2 polarizer display one of the polarizers is between the LC layer and the reflector. This results in parallax making this technology useless for high resolution displays. This problem doesn't occur in single polarizer reflective displays. By eliminating one of the polarizers the brightness of the display is also potentially higher. Single polarizer reflective displays are used for projection and direct view applications. For projection applications short switching times and a high contrast ratio are of key importance. For direct view applications a high brightness and contrast ratio for a wide viewing angle are important. Numerous LC modes are used for single polarizer reflective displays. Amongst others are hybrid-aligned nematic (HAN), dynamic-aligned nematic (DAP), optically compensated bend cells (OCB), hybrid field effect (HFE), mixed twisted nematic (MTN), self compensated twisted nematic (SCTN), twisted nematic (TN),... A description of these modes can be found in [11,12,16-19].

Reflective displays using polarizers generally only have a good contrast and brightness in the specular reflection direction. This is the reflection direction that has the same angle to the normal on the reflecting surface as the incoming light (Fig. 1.6). To increase the range of viewing angles with a good display contrast and brightness the reflected light is made more diffuse. The diffuse reflections are all the reflections different from the specular reflection. This can be done by using a diffuser on top of the cover glass [20-21] or by using rough surface reflector electrodes [22-23] (Fig. 1.6). The resulting light scattering will improve the brightness of the display in the non specular reflection directions. In the case of flat reflector electrodes the specular reflection on the cover glass coincides with the direction of maximum image contrast and brightness. Tilting the reflectors will result in a difference between these two directions (angle α in Fig. 1.7). This increases the image contrast [22-23].

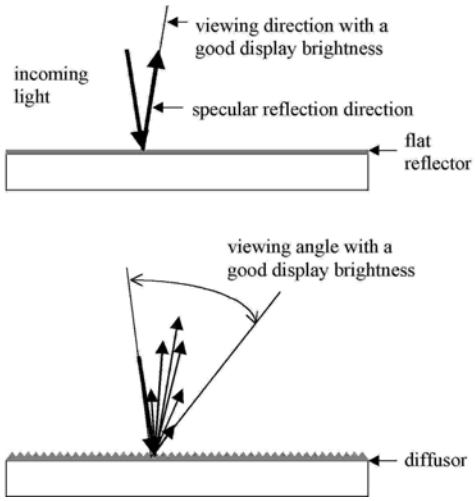

Fig. 1.6: When a display has a diffusor electrode light is reflected in directions different from the specular reflection direction. This increases the range of viewing angles with a good brightness compared to displays with a flat reflector electrode.

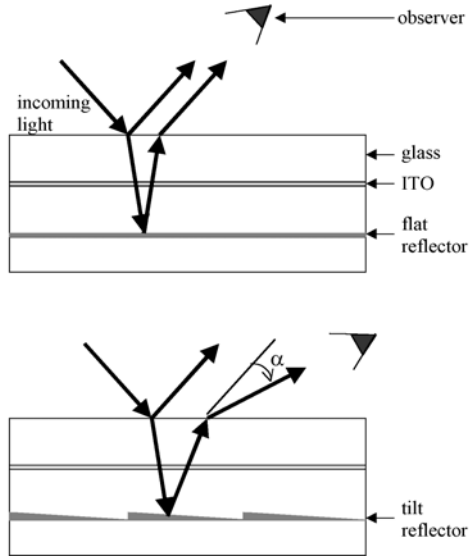

Fig. 1.7: By giving the reflector a tilt angle light modulated by the LC is reflected in a direction different from the reflections on the cover glass. This improves the contrast ratio in the direction with maximum image reflectance.

3.3 Polarizer-free reflective displays

Polarizer-free reflective displays typically have a high brightness but limited contrast. There are two different types of polarizer-free reflective displays: guest-host systems and scattering systems [11,12,14]. Guest host systems consist of a mixture of liquid crystal and dye with anisotropic absorption. The dye will align with the liquid crystal molecules. Depending on the alignment of the dye relative to the incoming light the incoming light will be transmitted or absorbed. In the case the dye is black a single display can switch between black and white. A full color display is obtained using color filters. In the case the dye has a color, a single display switches between white and color. Full color is obtained by stacking three single color displays [24].

There are two different scattering systems. On one hand there is cholesteric texture (chiral nematic) [14, 25-28] and on the other hand there is polymer dispersed liquid crystal. PNLC is also classified as a PDLC type of LC. Cholesteric texture has stable states at 0V. This is very favourable for the energy consumption of the display. Typical for cholesteric texture is that the LC molecules spontaneously form a helix. The axis of this helix is perpendicular to the axis of the LC molecules. One of the stable states is the planar cholesteric texture. In this case the axis of the helixes are perpendicular to the cover glass. The cholesteric texture will reflect one of the circular polarizations of the incoming light parallel with the helix axis. The reflected light has a wavelength $\lambda_r=n_aP$ with n_a=average refractive index of the cholesteric texture and P=pitch of the cholesteric texture helix. The wavelength bandwidth is $\Delta\lambda_r=\Delta nP$ with Δn=refractive index anisotropy of the cholesteric texture. The other circular polarization is transmitted by the cholesteric texture. Another stable state is the focal-conic texture. In this case the axis of the helices are aligned parallel to the cover glass and the cholesteric texture is slightly scattering. When the back plane of the display has a black absorber the focal-conic state of the cholesteric texture will

correspond with the dark state of the display. The transmitted circular polarization of the incoming light will also be absorbed by the backplane. There is also a third stable state: homeotropic texture. In this state the helix is unwound by external forces. Switching between two stable states is not as straightforward as with other LCs [26-27]. The waveform one has to apply depends on the current state and the desired state of the cholesteric texture. The switching voltages are also rather high although these problems can be solved using the appropriate driving electronics [29]. Two other disadvantages of cholesteric texture are the long switching times and the small wavelength bandwidth $\Delta\lambda_r$. These problems are partially solved by stabilizing the planar state of the cholesteric texture. The stabilization is achieved by a polymer network in the cholesteric texture (Polymer Stabilized Cholesteric Texture or PSCT) or by modifying the cell surface (Surface Stabilized Cholesteric Texture or SSCT). The stabilization of the planar state will reduce the switching time from the focal conic or homeotropic state. The modification of the cell surface (in the case of SSCT) or the introduction of a polymer network (in the case of PSCT) will cause some defects in the orientation of the helix axis. Not all helix' axis will be perpendicular to the cover glass. This will result in a broader wavelength bandwidth $\Delta\lambda_r$ but with a smaller peak. The color of the display will always be viewing angle dependent.

The optical principle of PDLC and PNLC has already been explained in paragraph 2.2. Reflective PDLC or PNLC displays have either an absorber or a reflector on the back plane of the display. In the case of an absorber only the light reflected by the PDLC (or PNLC) layer in the scattering state will reach the observer. In the case the absorber is replaced by a reflector the light transmitted by the PDLC in the scattering state will be reflected and pass the PDLC layer for a second time. The reflected light will be scattered once again. The reflective PDLC (or PNLC) displays with a reflector will have a much higher brightness. The brightness of the reflective displays with an absorber can be increased by increasing the cell gap of the display. This

will result in a higher switching voltage. The cell gap of reflective displays with a reflector can be very small without reducing the reflectance of the PDLC too much. As a consequence the switching voltage will be relatively low. The use of an absorber has the advantage of having a good dark state. This is not the case when using a reflector. As a consequence the contrast of display with a reflector will have a different dependency on the viewing angle and the type of illumination than the contrast of a display with and absorber. It is important for reflective displays to have PDLC with low switching voltages and high brightness and contrast.

3.4 Goals of this Ph.D. research

So far many of the measurements on the contrast ratio and brightness of reflective displays are done using measurement set ups for transmissive displays. This is not a good approach. Depending on the environment the reflective display has different types of illumination. The observer may also be blocking the illumination of the display especially in the case of mobile applications where the observer is close to the display. All these factors influence the contrast ratio and brightness of the display. During this Ph.D. research a method for analyzing the applicability of reflective displays has been determined. The contrast and brightness of the display are of special importance to determine the applicability. This measurement set up should allow us to determine the criteria for a high contrast in the case of reflective PDLC or PNLC displays with a reflector.

4 Microdisplays

4.1 Introduction

Microdisplays combine mature technologies of two different industries. On one hand there is the display industry and on the other hand there is the semiconductor industry. The technology used in microdisplays is already mature and both industries have the technology available in high volume end products. This reduces the development costs and the investment costs in production lines for microdisplays and microdisplay applications.

Besides the investment benefits microdisplays also have some technical benefits compared to other display technologies. Microdisplays use CMOS technology for the active matrix on the back plane of the display. CMOS allows the pixel size to be reduced to less than 15µm. Small size high resolution displays can be achieved using this technology. A 2560X2048 pixel microdisplay with an active display area of 38.4mm by 30.72mm has already been demonstrated [30]. However most microdisplays have a resolution of QVGA (120 by 160 pixels) to SXGA (1280 by 1024 pixels) with a dimension of 5X5mm^2 to 20X15mm^2 [31]. Another advantage is the high switching speed of CMOS compared to TFT. TFT technology is used in LCDs. Microdisplays use a reflective electrode while the electrode in LCDs is transmissive. The exception is the microdisplay technology of Kopin [31]. Reflective electrodes allow the transistors to be under the electrode. This increases the aperture ratio of the pixel compared to the aperture ratio of pixels for transmissive displays. The aperture ratio of a pixel is the ratio of the surface of the pixel used for displaying information to the physical surface of the pixel. The aperture ratio doesn't equal 1 due to the required insulator gaps between pixels. In the case of transmissive displays the pixel transistors have to be shielded to prevent photo current from being generated in the transistor. This pixel area where the light shield is, is always black reducing the aperture ratio. In microdisplays the via connecting the reflector

electrode with the underlying transistor is also visible and reduces the area for displaying information. However the aperture ratio of microdisplays (>95%) should be much higher than the aperture ratio of LCDs (70-80%) [35]. A higher aperture ratio means a higher optical efficiency for the display. The use of CMOS in the back plane of the display allows the integration of part of the driver electronics on the back plane of the display [32,33]. The power consumption of microdisplays is low. The power consumption is about 10mW for a mono color VGA (640 by 480 pixels) microdisplay and about 250mW for a SXGA full color microdisplay [31].

The small pixel size doesn't allow the naked eye to resolve all the information displayed on microdisplays. An optical system is required to enlarge the displayed information. The optical systems are either for personal viewer systems or for projector systems. In the case of personal viewer systems the optics create an enlarged virtual image. Personal viewer systems are typically used in mobile applications [34]. Important requirements for personal viewer systems are low weight, compact dimensions and ease of use. In the case of a projector system the optics create an enlarged real image. This image is projected on a screen. The observer can be either on the same side of the screen as the projector (front projector) or on the other side the screen (rear projector). Projector systems are typically used for high resolution and large area displays. High contrast and high optical efficiency are important parameters for projector systems. Resolution and contrast requirements are typically lower for personal viewer systems.

Although microdisplays all use CMOS technology for the active matrix the optical principle for displaying the information may be different. In the case of Liquid Crystal On Silicon or LCOS a liquid crystal layer is put on top of the silicon back plane. This is the type of microdisplays that are used in this Ph.D. research. Some other microdisplay technologies are mentioned here. An elaborate discussion of these technologies is beyond the scope of this introduction. In recent years Organic Light Emitting Diode or OLED on

silicon has evolved to an other promising microdisplay technology [35]. Another important microdisplay technology is the Digital Mircomirror Device™ or DMD™ of Texas Instruments™. This technology is promising for high end projection systems like digital cinema [36]. By flipping the micromirrors the light is either reflected or not reflected onto the projection screen.

Although LCOS combines two mature technologies, CMOS and LC, there are still some challenges to be overcome before LCOS itself can be considered a mature technology. These challenges are discussed in the next paragraph.

4.2 Challenges of LCOS

4.2.1 Technological challenges

When bringing CMOS and LC together in LCOS there are still some problems that have to be solved to make LCOS successful. First of all there are some technological problems concerning the silicon back plane of the microdisplay that can not be solved with standard CMOS [32, 33, 37-40]. Some of these problems are discussed in this paragraph. A first problem is that the silicon back plane requires reflective electrodes. These reflective electrodes must have a high reflectivity, be very flat and have a high aperture

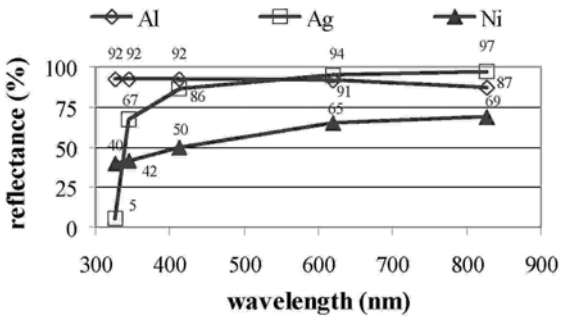

Fig. 1.8: Reflectivity of Al, Ag and Ni.

ratio to have a microdisplay with a good optical efficiency. Al or an Al(Cu) alloy is generally used as material for the reflector electrode [41,42]. These materials are commonly used in semiconductor metallizations and have a high reflectivity. Al has an average reflectivity of about 92% for wavelengths in the visible range. The reflectivity of Al(Cu) alloys is even somewhat higher in the red spectrum of the light. The reflectivity of other metals like Ag and Ni is not as interesting as that of Al or Al(Cu) (Fig. 1.8) [43]. The reflectivity of Ni is less in the visual range. The reflectivity of Ag varies more than the reflectivity of Al in the visual range. Ag has a better reflectivity in the red spectrum but less reflectivity in the blue spectrum.

There are several techniques to improve the flatness of the mirror electrodes. Some are done in the foundry, others are done outside the foundry. An in-foundry-solution is the Chemical Mechanical Polishing of the insulator layers under the Al reflector electrode [30,38,41,42]. Besides CMP a photo-definable organic layer under the Al reflector electrode can be used as a planarization layer. Benzocyclobutene (BCB) [40] and polyimide [32] (Fig. 1.9) have proven to be suitable materials for this layer. The processing of

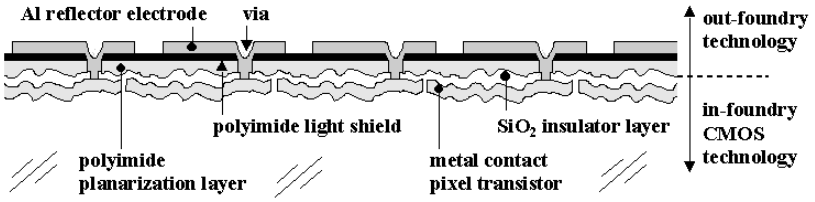

Fig. 1.9: Cross section of a microdisplay backplane with a polyimide planarization layer and light shield.

these layers is done outside the foundry. Both in-foundry and out-foundry techniques have proven to be very successful for the planarization of the reflector electrodes on a mirror scale. These techniques are not sufficient to have a flat backplane. The surface profile depends on the circuit design. The back plane will be thicker in areas with a high circuit density (active matrix and bonding pads) [31]. Another problem is the bow in the silicon die [44].

A part of the bow is inherently present in the naked silicon die. Another part of the bow is caused by the high temperature steps and the deposition of thin films during the manufacturing process. The surface profile caused by the circuit density is partly solved by adding dummy structures in the circuit and by an etch-back compensation step in the CMP step [31]. The flatness of the backplane on a die scale is important for LC that requires an uniform cell gap like Ferro-electric LC and to prevent a reduced contrast and optical throughput [45].

The back plane of a microdisplays also requires a light shield. This light shield prevents photo-currents to be induced in the transistors under the reflector electrodes. The microdisplays are exposed to high luminances especially in projector applications. The light shield is often a TiN layer [41-42,46] in combination with a labyrinth structure [30]. Another solution is the use of a polyimide layer (Fig. 1.9) [32,45].

The standard CMOS voltage is 3.3V or 5V. LCs require an analogue voltage in the range of $5V_{rms}$ to $10V_{rms}$. The exception is ferroelectric LC that uses digital driving voltages. This means that the standard CMOS technology has to be adapted to meet the requirements of the high voltage analogue LC driving voltage [30-33, 47].

4.2.2 Electro-optical challenges

There are some electro-optical effects due to the typical layout of the microdisplay. These will be discussed in the rest of the paragraph. In a LC display or microdisplay it is important to have a uniform cell gap across the display area. This is done by spraying or spinning spacers on the cover glass of the LCD. These spacers are in general plastic or glass rods or spheres with a diameter equal to the desired cell gap. This method can also be applied in LCOS. However one has to bare in mind that the pixel size in LCOS is considerably smaller than in conventional LCDs. The area on an active matrix consumed by a 4μm spacer can be neglected to the total area of a LCD pixel (>100μm). This is not the case for LCOS pixels (typically order

of 15μm). Another solution that has been suggested is to process SiO_2 spacers on the back plane of the microdisplay [41,42]. These spacers also reduce the display quality. There is also an assembly method where no spacers are on the active matrix of the microdisplay. BCB materials are used for this method [40]. The BCB material is patterned on top of the silicon back plane. It is not only used as a spacer material but also for the sealing of the LCOS. Since the patterning is very accurate the sealing ring can be patterned very close to the active matrix of the microdisplay. Compared to the sealing methods used in the assembly of LCDs this sealing ring consumes much less space reducing the required silicon area and back plane cost. The downturn of this 'spacerless' method is that the uniformity of the cell gap depends on the flatness of the cover glass and silicon backplane. The flatness of the silicon backplane is sometimes a problem [44].

As previously discussed LCOS has small pixels (typical size of 15μm) with a small insulator gap separating neighbouring pixels. When one pixel is switched on and a neighbouring pixel is switched off there will be a large electric field between these neighbouring pixels [48,49]. The occurrence of this electric field is called the fringe field effect. This electric field can be large compared to the vertical electric field between the pixel electrode on the back plane and the ITO electrode on the cover glass. Because the fringe field is not vertical but starts and ends on top of the neighbouring pixel electrodes, the fringe field has some negative effects on the optical properties of the display. Due to the fringe field the edge of a dark pixel adjacent to a white pixel will appear white and the edge of a white pixel adjacent to a dark pixel will appear dark. This leads to a reduction of the effective aperture ratio and hence of the contrast. Due to the fringe field some of the LC molecules may be differently aligned compared to LC in the centre of the electrode. In this case it is possible that the LC first passes a black state before reaching a white state. Because the LC starts from an intermediate state this transition will be rather slow compared to the rest of the LC in the rest of the pixel. It may appear that it is difficult to switch the new

information on a part of the pixel and that the old information sticks on the pixel. This is why this phenomenon is called image sticking. Because the LC switching in the domain affected by the fringe field is rather slow this may also result in flicker. Flicker occurs when the eye detects that the grey states of the LC are not stable during one frame. The fringe field effect can be reduced by reducing the cell gap.

Another problem in microdisplays and in reflective displays in general is the presence of a DC electric field across the cell gap. Due to this DC field the image is not stable but flickers. The reason for the flicker is that the optical response of the LC for the positive driving voltage is different from the optical response for the negative driving voltage. During the positive driving voltage V the optical response will correspond with the optical response when a voltage $V + V_{dc}$ is applied in a display with no DC voltage. During the negative driving voltage -V the optical response will correspond with the optical response when a voltage $-V + V_{dc}$ is applied in a display with no DC voltage. An increase of the refresh rate will reduce the flicker. In this case the contrast of the display will be reduced and the power consumption will rise. Flicker is also reduced by using row inversion, column inversion or pixel inversion instead of frame inversion. The optical response of the LC is a function of the rms value of the applied voltage. The DC component of the applied voltage has to be zero. Suppose the LC in the display has to be in a state that corresponds with an applied voltage of +V volts and the back plane potential is V_{BP}. In the case of frame inversion the pixels in the display will have during one frame an applied voltage of $V_{BP}+V$ and in the next frame an applied voltage of $V_{BP}-V$. In the case of row inversion during one frame the pixels in the even rows will have an applied voltage of $V_{BP}+V$ and the pixels in the uneven rows will have an applied voltage of $V_{BP}-V$. During the next frame the pixels in the even rows will have an applied voltage of $V_{BP}-V$ and the pixels in the uneven rows will have an applied voltage of $V_{BP}+V$. On a pixel level the flicker will be just as bad as with frame inversion. However an eye looking at a display with row inversion will experience less flicker

because the flicker in the even rows compensates for the flicker in the uneven rows. Column and pixel inversion is the same as row inversion but than for columns and pixels respectively. A disadvantage of the column, row and pixel inversion is an increase in the fringe field effect. Besides the flicker the DC voltage also causes image sticking. This is not solved by column, row or pixel inversion.

4.3 Goals of this Ph.D. research

In this Ph.D. a literature study will be made on different materials for the mirror electrodes. Another topic is to identify the reason for the DC voltage in reflective displays and suggest ways to solve this problem. Assembly and filling methods for PDLC and PNLC microdisplays will be analyzed and optimized. Finally an optical system has to be designed and built to demonstrate the possibilities of microdisplays for personal viewer applications.

5 Reflective color displays

5.1 Introduction

There are many ways to obtain reflective color displays. So far there is no straightforward method. Each LC technology has its own preferred approach for color displays. In this section the author wishes to give a short overview of some of the techniques for reflective color displays.

5.2 Color filters

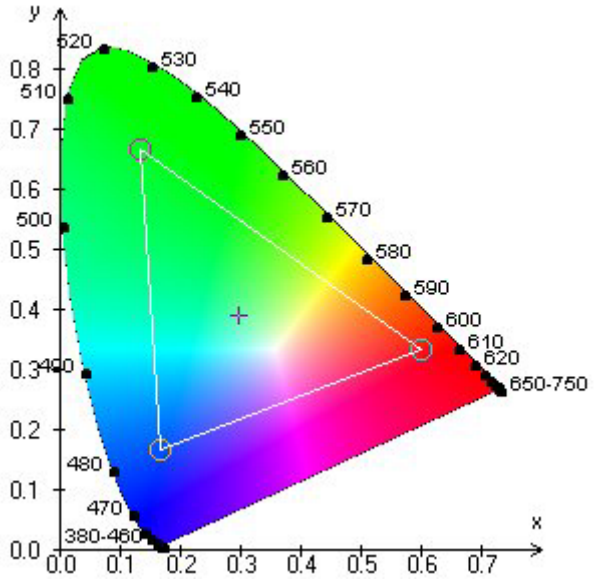

Fig. 1.10: The color range of a display is represented by the area inside the triangle in the chromaticity diagram. The color wavelengths are at the edge of the diagram in nm.

The standard way to obtain color in LCDs is by using color filters [50-55]. In this case each pixel consists of 3 subpixels. On top of each subpixel there is a color filter for one of the 3 base colors. The three base colors are red, green and blue or cyan, magenta and yellow. Each subpixel controls the intensity

of one of the base colors. The range of colors one can obtain with one set of base colors is represented in the chromaticity diagram [56]. The colors that can be produced by a set of color filters are the colors that are in the triangle of which the corners are determined by the base colors. The higher the color purity of the color filters are, the bigger the triangle will be so the more colors can be produced by the color filter set.

The operation principle of color filters is based on the absorption and transmission of light. Red color filters transmit the red light and absorb the other light. The higher the color purity of a color filter the more light the color filter will absorb so the darker the displays will be. This is an important disadvantage of color filters. In transmissive LCDs this problem can be compensated by using a backlight with a higher light output. In the case of reflective displays this can not be compensated since no light sources are used. In the case of transmissive displays a black matrix is applied. The black matrix prevents light from passing through the display in the gaps between the color filters and reaching the observer without being filtered. This is to prevent a reduction in color purity and contrast. In reflective displays a black matrix is not used because this would reduce the reflectivity of the display. For reflective displays a high reflectivity has a higher priority than color purity. Because a high reflectivity is a priority for reflective displays, manufacturers have developed special color filter material for reflective displays. The spectrum for red, green and blue are overlapping each other more than for transmissive LCDs and have a higher transmittance in their respective color spectrum. This will be discussed in more detail in the chapter 6: “Color displays using color filters”.

5.3 Color displays using diffraction of light

5.3.1 Principle

In this paragraph we discuss some technologies that use diffraction of light for color displays. The principle of these technologies is basically the same:

a grating that consist of 2 materials with different refractive index. At the interface of the consecutive layers in the grating light will be reflected. This will result in a color separation of the incoming white light (Fig. 1.11).

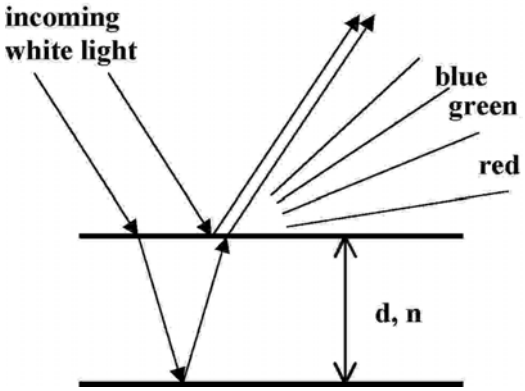

Fig. 1.11: Color separation of white light due to diffraction.

The color detected by an observer depends on the structure of the grating, the angle of incidence of the light, the angle of reflectance of the light and the refractive index of the material between the reflecting interfaces. When the grating consists of 2 reflecting interfaces on a distance d and a material with refractive index n between these layers then the wavelength of the reflected light λ in case of perpendicular illumination of the grating will be $\lambda=2nd$. The advantage of diffraction is the high color purity. The disadvantage is that observed color depends on the viewing angle. When the viewing angle equals θ and θ is relative to the normal on the grating then the detected light has a wavelength $\lambda=2nd\cos\theta$. In the case the display is in a personal viewer or a projector the dependency on the viewing angle is not important because the viewing angle is fixed.

5.3.2 Holographic Optical Elements

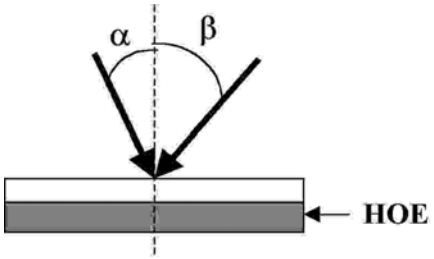

Fig. 1.12: The angles of the laser beams during curing of the HOE determine the angle of illumination and the angle of reflection.

The processing of Holographic Optical Elements (HOEs) starts with the curing of a photopolymer using 2 laserbeams [58-60] (Fig. 1.12). The first laser beam is the reference laser beam. The reference laser beam determines the angle for the illumination of the display. The second laser beam determines the angle of reflection and the reflection cone of the desired LCD reflection pattern. The two laser beams interfere. Where there is a constructive interference there is a strong curing of the photopolymer. In places with a destructive interference there is a weak curing of the photopolymer. In this way successive layers are created with a high and a low refractive index. The reflection of the light occurs at the interface of these layers. Dupont has developed 2 types of HOEs: transmissive HOEs and reflective HOEs.

An important advantage of reflective HOEs is that the angle of reflection for the image can be different from the specular reflections on the cover glass. This is especially important for reflective displays using TN type liquid crystals. In this way the viewing angle with the highest contrast coincides with the angle with the highest reflectance. When metallic reflectors are used for the display, the light reflected by the reflector is reflected in the same direction as the light reflected by the cover glass (Fig. 1.7). The specular reflection on the cover glass is not modulated by the liquid crystal and therefore results in a reduction of the contrast in the specular reflection

direction. By using a holographic reflector the contrast can be 70% higher [58] in the specular reflection direction of the holographic reflector compared to a display with a metallic reflector. This is because reflected light always consists of a diffuse component and a specular component. In the case of a holographic reflector the diffuse component of the reflected light is more concentrated around the specular reflection direction. As a consequence the reflectance in the specular reflection direction of a display using HOE reflectors can be 2 to 3 times [58] the reflectance of a display using metallic reflectors. The improvement in contrast and reflectance in the specular reflection direction is smaller for diffuse illumination. Some applications using HOEs show that viewing angle dependency of the reflectance, contrast and color spectrum is not very critical. Portable applications using HOEs have been developed by Sanyo and Motorola.

When using transmissive HOEs the direction of transmission depends on the wavelength and on the position. In this way it is possible to diffract the light reaching one pixel into its different color components red, green and blue. The different components are transmitted to one of the three subpixels. All the white light reaching one pixel is used in an effective way. This principle is interesting for projector applications.

5.3.3 Holographic PDLC and PNLC

In the case of holographic PDLC (HPDLC) or holographic PNLC (HPNLC) the diffractive grating is inside the PDLC or PNLC layer [61-68]. A cross section of the HPDLC or HPNLC shows consecutive layers of polymer and

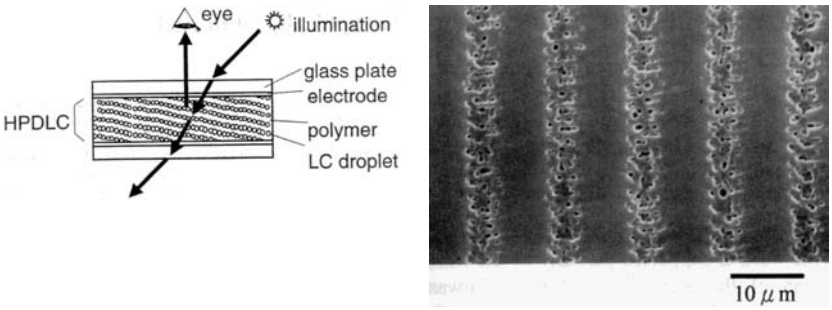

Fig. 1.13: Cross section of a HPDLC display (left) [67] and of a HDPLC layer (right) [63] showing the grating of consecutive polymer and LC droplet layers.

liquid crystal droplets (Fig. 1.13). When no voltage is applied across the HPDLC layer the liquid crystal in the droplets is randomly aligned. The difference in refractive index between the polymer and the grating of liquid crystal droplets results in diffraction of light. When there is a voltage across the display the liquid crystal molecules align parallel to the electric field. Incoming light experiences no difference in refractive index resulting in a transparent layer.

HPDLC is processed in a similar way as HOEs. The PDLC is cured with 2 identical laser beams. The prepolymer is cured in the places in the PDLC layer where there is positive interference between the 2 laser beams resulting in a polymer layer. Droplets with LC are formed in the places where there is destructive interference between the 2 laser beams. By changing the angle between the 2 laserbeams one can change the periodicity of the consecutive layers. By changing the angle of incidence of the 2 laser beams one can change the angle of the consecutive layers with the cover glass. This changes the angle of specular reflection for the incoming light on the HPDLC layer. The specular reflection direction on the cover glass is different from the specular reflection direction on the HPDLC layer. This increases the contrast in the direction with maximum reflectance. The periodicity of the different layers can also be changed by changing the wavelength of the laser beams.

The photo initiator in the prepolymer that starts the polymerization process has to be sensitive to the laser wavelength.

HPDLC has some disadvantages. The switching voltage is considerably higher compared to monochromatic PDLC displays. Switching voltages of 50V and higher for HPDLC are no exception. The switching voltage of monochromatic PDLC has an order of magnitude of about 5V. To achieve a full color reflective displays the display will consist of 3 stacked displays. Each of these displays will display the information for one of the 3 base colors. This is complex from a technological point of view and will be expensive because the display consists of 3 stacked displays. Parallax may also be a problem with stacked displays. In this case light modulated by one pixel is reflected or transmitted in the pixel area of a neighbouring pixel. This is especially a problem when not looking perpendicularly to the display. The effect is minimized by using thin glass substrates for the stacked displays. Companies like IBM have already demonstrated stacked displays [69]. The parallax effect is rather limited. The advantage of stacked displays is that no light is lost during the color separation.

5.3.4 Dielectric mirrors

Dielectric mirrors consist of different dielectric layers. Depending on the refractive index and the thickness of these layers a part of the light spectrum is reflected. The other part is transmitted. The advantage of the dielectric mirrors is the high color purity compared to color filters. They are also chemically and thermally very stable. Pixels with a dimension of 48μm by 130μm with a spacing between the pixels of 1μm have already been demonstrated [70]. This can be done by electron beam evaporation of SiO_2 and TiO_2 layers. The use of these mirrors in mono color reflective PDLC displays has already been demonstrated [71]. The dielectric mirror is on the backplane of the display. The display is white when the PDLC is scattering and has a color when the PDLC is transparent. In this case the display color is determined by the color that is transmitted by the dielectric mirror. Behind

the dielectric mirror there is a diffuser reflecting the transmitted spectrum. It is not easy to have a diffuser with on top of it flat dielectric layers. A transparent ITO electrode on top of the dielectric mirror is connected to the underlying transistors by a via.

5.3.5 Diffractive mirrors

When using diffractive mirrors the reflective electrodes are grid shaped. Reflective PDLC microdisplays using this technology have already been demonstrated [72]. This requires an etching process with an accuracy of a couple of 10nm. This is not evident.

5.4 Color sequential addressing

The information for the 3 base colors is simultaneously displayed when using color filters or diffraction of light. In the case of color sequential addressing the information for the 3 base colors is displayed in 3 consecutive time slots [73-77]. Once the display has switched to the appropriate grey levels for one of the composing colors the display is flashed with a LED (Light Emitting Diode) of the respective color. This is repeated for the other two composing colors. If the time slots are short enough (≈7ms) the interpretation of the information on the image by the eye will be the addition of the information on the 3 color images. The result is that the eye detects a full color image. LEDs are relatively simple components, meet the addressing speed required for color sequential addressing and have a high color purity with a high intensity.

The advantage of color sequential addressing is that each pixel doesn't have to be divided in subpixels. In this way a higher pixel resolution is achieved with the same display dimensions. The aperture ratio of the display will also be higher. A higher aperture ratio is beneficial for a higher display reflectance.

The disadvantage of color sequential addressing is that the principle only works when the time slots for displaying the information of each color are

sufficiently short. In the case the display refresh rate is 50Hz, this is a common display refresh rate, a new full color image is displayed every 20ms. This means that the time slot for displaying one color is about 6.7ms. So far only ferro-electric and TN type of LCs have switching times that allow this refresh rate. Color sequential addressing is not a problem for Digital Micromirror Devices (DMDs) of Texas Instruments or for Thin-film Mircomirror Arrays (TMAs) of Daewoo [78-79]. The switching speed of these display technologies is high enough to achieve grey scaling using digital addressing.

5.5 Goals of this Ph.D. research

After the PDLC and PNLC have been optimized for mono color reflective displays this Ph.D. will focus on full color reflective PDLC and PNLC microdisplays. The results of two different technologies will be discussed. One technology is based on color filters and the other is based on color sequential addressing. To reduce the switching times of PDLC and PNLC to levels compatible with color sequential addressing a new driving technique is used called Field Oriented Addressing.

6 Conclusion

First of all, the electro-optical properties of PDLC and PNLC test cells will be analyzed. This analysis has to point out the relationship between the display parameters (such as cell gap, UV parameters during curing, the cell assembly, the used filling process, DC voltage) and the display criteria (such as contrast ratio, switching voltage, switching time, hysteresis effect and brightness) in order to be able to optimize the display criteria. For this analysis three measuring set-ups are built. One measurement set-up is used to test the applicability of reflective displays in real life situations using only environmental light. Another measurement set-up is used to determine the cell gap of the displays. A third is used to measure the electro-optical properties of the PDLC and PNLC. Once the relationship between the display parameters and the display criteria has been determined this knowledge will be used to optimize the assembly of monochrome microdisplays. A lens system will be designed and built to demonstrate the applicability of PDLC and PNLC microdisplays in personal viewer applications. The last phase of the research project focuses on the introduction of full color in reflective PDLC and PNLC microdisplays. The first and most evident solution is the introduction of color filters in the microdisplay. Another technique called field oriented addressing will focus on the reduction of the PDLC and PNLC switching time to levels compatible with color sequential addressing.

References

[1] Drzaic, P.S., 1995, Theoretical considerations of droplet structures. In *Liquid Crystal Dispersions*, edited by H. L. Ong (Singapore: World Scientific Publishing), pp. 103-111

[2] Drzaic, P.S., 1995, Phase separation methods for PDLC films. In *Liquid Crystal Dispersions*, edited by H. L. Ong (Singapore: World Scientific Publishing), pp. 30-51

[3] Wu, B. G., Ma, Y. D., Li, T. S., "Novel Fast-Switching Polymer-Dispersed Liquid-Crystal Light Shutter and Display", 1992, *SID 92 Digest*, pp. 583-586

[4] Yamada, S., Tsuchiya, Y., Yazaki, M., Sakata, H., Sonehara, T., "Electro-optical properties of PDLC cells", 1998, *SID 98 Digest*, pp. 758-761

[5] Chung, D. B., Vu, E., Flack, R., Nicholson, B., "Recent Development in Polymer Dispersed Liquid Crystal Materials for Reflective Silicon Light Valve Application", 1998, *SID 98 Digest*, pp. 1127-1130

[6] Nolan, P., Jolliffe, E., Coates, D., "Film formation parameters affecting the electro-optic properties of low-voltage PDLC films", 1995, *SPIE Proc*., **2408**, 2

[7] Ginter, E., Lueder, E., Kallfass, T., Huttelmaier, S., Dobler, M., Hochholzer, V., Coates, D., Tillin, M., Nolan, P., "Optimized PDLCs for active-matrix addressed light valves in projection systems", 1993, *Proc. of Eurodisplay*, pp. 105-108

[8] Vinouze, B., Bosc, D., Guilbert, M., Trubert, C., "Active Matrix With Optimised PDLC for Reflective Direct View Liquid Crystal Display", 1994, *Proc. of IDRC '94*, pp. 472-475

[9] Park, W., Koh, Y., Park, S., "Improvement in electro-optical properties of Polymer Dispersed Liquid Crystal", 1998, *Proc. of Asia Display 98*, pp. 803-806

[10] Erdmann, J. H., Lackner, A. M., Sherman, E., Margerum, J. D., "Droplet-size effects and lighting techniques in direct-view PDLC displays", 1993, *Journal of SID*, **1/1**, 57

[11] Ogawa T., Fujita S., Iwai Y., Koseki H., "The Trends of Reflective LCDs for Future Electronic Paper", 1998, *Digest of SID 98*, pp. 217-220

[12] Fujita S., Yamaguchi H., Mizuno H., Ohtani T., Sekime T., Hatanaka T., Ogawa T., "A reflective color STN-LCD with a single polarizer and double retardation films", 1999, *Journal of SID*, **7/2**, 235

[13] Maeda T., Matsushima T., Okamoto E., Wada H., Okumura O., Iino S., "Reflective and transflective color LCDs with double polarizers", 1999, *Journal of SID*, **7/1**, 9

[14] Lowe A., "The Prospects for Polariser-free Reflective Liquid Crystal Dispalys", 1999, *Proc. of the 19th IDRC (Eurodisplay 99)*, pp. 433-436

[15] Ozeki M., Mori H., Shidoji E., Hirai Y., Koh H., Akatsuka M., "A Super Reflective Color LCD with White, Red, Blue, and Green Using Electrically Controlled Birefringence Technology", 1996, *SID Intl Symp Digest Tech Papers*, pp. 107-110

[16] Wu S.-T., Wu C.-S., Kuo C.-L., "Comparative studies of single-polarizer reflective liquid-crystal displays", 1999, *Journal of SID*, **7/2**, 119

[17] Kwok H.S., Chen J., Yu F. H., Huang H. C., "Generalized mixed-mode reflective LCDs with large cell gaps and high contrast ratios", 1999, *Journal of SID*, **7/2**, 127

[18] Beynon E., Saynor K., Tillin M., Towler M., "Single-polarizer reflective twisted nematics", 1999, *Journal of SID*, **7/1**, 71

[19] Ishinabe T., Miyashita T., Uchida T., "Optical design of R-OCB mode full-color reflective LCD with wide viewing angle and high contrast", 1998, *Journal of SID*, **6/4**, 243

[20] Iwata Y., Nakamura N., Arakawa F., Matsuoka T., "Novel Approach for Light Scattering Enhancement Using Internal Diffusing Sheet (IDS)", 1998, *Proc. of IDW '98*, pp. 275-278

[21] Shao X., Guo J., Wu S., Yuan J., Huang X., "Improving the display performance of reflective color LCDs with micro-cone-structure film", 1999, *Journal of SID*, **7/1**, 67

[22] Hiyama I., Itoh O., Kondo K., Arimoto A., "High-performance reflective STN-LCD with a blazed reflector", 1999, *Journal of SID*, **7/1**, 49

[23] Chang W.-C., Wen C.-J., Ting D.-L, Shiu J.-W., Chuang L.-S., Chang C.-C., "A Novel Reflective LCD with Diffusive Micro Slant Reflector (DMSR)", 1999, *Proc. of the 19th IDRC (Eurodisplay 99)*, pp. 49-52

[24] Nakai Y., Ohtake T., Sugahara A., Sunohara K., Tsuchida K., Tanaka M., Iwanaga H., Hotta A., Taira K., Mori M., Hiroyasu N., Akiyama M., Okajima M., "A reflective tri-layered guest-host color TFT-LCD", 1999, *Journal of SID*, **7/1**, 55

[25] Davis D., Khan A., Jones C., Huang X. Y., Doane J. W., "Multiple color high resolution reflective cholesteric liquid crystal displays", 1999, *Journal of SID*, **7/1**, 43

[26] Ma R.-Q., Yang D.-K., "Optimization of polymer-stabilized bistable black-white cholesteric reflective display", 1999, *Journal of SID*, **7/1**, 61

[27] Hashimoto K., Okada M., Nishiguchi K., Masazumi N., Yamakawa E., Taniguchi T., "Reflective color display using cholesteric liquid crystals", 1998, *Journal of SID*, **6/4**, 139

[28] Drzaic, P.S., 1995, Chiral nematic dispersions. In *Liquid Crystal Dispersions*, edited by H. L. Ong (Singapore: World Scientific Publishing), pp. 303-311

[29] J. Doutreloigne, H. De Smet, A. Van Calster, "A New Architecture for Monolithic Low-Power High-Voltage Display Drivers", 2000, *Conf. Record of the 20th IDRC*, 115-118

[30] De Smet H., Van de Steen J., Carchon N., Cuypers D., De Backere C., Vermandel M., Van Calster A., De Caussemaeker A., Witvrouw A., Ziad H., Baert K., Colson P., Schols G., Tack M., "The Design and Fabrication of a 2560X2048 Pixel Microdisplay Chip", 1999, *Proc. of Eurodisplay '99*, pp. 493-496

[31] Underwood I., 2001, Silicon Technology and VLSI Design for LCoS Microdisplays. In *2001 Seminar Lecture Notes Volume I: June 4*, edited by Morreale J. (San Jose, Society for Information Display), M-6/1-32

[32] Van den Steen J., Carchon N., Van Doorselaer G., De Backere C., De Baets J., De Smet H., De Vos J., Lernout J., Vanfleteren J., Van Calster A., "Technology and Circuit Aspects of Reflective PNLC Microdisplays", 1997, *SID Intl Symp Digest Tech Papers*, pp. 195-198

[33] Van Doorselaer G., Carchon N., Van den Steen J., Vanfleteren J., De Smet H., Cuypers D., Van Calster A., "Characterisation of paper-white reflective PDLC microdisplay for portable IT applications", 1998, *Proc. of Asia Display '98*, pp. 55-58

[34] Mukawa H., Yoshida T., Akutsu K., Sugiura M., Hashimoto S., "Novel Virtual Image Optics for Reflective Mircodisplays", 2000, *Conf. Rec. of the 20th IDRC*, pp. 96-99

[35] Prache O., "Full color SVGA+ OLED On Silicon Microdisplay", 2001, *International Symposium Digest of Technical Papers*, pp. 514-517

[36] Hornbeck L.J., Darrow D.J., Pettitt G.S., Walker B., Werner W.B., "DLP Cinema™ Projector Field Demonstrations: A Progress Report", 2000, *Proc. of 7th IDW*, pp. 1093-1096

[37] Stefanov M. E., Erdmann J. H., Gandhi J., "LCOS Microdisplay Manufacturing Technology", 2000, *Conf. Rec. of the 20th IDRC*, pp. 17-21

[38] Van Calster A., Bruyneel F., Cuypers D., Carchon N., Van Doorselaer G., Van den Steen J., De Smet H., "Miniature Reflective Displays", 2000, *Proc. of 7th IDW*, pp. 179-182

[39] Van Calster A., "Microdisplays for portable IT products and projection applications" 1998, *Proc. of IDW '98*, pp. 135-138

[40] Schuck M., Kazlas P., Radler M., McKnight D., Johnson K., "Post-processing and assembly of reflective microdisplays", 1999, *Journal of SID*, **7/2**, 93

[41] Colgan E.G., Doany F., Lu M., Rosenbluth A., Yang K.-H., Uda M., Shinohara M., Tomooka T., Tsukamoto T., "Optimization of light-valve mirrors", 1998, *Journal of SID*, **6/4**, 247

[42] Colgan E.G., Uda M., "On-chip metallization layers for reflective light valves", 1998, *IBM J. Res. Develop.*, Vol. **42**, No. **3/4**, 339

[43] Lide D. R. , 1990-1991, chapter12. In *Handbook of Chemistry and Physics, 71st edition,* (Boca Raton: CRC Press), pp. 87-102

[44] Bodammer G., Calton D. W., Underwood I., "Investigation of the Bow of Silicon Backplanes for Microdisplay Applications", 2001, *SID Intl Symp Digest Tech Papers*, pp. 439-441

[45] Ho G. S., Ou C. R., Yoo C. J., "The Optical Performance of Liquid Crystal under Cell Gap Variations in the Projection Display System", 2000, *Proc. of 7th IDW*, pp. 1045-1048

[46] De Backere C., Vermandel M., Van Calster A., "Light Shielding with Liquid Crystal On Silicon Displays", 1998, *Proc. of Asia Display '98*, pp. 415-418

[47] Moore P., Cacharelis P., Frazee J., Chung D., Luttrel R., Flack R., "A reflective-mode EEPROM-based silicon light-valve technology", 1999, *Journal of SID*, **7/2**, 85

[48] Lu M., Yang K. H., "Reflective Nematic LC Devices for LCOS Applications", 2000, *Conf. Rec. of the 20th IDRC*, pp. 1-7

[49] H. L. Ong, "Microdisplay: Nematic Electro-Optical Effects", 2000, *Conf. Rec. of the 20th IDRC*, pp. 8-12

[50] M. Tani et al., "Progress in Color Filters for LCDs", International Display Research Conference, pp.103-111, 1994

[51] M. Tani, "Color Filters for Reflective LCDs", SID International Symposium, pp. 287-290, Vol. XIX, 1998

[52] Y. Ishii et al., "Development of Highly Reflective Color TFT-LCDs", International Display Research Conference, pp.119-122, 1998

[53] Y. Hisatake et al., “An 8.4-in. Color Reflective TFT-LCD using CMY Colorfilters and Low-Temperature Poly-Si Technology”, International Display Research Conference, pp.131-134, 1998

[54] T. Sugiura, “Development of pigment-dispersed-type color filters for LCDs”, Journal of the SID, pp. 341-346, 1/3, 1993

[55] T. Sugiura, “Dyed color filters for liquid-crystal displays”, Journal of the SID, pp.177-180, 1/2, 1993

[56] Silverstein L. D., 2001, Color in electronic displays. In *2001 Seminar Lecture Notes Volume I: June 4*, edited by Morreale J. (San Jose, Society for Information Display), M-8/1-89

[57] Underwood I., 2001, Silicon Technology and VLSI Design for LCoS Microdisplays. In *2001 Seminar Lecture Notes Volume I: June 4*, edited by Morreale J. (San Jose, Society for Information Display), M-6/1-32

[58] A. G. Chen et al., “Holographic reflective liquid-crystal display”, Journal of the SID,3/4, pp. 159-163, 1995

[59] A. G. Chen et al., “Holographic Reflectors for Enhanced Reflective LCDs”, SID International Symposium, Digest of Technical Papers, Vol. 19, pp. 487-490, 1998

[60] K. Iwauchi et al., “Reflection Profiles of Holographic Color Reflectors”, International Display Research Conference, pp. 694-697, 1999

[61] G. P. Crawford et al., “Reflective color LCDs based on H-PDLC and PSCT technologies”, Journal of the SID, 5/1, pp. 45-48, 1997

[62] K. Tanaka et al., “Holographically formed liquid-crystal/polymer device for reflective color display”, Journal of the SID, 2/1, pp. 37-40, 1994

[63] A. Y.-G. Fuh et al., “Dynamical studies of holographic grating formed in polymer-dispersed liquid crystal films”, International Display Research Conference, pp.128-131, 1997

[64] K. Kato et al., “Alignment-controlled holographic polymer dispersed liquid crystal (HPDLC) for reflective display devices”, SPIE Vol. 3297, pp. 52-57, 1998

[65] C. C. Bowley et al., “Dual-domain Reflection from Holographically-formed PDLCs”, International Display Research Conference, pp.851-854, 1998

[66] K. Tanaka et al., “A liquid-crystal/polymer optical device formed by holography for reflective color display applications”, International Display Research Conference, pp. 109-111, 1993

[67] M. Date, ”Full-color reflective display device using holographically fabricated polymer-dispersed liquid crystal (HPDLC)”, Journal of the SID, 7/1, pp. 17-22, 1999

[68] H. Yuan et al., “High Efficiency Color Reflective Displays with Extended Viewing Angle”, International Display Research Conference, pp. 1136-1139, 1998

[69] Matsumoto K., Takeda K., Hasegawa M., Sueoka K., Taira Y., Gruber P. A., Doyle J. P., Rubino J.M., “Vertical Electrical Connections for Multi-layer Stacked Display”, 2001, *Proc. of Asia Display / IDW ’01*, pp. 347-350

[70] R. Sperger et al.,”High performance patterned all-dielectric interference colour filters for display applications”, International Display Research Conference, pp. 81-84, 1993

[71] Hugo J. Cornelissen et al., “Reflective direct-view LCDs using polymer-dispersed liquid crystal (PDLC) and dielectric reflectors”, Journal of the SID, 7/1, pp. 37-41, 1999

[72] P. Alvelda, “High-efficiency color microdisplays”, Journal of the SID,3/4, pp. 181-184, 1995

[73] H. Watanabe, “Reflective field sequential color LCD”, Eurodisplay, pp. 449-450, 1999

[74] H. C. Huang et al., “Color Sequential Miniature Silicon Display Using Reflective Twisted Nematic Mode”, International Display Research Conference, pp. 411-414, 1998

[75] T. Takahashi et al., “Implementation of A Field Sequential Fullcolor LCD, New Matrix LCD, And Optical Gates Using Ferroelectric Liquid Crystal Optical Diodes”, Eurodisplay late-news papers, pp. 13-16, 1999

[76] P. Alvelda et al., “SVGA and XGA LCOS Microdisplays for HMD Applications”, Eurodisplay late-news papers, 1999

[77] P. Alvelda et al.,”SVGA and XGA active matrix microdisplays for head-mounted applications”, Proceedings of SPIE, Vol. 3955, pp.109-119, 2000

[78] S.-G. Kim et al., “Actuated Mirror Array – A New Chip-based Display Device for the Large Screen Display”, International Display Research Conference, pp.329-334, 1998

[79] R. G. Fielding et al., “Colorimetry Performance of a High-Brightness DMD-Based Optical System”, SID International Symposium, pp. 767-770, 1996

CHAPTER 2:
Measurement set-ups

1 Introduction

The first objective of this Ph.D. is to optimize the characteristics of reflective PDLC and PNLC displays. In order to do this it is important to measure the different characteristics accurately. The characteristics of the displays can be split in three different categories. For the measurement of the characteristics of each category a different measurement set-up is designed and built.

A first set-up is used for measuring the electro-optical properties of the PDLC or PNLC layer in a reflective display. These include the switching speed, switching voltage, hysteresis, reflectance and contrast ratio of the PDLC and the PNLC.

A second set-up is used for the measurement of the cell gap of the display [1]. The influence of the cell gap on the electro-optical properties of the PDLC and PNLC can be analyzed with this set-up.

A third measurement set-up analyzes the influence of different types of illumination on the contrast ratio and reflectance of reflective displays [2,3]. With this set-up it is possible to compare the applicability of different reflective display technologies in environmental illumination conditions.

2 Measurement of the opto-electrical characteristics of PDLC and PNLC

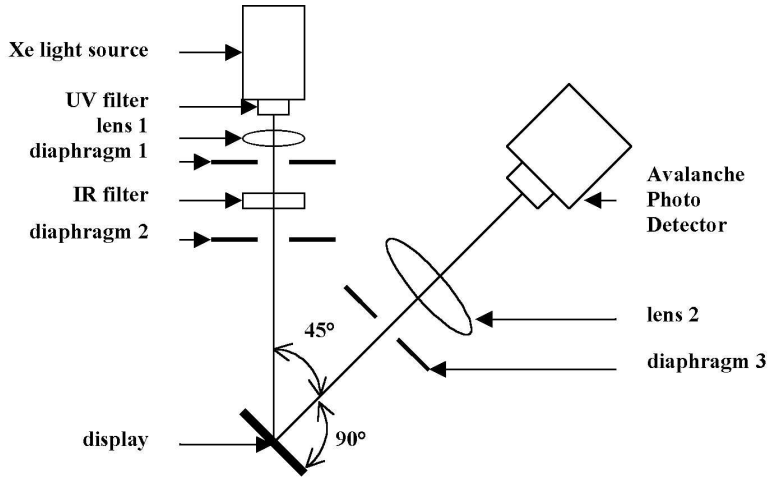

Fig. 2.1: Measurement set-up used for the measurement of the opto-electrical characteristics of PDLC and PNLC.

The set-up for the opto-electrical measurement of PDLC and PNLC has three basic components (Fig. 2.1). First of all we have the display itself. The displays are non emissive so an illumination system is required (the 2nd part). The opto-electrical properties are measured with the detector system (the 3rd part).

The detector system consists of an Avalanche Photo Detector, a lens and a diaphragm. The Avalanche Photo Detector is a silicon photodiode with a high sensitivity. Light falling on the detector generates a voltage which is a linear function of the light intensity. This voltage is detected by an oscilloscope. The lens in the detector system is used to focus the display on the detector. Diaphragm 3 determines the detection angle. The detection angle has an influence on the detected contrast ratio and reflectance of the display.

The illumination system produces a collimated light beam. The core of the illumination system is a Xe light source. The light output of the Xe light

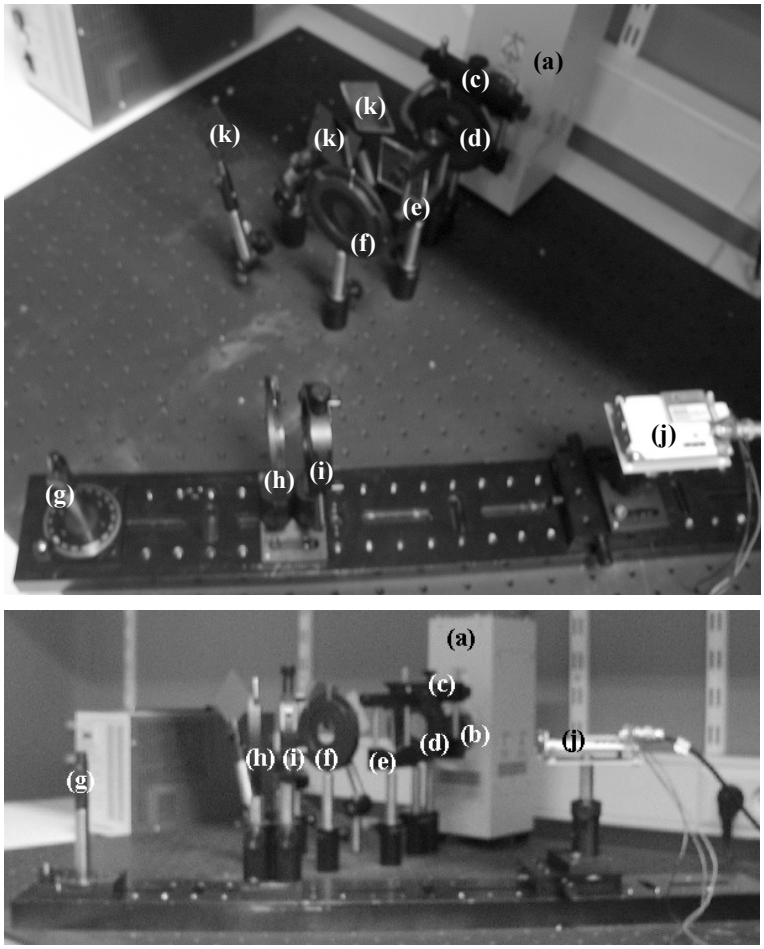

Fig. 2.2: Top view (top) and side view (bottom) of the measurement set-up of Fig. 2.1 showing the Xe light source (a), UV filter (b), lens 1 (c), diaphragm 1 (d), IR filter (e), diaphragm 2 (f), display holder (g), diaphragm 3 (h), lens 2 (i), detector (j) and grey filters (k).

source is very high and stable while the light spectrum is flat from the UV into the IR spectrum. Because we are only interested in the optical response in the visual spectrum the UV and IR are filtered out of the spectrum. The

filtering also prevents the UV or IR to heat the display or to damage or cure the PDLC/PNLC during the measurements. A lens and diaphragm 1 and 2 are used to convert the output of the light source into a collimated light beam. The high light output of the Xe light source and the high sensitivity of the Avalanche Photodiode are important for measurements in the non specular reflection direction. The intensity of the display illumination is controlled by putting grey filters in the optical path of the collimated light beam. Pictures of the measurement set-up are shown in Fig. 2.2.

The position of the display with respect to the light source and of the display with respect to the detector system changes the detected contrast ratio and the reflectance of the display considerably (see paragraph 3.5 “Applicability of reflective PDLC and PNLC displays for direct view applications”). The goal of this measurement set-up is to compare the opto-electrical properties (switching time, switching voltage, hysteresis, contrast ratio and reflectance) of displays, so the display processing and assembly can be optimized. For these experiments it is sufficient to use a measurement set-up with a fixed position of the display, the detector system and the illumination system. The different components of the measurement set-up are positioned in the same way as in Fig. 2.1.

For the measurement of the opto-electrical properties it is important to compensate the DC voltage in the cell gap of the display. This DC voltage is typical for reflective displays. The effects of this DC voltage have already been discussed in the paragraph “Microdisplays” in chapter 1. The origin of this DC voltage will be discussed in paragraph 3.4 “DC effect in reflective PDLC and PNLC displays”. The DC voltage is compensated by putting an inverse DC voltage across the cell gap.

With the measurement set-up of Fig. 2.1 the maximum light intensity is measured when the PDLC is scattering. This is different from measurements on transmissive displays. In general the specularly transmitted light is detected for transmissive displays. In the measurement set-up of Fig. 2.1 light in an off specular reflection direction is detected. For the switching of

the PDLC and PNLC between the transparent state and the scattering state a 50Hz square wave voltage is put across the PDLC or PNLC layer.

V_{90} is the voltage required to detect a light intensity of $I_{90} = I_{min}+0.1\Delta I$ with $\Delta I = I_{max}-I_{min}$. I_{min} is the minimum detected light intensity (for a voltage of $13V_{rms}$) and I_{max} the maximum detected light intensity (for a voltage of 0V) (Fig. 2.3). V_{th} (threshold voltage) is the voltage required to detect a light intensity of $I_{th} = I_{max} – 0.1\Delta I$. The contrast ratio = $(I_{max}-I_{noise})/(I_{min}-I_{noise})$ with I_{noise}= the default light intensity measured by the detector without a display

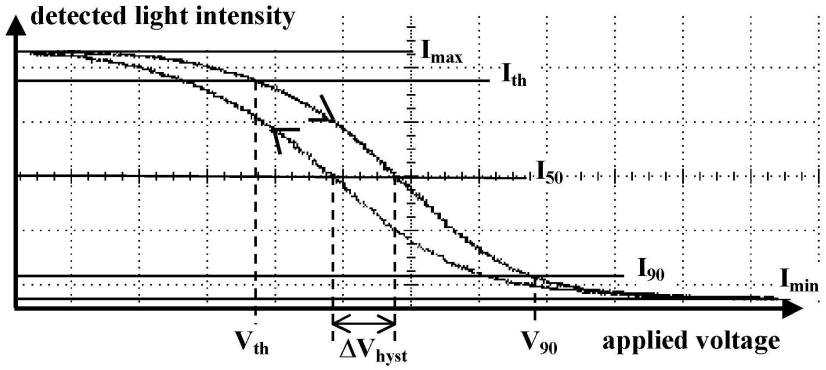

Fig. 2.3: Measurement showing the hysteresis in the optical response of a reflective PDLC display.

in the measurement spot. An oscilloscope is used for the readout of the detector. Like this the light intensity is measured in Volts. The order of magnitude for I_{max} is 10V, for I_{min} 0,1V and for I_{noise} 0,01V. The noise light intensity results from reflections on the walls in the measurement room and reflections on het display holder. The reported values for the hysteresis are measured by increasing the rms value of a 50Hz square wave from 0V to V_{90rms} (the rms value of V_{90}). The modulation frequency of the square wave is 0.4Hz. The absolute value of the hysteresis ΔV_{hyst} in V_{rms} is the difference between the two voltages for which the detected light intensity is $I_{50}=(I_{min}+I_{max})/2$. The relative value of the hysteresis equals $100\Delta V_{hyst}/V_{90}$. The switching time T_{rise} is the time needed to switch from scattering PDLC

with intensity I_{max} to transparent PDLC with an intensity I_{90}. T_{decay} is the time needed to switch from non scattering PDLC with an intensity I_{min} to scattering PDLC with an intensity of I_{th}. The values for the reflectance are measured relative to a white standard. The white standard used in the measurements is a Spectralon® Reflectance Standard SRS-99-010 (with a 99% reflectance in the range of 400nm to 950nm) of Labsphere®. The reflectance (in %) = $100(I_{max}-I_{noise})/(I_{white\_standard}-I_{noise})$ with $I_{white\_standard}$ = light intensity of the white standard for the same illumination conditions as the display and I_{max} and I_{noise} have the same definition as the one used for the contrast ratio.

3 Measurement of the cell gap in liquid crystal displays

3.1 Introduction

The cell gap of a Liquid Crystal Display (LCD) determines to a great extent the LCD's opto-electrical properties like contrast ratio, reflectance, switching speed and switching voltages. The control of the cell gap during the manufacturing process is very important. When a new type of Liquid Crystal (LC) is characterized a good knowledge of the cell gap is also required. Spacers are used to obtain the desired cell gap. However the actual cell gap can be smaller or bigger than the desired cell gap. This may be caused by the pressure used during assembly, the curing of the sealing glue of the displays, capillary forces during the filling of the displays, the cross-overs, dust particles, the spacer concentration,... The latter can be reduced to obtain a cell gap smaller than the spacer diameter especially in the case of plastic spacers. An accurate cell gap measurement method is an interesting tool for the optimization of the display assembly or for the characterization of a LC.

Some cell gap measurement methods have already been devised [4-6]. However these methods are only applicable for filled displays and are based on the polarization effect of the LC. These methods are not applicable for displays with an optical principle that is not based on the polarization of light but on the scattering of light like Polymer Dispersed Liquid Crystals (PDLC) and Polymer Network Liquid Crystals (PNLC). These polarizer free displays are becoming increasingly important for mobile applications due to their high optical efficiency [7,8] and resulting high energy efficiency. It would also be interesting to have a measurement method that allows the measurement of the cell gap before the filling of the LCDs. This would allow

a better monitoring of the stability of the cell gap during the entire display assembly process.

A measurement method based on the interference of light seemed to be an evident choice since the cell gap is determined by two reflecting layers in the display. Other papers [9-14] reporting on interferometry for distance measurements between reflecting surfaces are basically based on the same method: the two-wavelength interferometry. With the two-wavelength method distances shorter than the optical wavelength can be determined by measuring the phase difference between two interfering light beams with different wavelengths. The measurement equipment that is used for the two-wavelength interferometry is not commonly used in other set-ups for display measurements.

The method presented in this Ph.D. is based on the spectral analysis of white light reflected by the display. One advantage of this method is that it allows the cell gap measurement of LCDs before and after the filling with LC. This method is not only limited to LCDs with an optical principle based on the polarization of light like TN (Twisted Nematic), FLC (Ferro-electric Liquid Crystal), VAN (Vertically Aligned Nematic),... It is also possible to measure the cell gap in LCDs with an optical principle based on the scattering of light like PDLC and PNLC. Another advantage of the method is that the components can be used for other display measurements like colorimetry.

3.2 Concept of the measurement method

3.2.1 Basic theory

The concept of the measurement methods is based on the interference pattern of the light reflected by a layer with two reflecting surfaces. Assume the situation as described in Fig. 2.4. We define the coefficient of reflection $R1$ as the ratio of the amplitude of the light reflected by surface 1 to the amplitude of the total incident light on surface 1. Surface 2 has a coefficient of reflection $R2$. If the total incident light equals $I=\cos(\omega t)$ and we assume

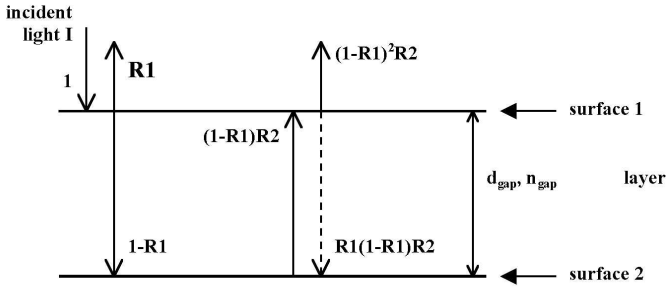

Fig. 2.4: Two reflecting surfaces divided by a layer causing light interference. The dotted line indicates the first internal reflection.

no absorption of light in surface 1 and 2 then we can write that the total reflected light R is

$$R = R1\cos(\omega t) + \sum_{k=1}^{\infty} R1^{k-1} R2^{k} \left(1 - R1\right)^{2} \cos\left[\omega\left(t - kt_0\right)\right] \qquad \text{Eq. (2.1),}$$

where $\omega=2\pi c/\lambda$ and $t_0=2d_{gap}n_{gap}/c$, c=speed of light in vacuum; λ=wavelength; d_{gap}=thickness of the layer; n_{gap}=refractive index of the layer. The cosine factors in Eq. (2.1) for $k>1$ are caused by internal reflections. Since $R1<1$ and $R2<1$ the magnitude of the cosine factors for $k>1$ is much smaller than for $k=1$. Therefore we neglect the internal reflections so

$R = R1\cos(\omega t) + (1-R1)^2 R2\cos(\omega t - 4\pi n_{gap} d_{gap}/\lambda)$ Eq. (2.2).

Thus the reflected spectrum is

$|R(\lambda)|^2 = R1^2 + ((1-R1)^2 R2)^2 + 2\, R1(1-R1)^2 R2\cos(4\pi n_{gap} d_{gap}/\lambda)$ Eq. (2.3).

The periodic term in Eq. (2.3) causes what is generally known as an interference pattern (Fig. 2.5). The periodicity of the reflected interference spectrum unambiguously determines the optical thickness of the cell gap $n_{gap}d_{gap}$. If for instance λ_1 and λ_2 are two wavelengths with extrema in Eq. (2.3) then $\cos(4\pi n_{gap}d_{gap}/\lambda)= \pm 1$ for $\lambda=\lambda_1$ and $\lambda=\lambda_2$. So

$2n_{gap}d_{gap} = k_1\lambda_1/2$ Eq. (2.4),

$2n_{gap}d_{gap} = k_2\lambda_2/2$ Eq. (2.5),

where k_1 and k_2 are natural numbers. Suppose $\lambda_1>\lambda_2$ then

$k_2 = k_1 + x$ Eq. (2.6),

where x is a natural number.

Based on Eq. (2.4), Eq. (2.5) and Eq. (2.6) we can write

$$n_{gap} d_{gap} = \frac{x \lambda_1 \lambda_2}{4(\lambda_1 - \lambda_2)}$$ Eq. (2.7).

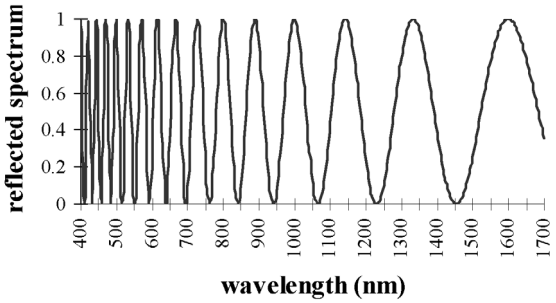

Fig. 2.5: Plot of the equation R=A+Bcos($4\pi n_{gap} d_{gap}/\lambda$), which is similar to the interference pattern of Eq. (2.3), with A=B=0.5 and $n_{gap} d_{gap}$=4μm.

The value of x-1 indicates the number of extrema in $|R(\lambda)|^2$ between the wavelengths λ_1 and λ_2 (we refer to x as the distance between λ_1 and λ_2). In theory $n_{gap} d_{gap}$ can be determined if the wavelengths for a consecutive maximum and minimum (x=1) are known. If several wavelengths with extrema are known it is better to choose the distance x between the two extrema as high as possible. This results in a bigger difference λ_1-λ_2 in the denominator of Eq. (2.7) improving the accuracy of the calculation of $n_{gap} d_{gap}$. x=2 when λ_1 and λ_2 are two wavelengths with consecutive maxima in $|R(\lambda)|^2$. In this case we can write based on Eq. (2.7)

$$n_{gap} d_{gap} = \frac{\lambda_1 \lambda_2}{2(\lambda_1 - \lambda_2)}$$ Eq. (2.8).

Equation (2.8) is also valid for two wavelengths with consecutive minima in $|R(\lambda)|^2$. By measuring across a broad spectrum we are able to detect several maxima and minima in the reflected spectrum so we are able to calculate

$n_{gap}d_{gap}$ several times using Eq. (2.8). This allows us to do a statistical analysis of the calculated cell gap values increasing the accuracy of the cell gap determination.

Another way to determine the optical thickness of the cell gap is by analyzing the Fourier Transform (FT) of $|R(1/\lambda)|^2$, $|R(f)|^2$ = FT($|R(1/\lambda)|^2$). $|R(1/\lambda)|^2$ is the measured spectrum as a function of the wavenumber $1/\lambda$. Based on Eq. (2.3) and knowing that FT(constant)=constant*$\delta(f)$ and FT[$\cos(4\pi n_{gap}d_{gap}/\lambda)$]=[$\delta(f-2n_{gap}d_{gap})$ + $\delta(f+2n_{gap}d_{gap})$]/2 we can write

$$|R(f)|^2 = [R1^2 + ((1-R1)^2R2)^2]\delta(f) + R1\,(1-R1)^2R2[\delta(f-2n_{gap}d_{gap}) + \delta(f+2n_{gap}d_{gap})] \quad \text{Eq. (2.9),}$$

where $\delta(f)$ is a Dirac pulse. In this case $n_{gap}d_{gap}$ is determined by the spatial frequency where we have a Dirac pulse in the Fourier Transform of the reflected spectrum. Because the dimension of $1/\lambda$ is 1/meter the dimension of the frequency f in $|R(f)|^2$ = FT($|R(1/\lambda)|^2$) will be meter. To prevent confusion between the frequency of light (dimension Hz) and the frequency f in $|R(f)|^2$ (dimension meter) we will refer to the latter frequency as the spatial frequency.

In the third method an Inverse Fourier Transform (IFT) is used. The measured spectrum $|R(\lambda)|^2$ will have some noise, which affects the accuracy of the cell gap determination. The noise can be filtered out in the spectrum of $|R(f)|^2$. On this filtered spectrum we perform an IFT. This results in a spectrum similar to $|R(1/\lambda)|^2$. Based on this spectrum the cell gap can be determined in the same way as in the first method. Because the noise is filtered out the cell gap determination will be more accurate.

3.2.2 Empirical model for LCD measurements

We describe an empirical model based on the physics of the display. In our model we take into account that there are more than two reflecting surfaces. In Fig. 2.6 we see a cross section of the displays used in our measurements

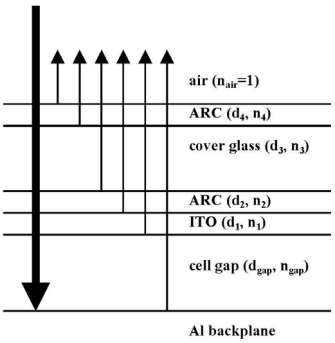

Fig. 2.6: Cross section of a display used in our measurements.

with their different reflecting surfaces. Some of the displays do not have an ARC layer (Anti Reflective Coating) between the cover glass and the ITO layer (Indium Tin Oxide). When the LCD is not filled with LC the cell gap only contains air. We assume that the optical path in the cell gap $n_{gap}d_{gap} \cong d_{gap}$ since $n_{gap} \cong 1$ for air. In the case the display is filled with LC the refractive index n_{gap} no longer equals 1. In order to have an accurate measurement of the cell gap value it is necessary to have a good knowledge of the value of n_{gap}.

There will also be internal reflections in the different layers. However these are neglected in the model. The magnitude of these internal reflections is strongly reduced even after the first internal reflection. This is confirmed by the measurements (Fig. 2.8 to Fig. 2.13). The total reflected light will be

$$R = \beta_1\cos(\omega t) + \beta_2\cos(\omega t - 4\pi n_4 d_4/\lambda) + \beta_3\cos[\omega t - 4\pi(n_4 d_4 + n_3 d_3)/\lambda] + \beta_4\cos[\omega t - 4\pi(n_4 d_4 + n_3 d_3 + n_2 d_2)/\lambda] + \beta_5\cos(\omega t - 4\pi(n_4 d_4 + n_3 d_3 + n_2 d_2 + n_1 d_1)/\lambda) + \beta_6\cos(\omega t - 4\pi(n_4 d_4 + n_3 d_3 + n_2 d_2 + n_1 d_1 + d_{gap})/\lambda) \quad \text{Eq. (2.10).}$$

The coefficients β_1 to β_6 are a function of the coefficients of reflection of the several surfaces in a similar way as the coefficients of the cosine terms in Eq. (2.2). The reflected spectrum $|R(\lambda)|^2$ will consist of cosine components with spatial frequencies equal to two times the different optical paths of the reflected light 0, n_4d_4, $n_4d_4 + n_3d_3$, $n_4d_4 + n_3d_3 + n_2d_2$, $n_4d_4 + n_3d_3 + n_2d_2 + n_1d_1$, $n_4d_4 + n_3d_3 + n_2d_2 + n_1d_1 + d_{gap}$ and the spatial frequencies that equal two times the difference between two of these optical paths. The latter spatial frequencies appear during the calculation of $|R(\lambda)|^2$ when components of the form $\cos(a)\cos(b) + \sin(a)\sin(b) = \cos(a-b)$ are found. From a technical point of view d_2 and d_4 can be controlled very accurately and are about 100nm. Since they are both made of the same material we can assume that $n_4d_4 \cong n_2d_2$. n_3d_3 is much larger than the other optical paths. d_3 is about 0.75mm while the other thickness range from 100nm (d_1, d_2, d_4) to a few microns (d_{gap}). The high spatial frequency components with a spatial frequency higher or equal to $2n_3d_3$ are negligible in the measured spectrum (see Fig. 2.8) and will be omitted. Therefore we can write based on Eq. (2.10):

$$|R(\lambda)|^2 = A_1 + A_2\cos(4\pi n_4d_4/\lambda) + A_3\cos(4\pi n_1d_1/\lambda) + A_4\cos(4\pi d_{gap}/\lambda) + A_5\cos[4\pi(d_{gap}+n_1d_1)/\lambda] + A_6\cos[4\pi(n_1d_1+n_2d_2)/\lambda] + A_7\cos[4\pi(d_{gap}+n_1d_1+n_2d_2)/\lambda] \quad \text{Eq. (2.11).}$$

Based on our measurements (Fig. 2.8) we see that the average value A_1 is decreasing with the wavelength λ in a linear way. This can be explained by the higher absorption of light in the ARC and ITO layer, especially for wavelengths in the infra red. Therefore the average value A_1 is replaced by a coefficient linearly dependent on the wavelength λ. The same is done for A_2 to A_7 to anticipate for any wavelength dependency of A_2 to A_7. For the displays with no ARC between the cover glass and ITO layer A_6 and A_7 are 0 so

$$|R(\lambda)|^2 = A_1 + A_2\cos(4\pi n_4d_4/\lambda) + A_3\cos(4\pi n_1d_1/\lambda) + A_4\cos(4\pi d_{gap}/\lambda) + A_5\cos[4\pi(d_{gap}+n_1d_1)/\lambda] \quad \text{Eq. (2.12).}$$

3.2.3 Principle of measurement of the cell gap of filled LCDs

If we want to measure the cell gap of a filled LCD we have to know the ordinary refractive index n_o of the LC. The refractive index of a LC is anisotropic. This is an essential property of LCs and forms the basis for their use in displays. The refractive index of a LC molecule is modelled by a tensor. A LC molecule is a long stretched molecule. One component of the refractive index is aligned parallel to the long axis of the LC molecule and has a value of n_e (the extraordinary value of the refractive index) (Fig. 1.1). The two other components are perpendicular to the long axis and are perpendicular to each other. They both have the same value n_o (the ordinary value of the refractive index). It is clear that for randomly oriented LC molecules the LC changes the polarization of the incident light and the basic theory of paragraph 2.1 no longer applies. However in most LCD technologies the LC molecules are aligned parallel to the incident light either in the 'ON' or the 'OFF' state of the LCD. In the case of PDLC, TN,... and other LCs with a dielectric anisotropy $\Delta\varepsilon=\varepsilon_e-\varepsilon_o > 0$ a voltage has to be applied during the measurements to align the LC molecules parallel to the incident light. For LCs with a $\Delta\varepsilon < 0$ (this is the case for VAN) no voltage must be applied during the measurements. When the LC molecules are aligned parallel to the incident light the refractive index in the plane perpendicular to the propagation direction of the light is uniform and equal to n_o. The basic theory of paragraph 3.2.1 is then applicable with $n_{gap} = n_o$.

3.3 Measurements

3.3.1 Measurement set-up

The measurement set-up consists of four basic components: a microscope, a halogen light source, a spectrumanalyzer and a PC (Fig. 2.7). The light from the halogen lamp is transformed by a lens into a collimated light beam and is

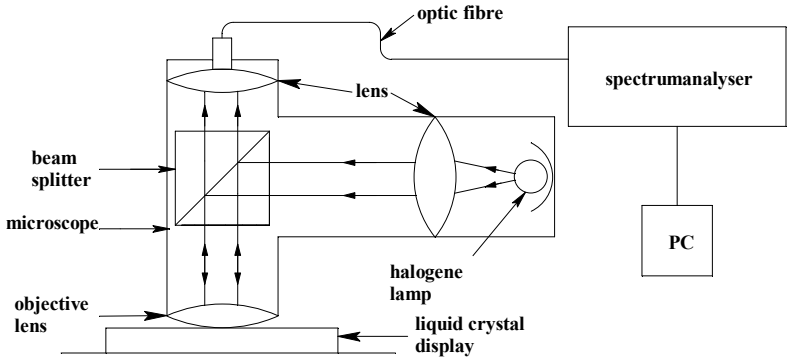

Fig. 2.7: Schematic layout of the measurement set-up.

reflected by a beam splitter through the objective of the microscope. This results in a measurement spot with a diameter of 1mm. The display to be measured is under the objective and reflects the light into the objective, through the beam splitter and into a glass fibre. The glass fibre guides the light to the spectrumanalyzer. This analyzer has a good sensitivity for wavelengths in the 465nm to 1650nm range. The resolution of the spectrumanalyzer is 5nm. The spectrum was averaged over 100 measurements. First the spectrum reflected by the backplane of the display without a cover glass on top of it is measured. This spectrum is stored in the memory of the spectrumanalyzer and is used as the reference spectrum without an interference pattern. Like this we are able to measure the spectrum reflected by the assembled display relative to the spectrum reflected by the backplane without any further calculation. This relative spectrum will have the interference pattern required for determining the cell gap. The measurements from the spectrumanalyzer are transferred to a PC for further analysis.

Two types of displays are used in the experiments. One type has the same cross section as in Fig. 2.6. Another type doesn't have an ARC layer between the ITO and the cover glass. In paragraph 3.3.2 to 3.3.4 the cell gap of the displays is measured before the displays are filled with LC so $n_{gap}d_{gap} \cong d_{gap}$.

3.3.2 Cell gap based on the interference spectrum

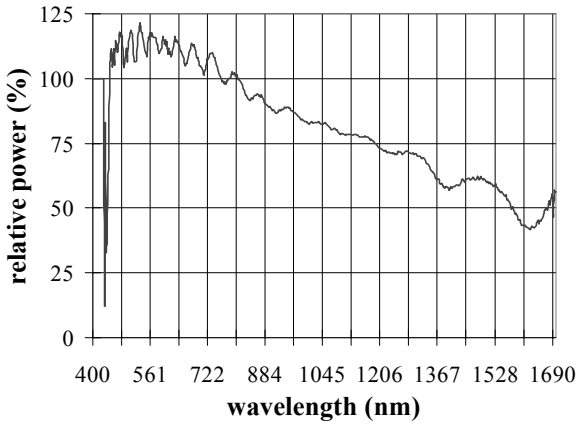

Fig. 2.8: Example of a measurement. The reflected spectrum of the display is measured relative to the spectrum reflected by the Al backplane.

The first method to determine d_{gap} is based on Eq. (2.7) and Eq. (2.8). An example of the measured spectrum $|R(\lambda)|^2$ clearly shows several extrema (Fig. 2.8).The cell gap was determined based on Eq. (2.7) with the highest possible value for x. This means the values for λ_1 and λ_2 refer to the highest and lowest wavelength respectively corresponding with an extremum in the measured spectrum $|R(\lambda)|^2$. This method is referred to as the Two Peaks Method (TPM) in the rest of this PhD. The results are in the 2 columns on the left of Table 2.1. Displays 1 and 2 have 4.71μm spacers, displays 3 and 4 have 3.10μm spacers.

Because the detected spectrum has several peaks (Fig. 2.8), we are able to determine a series of d_{gap} values based on Eq. (2.8). Using Eq. (2.8) the cell gap is determined based on the wavelengths corresponding with neighbouring maximums and minimums (x=2 in Eq. (2.7)). As can be seen in Fig. 2.8 some peaks are not easy to determine accurately, for instance for wavelengths shorter than 450nm and for wavelengths in the 1045nm to 1206nm range. This is due to noise in the light source and the detector,

absorption in the ITO and ARC layer, cell gap variation in the measurement spot and because we do not have a simple double layer structure as in Fig.

	TPM		MPM		
Display	Cell gap d_{gap} (nm)	Distance between two extrema, x	Average cell gap d_{gap} (nm)	99% error margin Δ (nm)	No. of values, n
1	4962	27	4950	309	28
2	6044	27	5986	450	25
3	3210	20	3198	240	18
4	3540	19	3626	138	20

Table 2.1: This table contains the results of the cell gap determination.

2.4 but a multilayer structure as in Fig. 2.6. This may result in some non plausible values for the cell gap d_{gap}. After having eliminated these values a statistical analysis of the rest of the d_{gap} values is made based on the Student distribution and the 99% error margin Δ is determined (Table 2.1). The Student distribution is similar to the normal distribution and it is used when the number of values n for a certain unknown (in this case the cell gap d_{gap}) is less than 30. The chance that the real value of the cell gap d_{gap} is within the interval $d_{avg} \pm \Delta$ is 99% where

$$\Delta = t_{995} \frac{s}{\sqrt{n-1}} \qquad \text{Eq. (2.13)}$$

$$s = \sqrt{\frac{\sum_{i=1}^{n} (d_{avg} - d_i)^2}{n}} \qquad \text{Eq. (2.14).}$$

t_{995} is the typical statistical unit of the Student distribution and depends on the number of values n. t_{995} decreases as the number of values n increases (t_{995} =63.66 for n=2 and t_{995} =2.76 for n=30). d_i for i=1 to n are the different calculated values for the cell gap with an average value $d_{avg.}$ This method is

referred to as the Multiple Peaks Method (MPM) in the rest of this PhD. The 3 columns on the right in Table 2.1 show the results for 4 displays.

3.3.3 Method based on the Fourier Transform

A second method to determine the cell gap d_{gap} is based on the FT of $|R(1/\lambda)|^2$ (see Eq. (2.9)). A discrete FT of $|R(1/\lambda)|^2$ is calculated based on the Fast Fourier Transform (FFT). For the FFT of $|R(1/\lambda)|^2$ (referred to as $|R(k*F_0)|^2$) we use the spectrum between the wavenumbers $(1653.2\text{nm})^{-1}$ and $(465\text{ nm})^{-1}$. Like this we have a spatial frequency resolution $F_0 = (465^{-1} - 1653.2^{-1})^{-1} = 647.0$nm in the spectrum of $|R(k*F_0)|^2$. The variable k is a natural value from 0 up to N-1. For a FFT N has to be a power of 2. In the performed FFT N=256. In Fig. 2.9 one can see the peak due to the cell gap as predicted by Eq. (2.9). Please note that only the positive spatial frequencies $k*F_0$ for k = 0 to 127 are displayed in the figures containing a FFT ((Fig. 2.9) and (Fig. 2.11)).

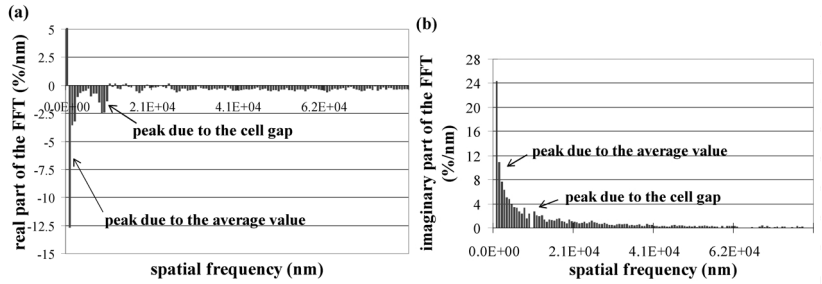

Fig. 2.9: Real part (a) and imaginary part (b) of the FFT of the measured spectrum $|R(1/\lambda)|^2$.

The peak at very low spatial frequencies in Fig. 2.9 is due to the wavelength dependency of the average value of $|R(1/\lambda)|^2$. We see that the peak due to the cell gap is almost absorbed by the peak due to the average value. This is especially true for small cell gaps because the peak frequency due to the cell gap decreases as d_{gap} decreases (see Eq. (2.9)). Like this the detection of the peak frequency for small cell gaps d_{gap} in the spectrum of the FFT of

$|R(1/\lambda)|^2$ could be a problem. This is solved by subtracting from $|R(1/\lambda)|^2$ its average value (Fig. 2.10). This average value is simulated by a polynomial of the form $a(1/\lambda)^2+b(1/\lambda)+c$ and is fit to the measured $|R(1/\lambda)|^2$. The subtraction of the average value from $|R(1/\lambda)|^2$ can be regarded as filtering the measured spectrum by an analogue high spatial frequency pass filter.

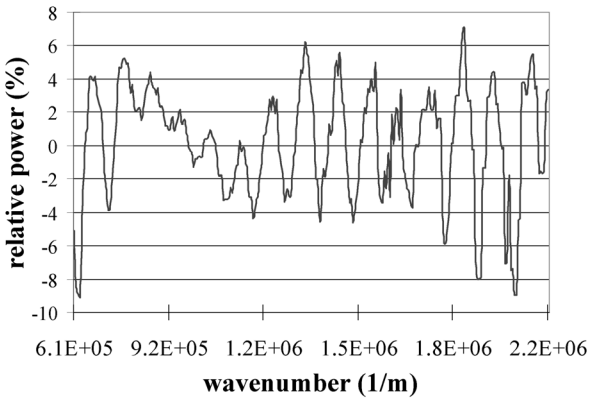

Fig. 2.10: Example of a spectrum $|R(1/\lambda)|^2$ after the average value is filtered out.

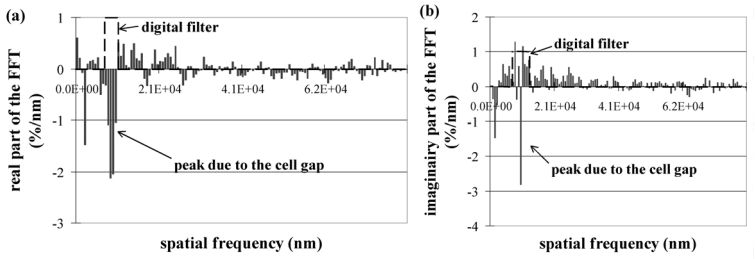

Fig. 2.11: Real part (a) and imaginary part (b) of the FFT of a spectrum $|R(1/\lambda)|^2$ after the average value is filtered out. Notice the better definition of the peak due to the cell gap compared to Fig. 2.9. The digital filter used for the Inverse FFT is indicated.

The result of the FFT of the analogue filtered $|R(1/\lambda)|^2$ (Fig. 2.11) results in a spectrum with a better defined peak compared to the FFT of the unfiltered

$|R(1/\lambda)|^2$ (Fig. 2.9). The results for the cell gaps corresponding to the peak spatial frequencies are in Table 2.2. A first remark is that the resolution F_0 of the spatial frequency of $|R(k*F_0)|^2$ is only 647.0nm. This means that we are only able to determine the cell gap d_{gap} with an accuracy of 647.0/2≅324nm since the peak spatial frequency f=2d_{gap}. This is why the peak spatial frequency is not necessarily the same for the imaginary part, the real part and the modulus of $|R(k*F_0)|^2$ (Table 2.2). The resolution of the FFT can be increased by measuring the interference pattern across a broader spectral range. Fig. 2.11 also demonstrates that the peak sometimes has a certain spread. This is caused by the noise of the light source and the detector and by the cell gap variation of the display in the measurement spot.

	FFT results: d_{gap} (nm) based on:			IFFT results (nm)	
Display	Re FFT	Im FFT	|FFT|	Average d_{gap}	99% error Δ
1	5179	4855	5179	4919	268
2	6150	5826	5826	6080	246
3	3236	2913	3236	3237	165
4	3561	3561	3561	3534	82

Table 2.2: Cell gap values determined with FFT and IFFT.

3.3.4 Method based on the Inverse Fourier Transform

A third method is based on the following idea. Due to the limited spatial frequency resolution of $|R(k*F_0)|^2$ and the spread in the peak frequency of $|R(k*F_0)|^2$ the peak in the spectrum $|R(k*F_0)|^2$ does not necessarily correspond with the cell gap value. However all the information to determine the cell gap is in the spectrum $|R(k*F_0)|^2$. By performing an Inverse FFT (IFFT) on $|R(k*F_0)|^2$ we obtain again the analogue signal as in Fig. 2.10. Before we perform the IFFT we filter out all the spatial frequencies in $|R(k*F_0)|^2$ that are not linked to the cell gap d_{gap} (Fig. 2.11). This analogue

signal will be free of noise allowing a more accurate cell gap determination based on MPM (see Table 2.2).

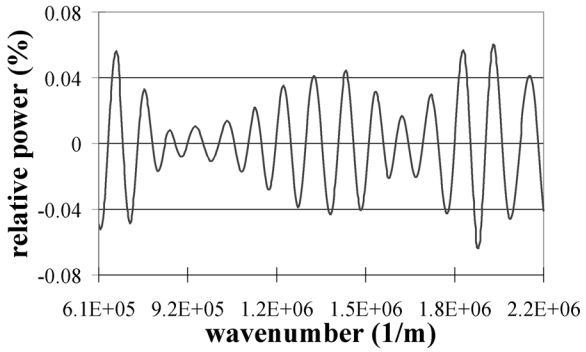

Fig. 2.12: Example of the IFFT of the digitally filtered $|R_2(k*F_0)|^2$.

The spatial frequencies in $|R(k*F_0)|^2$ that contribute to the cell gap are the peak frequency and its spread. The filtering of the spectrum $|R(k*F_0)|^2$ is done by multiplying $|R(k*F_0)|^2$ by the digital filter $|H(k*F_0)|^2$. $|H(k*F_0)|^2 = 1$ for the spatial frequencies that contribute to the cell gap and $|H(k*F_0)|^2 = 0$ for the other spatial frequencies (Fig. 2.11). The resultant analogue signal after performing an IFFT on $|R_2(k*F_0)|^2 = |H(k*F_0)|^2 * |R(k*F_0)|^2$ is displayed in Fig. 2.12. This analogue signal clearly has less noise than the analogue signal in Fig. 2.10. The cell gap determination and 99% error margin are determined in a similar way as with the MPM based on the Student distribution (Table 2.2).

3.3.5 Method based on an empirical model

The cell gap values in Table 2.1 and Table 2.2 are confirmed by fitting an empirical model to the reflected spectrum $|R(\lambda)|^2$ as described by Eq. (2.11) and Eq. (2.12) (Fig. 2.13). This means that the assumption is correct that the influence of the internal reflections on the interference pattern may be neglected. The accuracy of the fitted model is described by the correlation

factor (see Table 2.3). Displays 1 and 3 have an ARC between the ITO and glass layer, displays 2 and 4 do not.

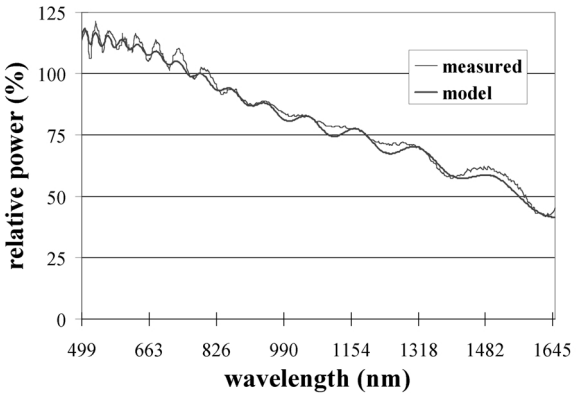

Fig. 2.13: Comparison between a measured spectrum and the empirical model for display 1.

Display	Cell gap d_{gap} (nm)	Correlation factor
1	4984	0.996
2	5836	0.982
3	3303	0.993
4	3468	0.981

Table 2.3: In this table we have the cell gap and the correlation factor between the measured spectrum and the fitted model.

3.3.6 Cell gap measurement of a filled LCD

The applicability of the measurement set-up for the measurement of the cell gap of filled displays is demonstrated for a display filled with PDLC. The LC molecules have to be aligned parallel to the incident light during the measurement as has been explained in paragraph 3.2.3. In the case of PDLC this is done by applying a voltage across the PDLC. A clear interference pattern is visible in the spectrum reflected by the filled display (Fig. 2.14). Only wavelengths in the visible spectrum are used for the calculation of the cell gap of the filled display. In this range of the spectrum the ordinary

refractive index of PDLC n_o = 1.527 [15]. The cell gap was calculated on 5 different spots on the display before and after the filling (Table 2.4) based on

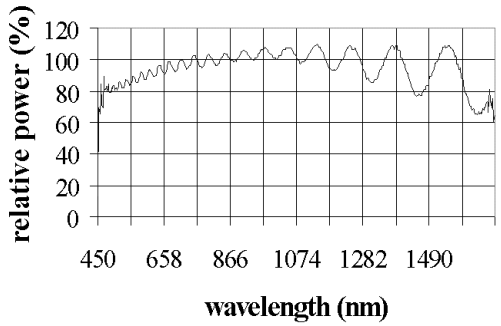

Fig. 2.14: Interference pattern in the light spectrum reflected by a display filled with PDLC.

	Cell gap (nm)	
Spot	Before filling	After filling
1	4589	4301
2	4521	4317
3	4510	4387
4	4346	4218
5	4570	4281

Table 2.4: Measured values for the cell gap on 5 different spots before and after the filling of the display with PDLC.

	Cell gap (nm)	
Method	Before filling	After filling
TPM	4589	4301
MPM	4578±647	4235±411
IFFT	4421±156	4174±246

Table 2.5: Comparison of the calculated cell gap values for the different methods before and after the filling of the display.

TPM. The cell gap on spot 1 was also calculated with some of the other methods (Table 2.5). When we compare the cell gap values before and after

the filling of the display we notice a reduction of the cell gap by an average of 200nm. This can be caused by the capillary forces during the filling of the display.

3.3.7 Error margin of the measurement set-up

Depending on the used method different values for the cell gap were calculated in the previous paragraphs. These values are not contradictory taking into account the statistical error margins. However it is not certain that the calculated values for the cell gap are indeed the real values for the cell gap. An independent measurement based on a measurement set-up different from the one in Fig. 2.7 is needed to verify this. One possible error in the measurements could be caused by the objective lens in the microscope. Due to this lens the display is illuminated by a convergent wave while the models for the calculation of the cell gap are based on a plane wave model. The convergence of the light wave is small and has a limited influence on the cell gap calculation. The only way to confirm this is with an independent measurement set-up.

An accurate calibration of the measurement set-up on a display is difficult because of the variation of the cell gap across the display. In this case the position of the measurement spot on the display is critical. It is also difficult

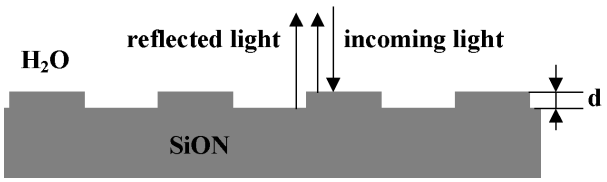

Fig. 2.15: Principle of the calibration: the thickness of the grooves *d* of the SiON grating is determined with the cell gap measurement set-up and the TENCOR alpha-step 200.

to find an alternative measurement set-up for an accurate cell gap measurement that is not based on light. That is why for the calibration of the measurement set-up a grating is used (Fig. 2.15). The use of a grating for the

determination of the error margin has two advantages. The first advantage is that the thickness of the grooves in the grating can be measured with an alpha-step 200 of TENCOR. The alpha-step 200 measures the profile of the grating by means of a stylus and with a resolution of 5nm. The second advantage is that the thickness of the grooves d in the grating can be made very accurately across a big surface. This is because the grating is made by Plasma Enhanced Chemical Vapour Deposition (PECVD) of SiON on a Si wafer and Reactive Ion Etching (RIE). The position of the measurement spot on the grating is less critical allowing a calibration with a higher accuracy. In the case the display is filled with LC the cell gap contains a medium with a wavelength dependent refractive index. During the measurements with the set-up of Fig. 2.7 the grating is submerged in water to simulate this. The refractive index of water is n_{water} = 1.33 at 20°C in the range of 589.32nm to 706.52nm [16]. The only disadvantage is that the method with the empirical model for LCDs (paragraph 3.2.2) since there are no multiple reflections in gratings. However it has already been proven in the previous paragraphs that the results obtained with the empirical model correspond with the results of the other methods.

Method	Groove thickness (nm)	Error margin (nm)
TPM	4128	–
MPM	4002	480
IFFT	4121	206
Tencor	4050	5

Table 2.6: Results of the groove thickness of the grating obtained with the cell gap measurement set-up and with the Tencor alpha-step 200.

The results of Table 2.6 show a good correspondence between the values of the gap obtained with the cell gap measurement set-up and the value obtained with the Tencor alpha-step 200. The statistical error margins seem to be a good measure for the error margin. The gap calculation based on TPM has the highest error. The error is 78nm or about 1.9% of the calculated

value of 4128nm. This is a good result compared with other measurement methods [5].

3.4 Discussion

In Table 2.1 and Table 2.2 we see a rather big difference in the 99% error margin for the different displays. The reason for this is that the accuracy of the measurement not only depends on the stability of the light source and the detector but also on the uniformity of the cell gap in the measurement spot. From a technical point of view there will always be some cell gap variation within a certain spot. The bigger the variation of the cell gap in the measurement spot is, the bigger the spread of the peaks in $|R(f)|^2$ will be (see Fig. 2.11). The calculated values of the cell gap should be regarded as an average value of the cell gap within the measurement spot.

A good knowledge of the ordinary refractive index n_o is required for the calculation of the cell gap of filled displays. This index may vary as a function of the wavelength especially for wavelengths outside the visual spectrum. In general n_o will be about 1.5 in the visual range [17]. The value of n_o is also temperature dependent. However the temperature during measurement can be controlled. Another aspect in the measurement of filled displays is the alignment of the LC molecules parallel to the incident light. This is not always easy to achieve especially for the LC molecules at the interface with other layers. These layers may be ITO or Al electrodes, alignment layers (TN and VAN), the polymer matrix (PDLC),... Especially in the case of PDLC this could be a problem. PDLC consists of LC droplets encapsulated in a polymer matrix. This means the ratio of the surface at the interface between LC and non LC (polymer) to the volume of the LC is the highest for PDLC compared to other LCs. A perfect alignment of the LC in PDLC is not evident. The influence of this effect on the accuracy of the cell gap calculation is investigated. This is done by illuminating the display with s-polarized light. If the LC is not perfectly aligned the display will reflect not only s-polarized light but also p-polarized light resulting in an error. An

analyzer in front of the detector blocks the p-polarized light. The cell gap is calculated based on the reflected s-polarized light. The results for the cell gap based on polarized light (Table 2.7) confirm the results based on non-polarized light (Table 2.5). This means that the effect of not perfect alignment of the LC doesn't introduce a significant error in the calculations and can be neglected.

Method	Cell gap (nm)
TPM	4254
MPM	4248±573
IFFT	4274±245

Table 2.7: Cell gap based on measurements with polarized light.

The methods based on the fitting of an empirical model and on FFT are not the most appropriate methods to calculate the cell gap of filled displays. It is hard to allow for the wavelength dependence in these methods or to restrict oneself to wavelengths where the refractive index is constant. Either the complexity of the measurements would increase a lot or the accuracy of the measurements would be reduced.

The accuracy of the measurements can be improved by optimizing the measurement. A first improvement would be the use of a light source that is more stable than the halogen lamp and still emits light across a broad spectrum. A stabilised xenon lamp could be a solution for this. A higher accuracy could also be obtained with a detector with a good sensitivity and signal to noise ratio across a broader spectrum. A third improvement would be to measure the spectrum of the light source and the spectrum reflected by the display simultaneously. The interference pattern is obtained by referencing the spectrum reflected by the display to the spectrum of the light source. The interference pattern would be independent from the stability of the light source if both spectrums are measured simultaneously.

Measurements have demonstrated that these methods are also applicable for transmissive LCDs. In a transmissive LCD the Al backplane in Fig. 2.6 is

replaced by a glass substrate with on top of it an ITO-layer (the ITO-layer is at the side of the cell gap).

3.5 Conclusion

The values for the cell gap calculated with the different methods correspond. The calibration of the measurement set-up indicates a relatively small error margin (less than 2%). The measurement of filled displays showed a good interference spectrum and acceptable cell gap values. In conclusion all of the proposed methods allow the calculation of the cell gap of LCDs. The statistical 99% error margin seems to be a good measure for the error margin between the calculated and the real cell gap. This error margin is the smallest for the cell gaps calculated with the IFFT. This is the result of the filtering techniques.

4 Analysis of the applicability of reflective displays for direct view applications

4.1 Introduction

Reflective displays are an important new display technology especially for mobile direct view applications. The energy consumption of these displays is low compared to transmissive LCDs because they don't require a backlight. Instead these displays use environmental light as a light source. The challenge for direct view reflective displays is that the contrast ratio and the reflectance have to be high for all illumination conditions.

There are already standards for measuring the influence of the environment on the contrast ratio and reflectance of emissive and transmissive displays [18-21]. However these standards focus on the measurement of glare and not on the applicability of reflective displays that use environmental light as the only light source. The challenge is to simulate the infinite number of types of illumination produced by the environment while keeping the measurement set-up relatively simple. The measurement set-up has to give a better insight in the applicability of any kind of reflective display technology. This would make it a tool to determine the impact of changes in display technology on the applicability of the display and to compare different display technologies.

4.2 Principle of the measurement set-up

All the different types of environmental illumination are basically made up of diffuse and directed light components. Another important factor in the illumination of the display is the position of the observer. Contrary to the emissive or transmissive displays the observer is on the same side of the reflective display as the illumination source. This means the observer can block the illumination of the display partially or even completely. Other

measurement set-ups don't take the observer into account [21]. This is comparable with the situation where the observer is at a very large distance from the display. This is not always the case especially not for mobile applications where the observer is close to the display. As a result a measurement set-up for diffuse (Fig. 2.17 and Fig. 2.18) and directed (Fig. 2.19) illumination is built. Both set-ups have the influence of the observer incorporated as will be explained further on.

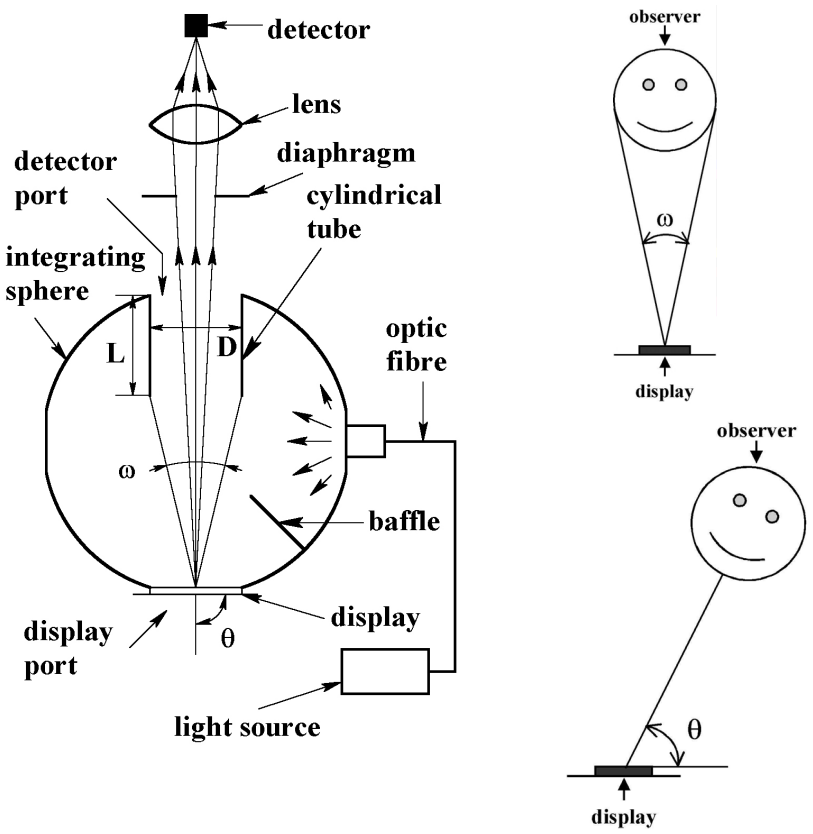

Fig. 2.17: Measurement set-up for diffuse illumination and an illustration of the angles ω and θ.

Fig. 2.17 illustrates the measurement set-up for diffuse illumination. The diffuse illumination is obtained by coupling light into an integrating sphere with an optic fibre. A halogen lamp is used as a white light source. The

display is placed at one opening of the sphere: the display port. Opposite to the display port is another opening in the sphere: the detector port. The detector port simulates the observer and will resemble a dark area because the environment outside the integrating sphere is dark. The detector, an avalanche photodiode, is at a distance from the detector port. By using a lens

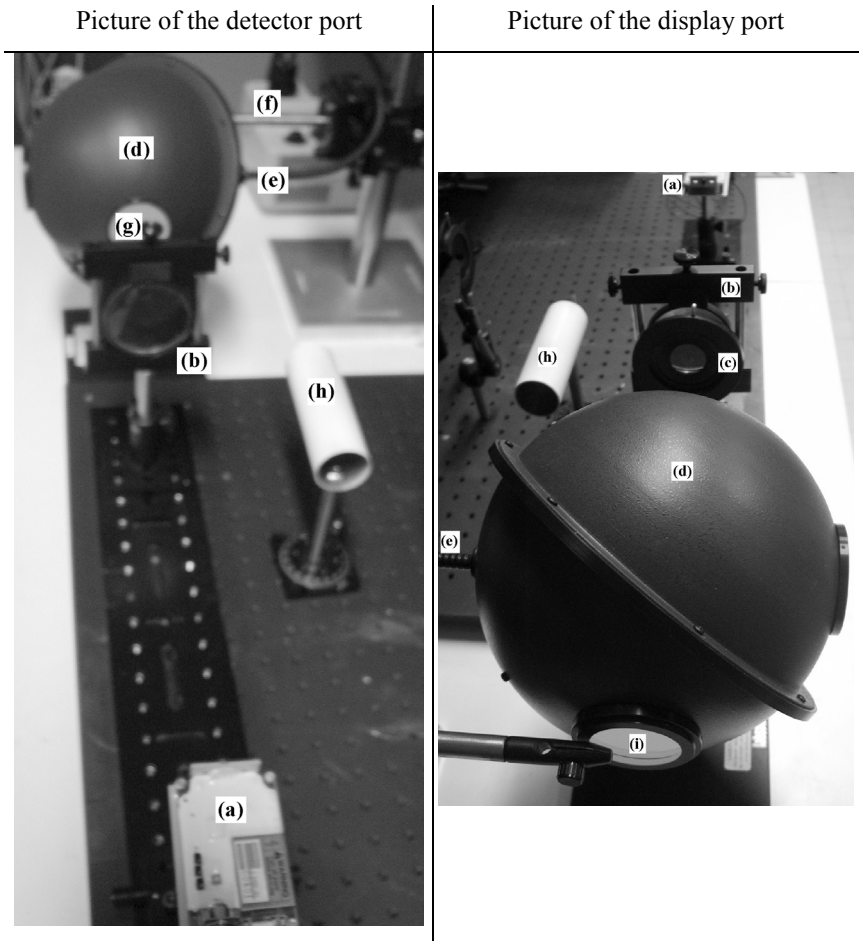

Fig. 2.18: Pictures of the measurement set-up for diffuse illumination showing the detector (a), lens (b), diaphragm (c), 8 inch integrating sphere (d), optic fibre (e), light source (f), detector port (g), unmounted cylindrical tube (h) and display port (i).

the detector only measures light coming from the display. The distance of the observer to the display is simulated by changing the dark area. The dark area is defined by the polar angle ω with $\omega=2\text{Arctg}[D/(2(d_{sphere}-L))]$ and d_{sphere}=diameter of the integrating sphere (Fig. 2.17). In the set-up of Fig. 2.17 ω is changed by changing the diameter D (for small ω's) of the detector port or by inserting a cylindrical tube with length L (for big ω's) in the sphere at the detector port. The outside of the cylindrical tube has a white scattering coating. This limits the influence of the cylindrical tube on the uniformity of the diffuse illumination. The closer the observer is to the display the bigger ω will be. The angle of inclination θ is the polar angle between the viewing direction and the display surface. By changing θ one changes the inclination angle of the display to the observer.

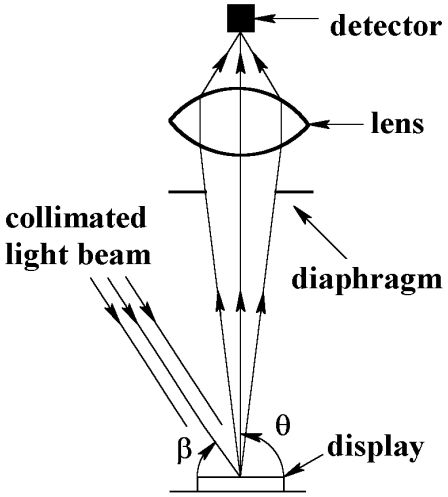

Fig. 2.19: Measurement set-up for directed illumination.

Fig. 2.19 illustrates the measurement set-up for a single source of directed illumination. The illumination source is a collimated light beam coming from a xenon light source. The light source is at the same side of the display as the detector, an avalanche photodiode. In the case of directed illumination the observer only blocks the illumination when the observer is in the path of

the light beam. This means that measurements with this set-up are only valid for situations where the observer is not in the path of the light beam.

4.3 Discussion

The measurement set-ups of Fig. 2.17 and Fig. 2.19 do not simulate all the possible illumination conditions. In reality the illumination can be a combination of directed and diffuse illumination with different luminance, light spectrum or obscuration. We would need an infinite number of set-ups to simulate all the possible combinations. Another solution would be to use the Bidirectional Reflectance Distribution Function (BRDF) of the light reflected by the display. Once the BRDF of a display has been determined for one type of illumination it is possible to determine the reflectance of the display for any other type of illumination [22-24]. The difficulty with this method is that one requires a good model of the reflectivity of the display. This shifts the problem from designing a relevant measurement set-up to the modelling of the displays, modelling of the illumination and the calculation of the reflectivity for different types of illumination.

4.4 Conclusion

A method has been devised to evaluate the applicability of reflective displays. The method is based on the fact that all light can be split in a diffuse and a directed component. Two measurement set-ups are used for the analysis of reflective displays: one for diffuse illumination and one for directed illumination. The influence of the observer is also incorporated in the measurement set-ups. This is important especially for mobile applications where the observer is close to the display. The observer may prevent major parts of the environmental light from reaching the display.

5 Conclusion

Three different aspects of the displays have to be characterized. The first is the characteristics of the PDLC and PNLC. The second is the cell gap of the display and finally the applicability of reflective displays in different environments with different types of illumination. Methods to measure these aspects are devised and respective measurement set-ups have been designed and built during this PhD.

References

[1] Bruyneel F., De Smet H., Vanfleteren J., Van Calster A., "Method for measuring the cell gap in liquid crystal displays", 2001, in *Optical Engineering*, **Vol. 40 No. 2**, pp. 259

[2] Bruyneel F., De Smet H., Van Calster A., Egelhaaf J., "Comparison of reflective PNLCDs and reflective single polarizer Heilmeier Guest Host displays", 2001, in *Journal of SID*, **Vol. 9 No. 4**, pp. 313-318

[3] Bruyneel F., De Smet H., Van Calster A., Egelhaaf J., "Measurement and evaluation of the applicability of reflective displays for direct view applications", 2000, in *Proc. 7th IDW*, pp. 45-48

[4] G. Rho, J. S. Kim, J. K. Kim, "Simultaneous measurement of pretilt angle and cell gap of LC cells by using an improved crystal rotation method", *ASIA DISPLAY 98*, pp. 245-248 (1998)

[5] K. H. Yoon, S. H. Ahn, J. H. Kim, W. Y. Kim, S. B. Kwon, "A novel method for measuring both the twist angle and the cell gap of LC cell using spectral analysis", *ASIA DISPLAY 98*, pp.1131-1134 (1998)

[6] S. T. Tang, H. S. Kwok, "A new method to measure the twist angle and cell gap of liquid-crystal cells", *SID 98 DIGEST*, pp. 552-555 (1998)

[7] J. Van den Steen, N. Carchon, G. Van Doorselaer, C. De Backere, J. De Baets, H. De Smet, J. De Vos, J. Lernout, J. Vanfleteren, A. Van Calster, "Technology and circuit aspects of Reflective PNLC microdisplays", *SID 97 DIGEST*, pp. 195-198 (1997)

[8] A. Van Calster, "Microdisplays for portable IT products and projection applications", *IDW '98*, pp. 135-138 (1997)

[9] C. Polhemus, "Two-Wavelength Interferometry", *Applied Optics*, Vol. 12, No. 9, pp.2071-2074 (1973)

[10] H. Kikuta, K. Iwata, R. Nagata, "Distance measurement by the wavelength shift of laser diode light", *Applied Optics*, Vol.25, No.17, pp. 2976-2980 (1986)

[11] R. Dändliker, R. Thalmann, D. Prongué, "Two-wavelength laser interferometry using superheterodyne detection", *Optics Letters*, Vol. 13, No. 5, pp. 339-341 (1988)

[12] M. Suematsu, M. Takeda, "Wavelength-shift interferometry for distance measurements using the Fourier transform technique for fringe analysis", *Applied Optics*, Vol. 30, No. 28, pp. 4046-4055 (1991)

[13] E. Fischer, E. Dalhoff, S. Heim, U. Hofbauer, H. J. Tiziani, "Absolute interferometric distance measurement using a FM-demodulation technique", *Applied Optics*, Vol. 34, No. 25, pp. 5589-5594 (1995)

[14] M. Hart, D. G. Vass, M. L. Begbie, "White-light measurement for high-performance liquid crystal spatial light modulators", *Proc. SPIE*, Vol. 3015, pp. 21-31 (1997)

[15] P. Nolan, E. Jolliffe, D. Coates, "Film formation parameters affecting the electro-optic properties of low-voltage PDLC films', *Proc. SPIE*, Vol. 2408, pp. 2-13 (1995)

[16] D. R. Lide, *CRC Handbook of Chemistry and Physics*, CRC Press, Boca Raton, pp. 10-287 (1990)

[17] W. Becker, *The Merck Group Liquid Crystal Newsletter No. 13*, Merck KGaAs, Darmstadt (1998)

[18] MIL-L-85762A, Military Specification, "Lighting, aircraft, interior, night vision imaging system (NVIS) compatible"

[19] ISO 9241 "Ergonomic Requirements for Office Work with Visual Display Terminals", Part 7 "Requirements for Displays with Reflections"

[20] M. Lindfors, "Accuracy and repeatability of the ISO 9241-7 test method", Displays, Vol. 19, Issue 1, pp. 3-16, 1998

[21] N. Umezu, Y. Nakano, T. Sakai, R. Yoshitake, W. Herlitschke, S. Kubota, "Specular and diffuse reflection measurement feasibility study of ISO9241 Part 7 method", Displays, Vol. 19, Issue 1, pp. 17-25, 1998

[22] John C. Stover, 1995, Scatter Predictions. In 'Optical scattering : measurement and analysis – 2nd edition", published by SPIE – The International Society for Optical Engineering, Bellingham, pp. 177-210

[23] E.F. Kelley, G.R. Jones, T.A. Germer, “Display reflectance model based on the BRDF”, Displays, Vol. 19, Issue 1, pp. 27-34, 1998

[24] E.F. Kelley, G.R. Jones, T.A. Germer “ The three components of reflection”, Information Display, Vol. 14, No. 10, 1998, pp. 24-29

CHAPTER 3:
Characterization of PDLC and PNLC for reflective displays

1 Introduction

PDLC and PNLC are two different materials but their optical principle is the same. The morphology of a PDLC layer is different from a PNLC layer. A Polymer Dispersed Liquid Crystal layer is a polymer layer with dispersed droplets of liquid crystal (Fig. 1.2). The droplets of liquid crystal are formed during the polymerization of the polymer. A Polymer Network Liquid Crystal layer consists of a polymer network that is submerged in a LC layer (Fig. 1.3). The LC molecules are not concentrated in droplets as is the case for PDLC. There are different types of polymerization depending on the type of polymer. For this research the prepolymer component in the PDLC mixture is PN393 of Merck. PN393 is in its turn a mixture of a photo-initiator and an acrylate type of monomer. The LC that is used, is TL213 of Merck. PNLC also has an acrylate type of monomer. The manufacturer of PNLC, Dainippon Ink & Chemicals, only supplies premixed mixtures of the prepolymer and the LC. The prepolymer and the LC can not be individually obtained. Other types of PDLC or PNLC have not been characterized since they were not commercially available at the time of the research. Since in the past a lot of research has been performed on the PDLC of Merck and the PNLC of DIC we expect these LCs to have the best performance.

For both PDLC and PNLC the prepolymer is polymerized by a Photoinitiated Polymerization-Induced Phase Separation (PIPS) process. The morphology of the PDLC and PNLC film determines the electro-optical properties of the PDLC and PNLC. The PDLC and PNLC layer has a different morphology depending on the temperature during curing, the

intensity of the UV illumination and the duration of the UV curing step. This research focuses on the influence of the UV cure time [1] and UV intensity on the electro-optical properties of the PDLC and PNLC displays. The results of different experiments are compared with what is known in literature. Other aspects like the polymerization process, the phase separation and the morphology of the polymer film and LC droplets are not analyzed. An extensive study of these aspects requires specialized equipment that was not present in the lab at the time of the PhD. The cell gap of the display also plays an important role in the electro-optical properties of the PDLC and PNLC, especially the switching voltage and the reflectance. A large cell gap results in a high reflectance. The downside of a large cell gap is the high switching voltage. How the electro-optical parameters are influenced by the cell gap is analysed in this PhD. Another aspect is the difference in LC alignment in the droplets in the bulk of the PDLC or PNLC layer and in the droplets at the interface with the electrodes. PDLC and PNLC with a cell gap below or above a certain value for the cell gap will behave very differently. The reason for this is the absence of bulk PDLC or bulk PNLC below a certain value of the cell gap [1,2]. The cover glass of the displays used for the characterization of the PDLC has an ITO electrode on one side and an anti reflective coating on the other side. The backplane of the displays consists of a flat Al electrode on glass.

Former research on PDLC and PNLC was mainly focussing on transmissive displays and displays with an absorber on the backplane. The use of PNLC and PDLC in displays with a reflective electrode is far from a general trend. However this approach has some considerable advantages. An analysis of the applicability of a single polarizer Guest Host Heilmeier reflective display and of a reflective PNLC display for direct view applications is made. The comparison of both display types demonstrates the advantages of LC based on the scattering of light, like PDLC and PNLC, in reflective displays with a flat Al reflector electrode [3,4].

2 Characterization of PDLC for reflective displays

2.1 Preparation of the PDLC mixture

The components of the PDLC mixture used in this Ph.D. research are supplied by Merck. These components are the prepolymer PN393 and the LC TL213. Merck recommends to mix these components in a ratio of 20%wt PN393 and 80%wt TL213 [5]. This ratio is used for all the PDLC mixtures

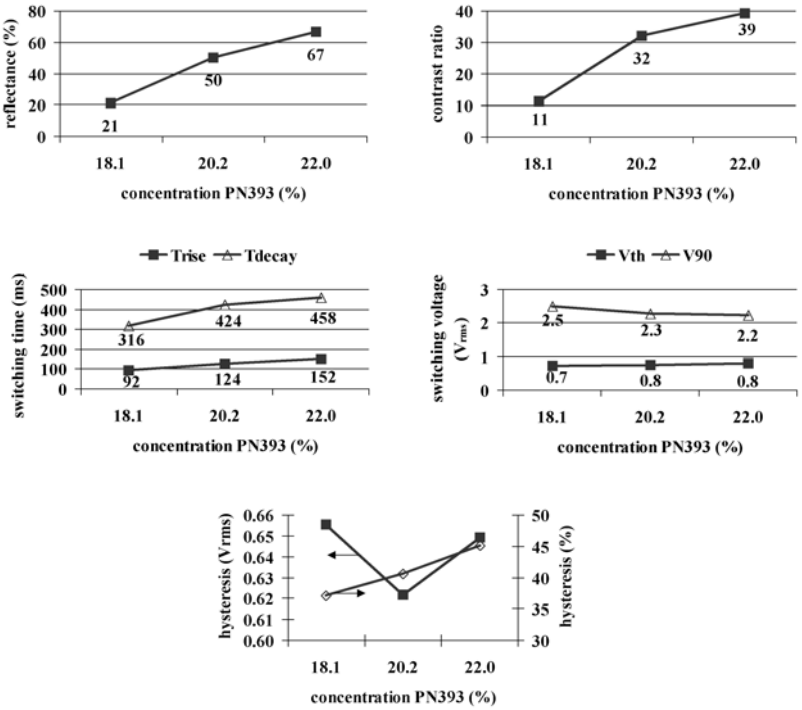

Fig. 3.1: Electro-optical properties as a function of the PN393 concentration in the PDLC mixture.

in the experiments. In case another mixture ratio is used some characteristics seem to improve while others deteriorate. This is also the conclusion of a comparison of the electro-optical properties of PDLC with different mixture

ratios (Fig. 3.1). In these experiments the electro-optical properties are measured of PDLC containing 18,1%wt, 20,2%wt and 22,0%wt PN393. The PDLC is cured with a Hg lamp and with an UV intensity of 12,5mW/cm^2 for 180s. The cell gap of the displays is 5,3µm.
PDLC with 18,1%wt PN393 has the smallest switching times. On the other hand PDLC with 22,0%wt PN393 has the highest contrast, reflectance and lowest switching voltage. A concentration of PN393 below 20,2%wt seems to have a big impact on the electro-optical properties of PDLC. The electro-optical properties are less sensitive to the concentration of PN393 once this concentration is higher than 20,2%wt. The suggestion of Merck to use PDLC with 20,2%wt PN393 is a good compromise for the electro-optical properties.

2.2 Influence of the UV parameters

2.2.1 Spectrum of the UV light sources

In general the curing of the PDLC and PNLC is characterized by the cure time and the UV intensity at 360nm. We have found that this is not sufficient to characterize the curing. PDLC displays cured with the same UV intensity and cure time show different electro-optical characteristics when using illumination sources with a different UV spectrum. The UV spectrum of the light source seems to play an important role in the PIPS. In our experiments two different types of UV light sources are used for the curing of PDLC and PNLC. One has a 200W Hg lamp and the other has a 200W HgXe lamp. The 200W Hg lamp is mounted in an aligner for microlithography. The 200W HgXe lamp is mounted in an UV spot light source. A specialized fibre system and lens system is used to transform the light output of the HgXe lamp into a collimated light beam. The HgXe light source has a 300nm-450nm reflector and a cut off filter for wavelengths larger than 600nm. The highest UV intensity at 360nm with the Hg lamp is only 12,5mWcm^{-2}. The HgXe lamp is capable of curing with higher UV intensities. In our

experiments UV intensities of up to 80mWcm^{-2} are used, although even higher UV intensities are possible with the HgXe light source.

	illuminination source for curing	
	Hg	HgXe
reflectance (%)	15	17
contrast ratio	14	9
V_{th} (V_{rms})	0.9	2
V_{90} (V_{rms})	3.3	7.5
T_{rise} (ms)	7	2
T_{decay} (ms)	270	140
hysteresis (V_{rms})	0.8	0.6

Table 3.1: PDLC characteristics cured with a Hg and a HgXe lamp cured with different UV curing times.

PDLC cured with the Hg light source and the HgXe light source show different characteristics (Table 3.1) using the same UV curing parameters: UV intensity of 8.6mW/cm^2 and a cure time of 180s. The UV intensity is measured with a photodiode with a peak sensitivity at 360nm.

The hysteresis and reflectance are more or less the same. The switching voltage V_{th} and V_{90} of PDLC cured with a Hg illumination source is half the switching voltage of PDLC cured with a HgXe light source. The opposite is true for the switching time T_{rise} and T_{decay}. The higher switching voltage and the lower switching speed of the PDLC cured with HgXe light source indicate that the droplet size is smaller for PDLC cured with a HgXe light source. Similar relations are found when comparing PDLC cured with different light sources as when comparing PDLC cured with different UV intensities (see next paragraph). The only remaining difference in the UV curing parameters is the used UV source. The measurements suggest that the curing power of the HgXe lamp is higher than that of the Hg lamp. It seems that the UV spectrum has an influence on the PDLC characteristics. A Hg lamp has a different spectrum from a HgXe lamp (Fig. 3.2). Both lamps have peaks in the UV spectrum for about the same wavelengths. When comparing

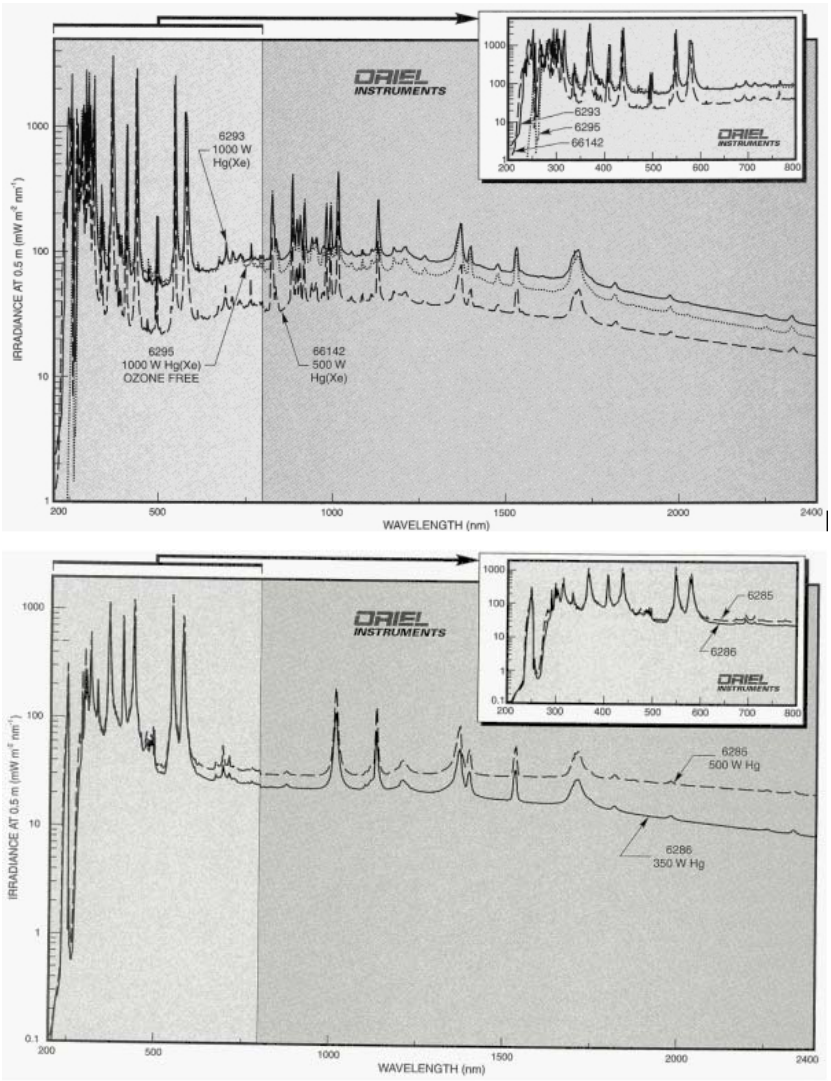

Fig. 3.2: The shape of the UV spectrum of a 500W Hg(Xe) lamp (top) is different from a 500W Hg lamp (bottom).

a 500W HgXe lamp with a 500W Hg lamp one sees that the peaks in the irradiance of the HgXe lamp are relatively higher to the main value of the irradiance than the peaks of the Hg lamp. The absolute values of the peaks in

the spectrum of the 500W HgXe lamp are also higher. The different shape of the UV spectrum makes it hard to measure and compare the UV intensity of different lamps even with a small bandwidth detector. This can be solved by mentioning not only the UV intensity and UV cure time but also the type of UV source used for the curing of the PDLC. In conclusion when specifying the UV parameters it is not only important to specify the UV intensity and UV cure time but also the type of UV source.

2.2.2 UV intensity

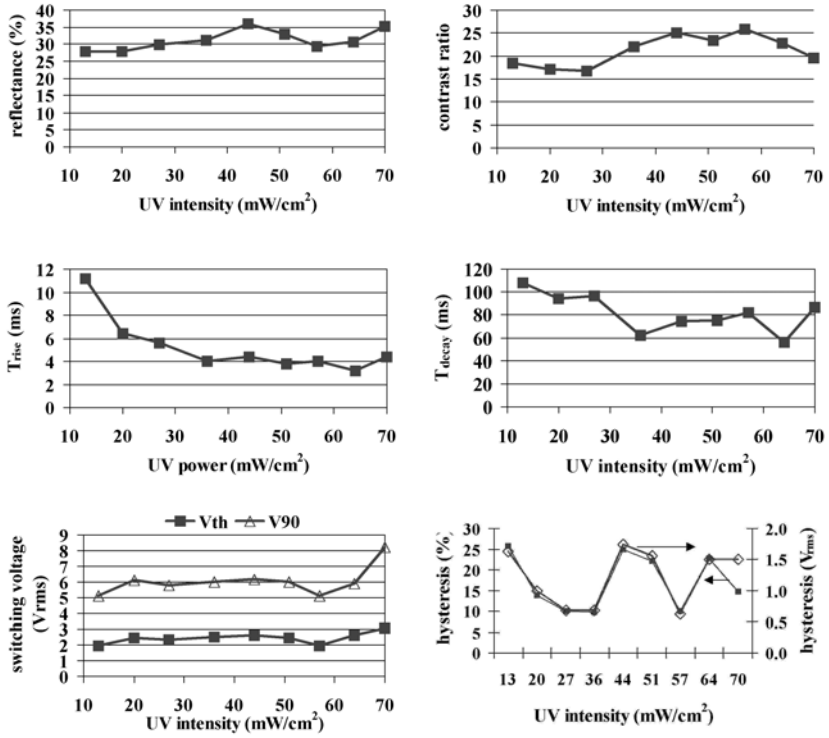

Fig. 3.3: Electro-optical properties of PDLC cured with a HgXe light source and different UV intensities using an IR filter.

The influence of the UV intensity on PDLC is analyzed by measuring the opto-electrical properties of PDLC displays cured with a constant UV energy

of 1550mJcm^{-2}. In this paragraph the PDLC is cured with a HgXe illumination source. The intensity of the UV illumination is controlled by changing the distance of the display to the illumination source. The UV intensity during curing is measured with a photodiode with a peak sensitivity at 360nm. The display cell gap is 4μm.

PDLC is cured with different UV intensities ranging from 13mWcm^{-2} to 70mWcm^{-2}. The reflectance, the contrast and the switching voltage seem to be only slightly dependent on the UV intensity. The general trend of these parameters is that their value slightly rises for higher UV intensities (Fig. 3.3). The switching times, T_{rise} and T_{decay}, are more sensitive to the UV intensity. The higher the UV intensity is the smaller the switching times are.

The UV intensity influences the speed of the polymerization during the PIPS. The higher the UV intensity the more polymerization processes will be initiated. Due to the smaller mesh size in the polymer matrix the LC molecules will migrate in smaller droplets during the PIPS. A smaller droplet diameter means that the number of LC to polymer interfaces the light has to pass before exiting the PDLC layer will increase. This explains the slight increase in reflectance for higher UV intensities. A smaller droplet diameter will result in a higher reorientation field *E* [6] with

$$E = \frac{1}{al}\sqrt{\frac{K\left(l^6 - 1\right)}{\varepsilon_0 \Delta\varepsilon}} \qquad \text{Eq. (3.1)}$$

and ε_0 = free space permittivity, $\Delta\varepsilon$ = dielectric anisotropy, *K* = an elastic constant expressing the elastic forces resisting the LC alignment parallel to the electric field and the surface anchoring forces at the LC-polymer interface, $l = a/b$ = shape anisotropy factor with *a* = major semi-axis of the LC spheroid and *b* = minor semi-axis of the LC spheroid. Because the displays used in the experiments of Fig. 3.3 all have the same cell gap the switching voltages will be higher for higher UV intensities. Higher reorientation fields mean that the threshold electric field E_{th} will also be higher.

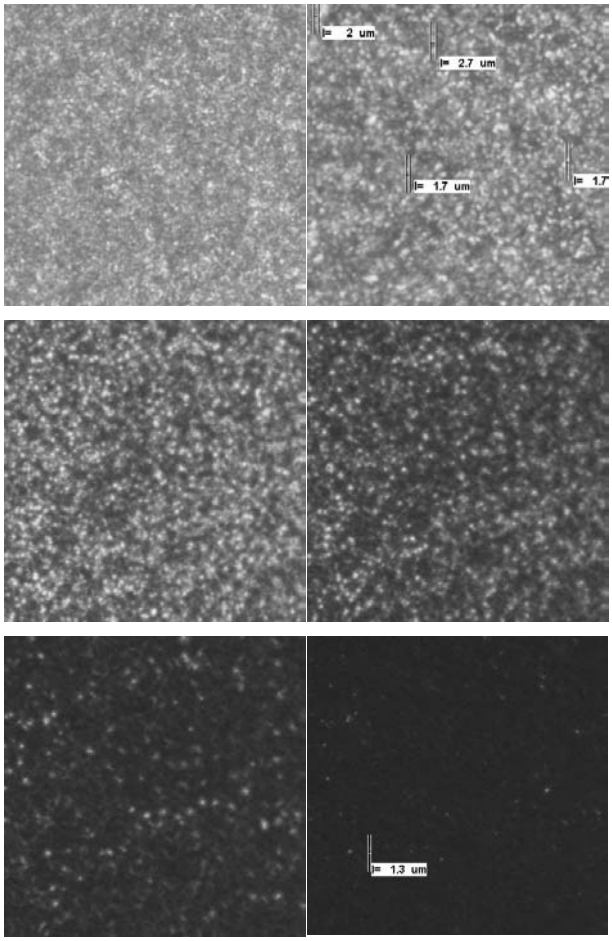

Fig. 3.4: Pictures of the transition of scattering PDLC (top left) to transparent PDLC (bottom right) taken with a microscope using crossed polarizers. The applied electric field in the PDLC rises from left to right and from top to bottom.

The influence of the droplet diameter on the reorientation field is also observed when switching the PDLC between the scattering state and the transparent state (Fig. 3.4). Pictures taken of PDLC with a microscope and crossed and parallel polarizers show that at low and intermediate voltage LC

droplets with intermediate and small diameters are scattering. At high voltage (>> V_{90}) only droplets with small diameters are scattering. So even at high voltage the reorientation field for these droplets is not high enough while other droplets with intermediate or big diameter have turned transparent.

According to the theory [7]

$$T_{decay} \cong \frac{2\gamma}{\varepsilon_0 \Delta\varepsilon E_{th}^2} \qquad \text{Eq. (3.2)}$$

$$T_{rise} \cong \frac{\gamma}{\varepsilon_0 \Delta\varepsilon \left(E_{appl}^2 - E_{th}^2\right)} \qquad \text{Eq. (3.3)}$$

with γ = rotational viscosity coefficient, ε_0 = free space permittivity, $\Delta\varepsilon$ = dielectric anisotropy and E_{appl} = applied electric field within the LC. Since E_{th} increases with increasing UV intensities the switching times, T_{rise} and T_{decay}, will decrease with increasing UV intensities. This is confirmed by the measurements (Fig. 3.3).

Hysteresis is influenced by a number of factors [8]. These include the difference in T_{rise} and T_{decay}, optical effects due to the difference in LC alignment when starting from the scattering state or the transparent state, defect structures in the LC droplets, internal electric fields in the PDLC film, surface anchoring or alignment effects,… However it is hard to predict the magnitude of the hysteresis or how to reduce it. The measurements show no trend between the UV intensity and the hysteresis. This confirms the results of Merck for displays with an absorber [5]. The random variation in hysteresis for different UV intensities can be explained for instance by the droplet anisotropy. In chapter 4, “Assembly and filling of PDLC and PNLC microdisplays”, it is shown that the cell gap of the PDLC displays may be unstable after the curing of the PDLC. The instability of the cell gap varies from display to display and is hard to predict. The instability of the cell gap will lead to a change in anisotropy of the droplet diameter. Since the cell gap

instability is random and hard to predict the anisotropy in droplet diameter and the hysteresis of the PDLC display will also be hard to predict.

The measurements on reflective PDLC displays regarding the relation between the UV intensity and the electro-optical properties are in line with previous reports in literature on transmissive displays and displays with an absorber. A high UV intensity reduces the LC droplet diameter. This results in higher reflectance, contrast and switching voltages and in shorter switching times.

2.2.3 UV cure time

The stability of the PDLC benefits from a higher UV curing time because more monomers will have polymerized [5]. The influence of the UV cure time on the stability of the PDLC characteristics is analyzed by curing the PDLC with an UV intensity of 44mWcm^{-2} using a HgXe light source. PDLC displays cured for UV cure times between 2s and 12s are measured.

The characteristics of the PDLC are measured for a first time immediately after curing. They are measured for a second time one week after curing. During this week the displays are stored in a container sealed from UV light. The measurements (Fig. 3.5) indicate that the reflectance is stable in time. The switching time and switching voltage are not stable in time, especially for cure times shorter than 6s. The general trend is that after 1 week the switching voltage has decreased while the switching time has risen. The relation between the switching voltage and the switching time can be explained by Eq. (3.2) and Eq. (3.3). The polymerization continues after the curing especially for cure times < 6s. This polymerization doesn't change the droplet diameter. This would explain only the evolution of the switching time and switching voltage but not the stability of the reflectance. A better explanation is that the polymerization changes the surface of the droplet's polymer wall. This would affect the surface anchoring energy and explain why the switching voltage and switching time changes while the reflectance remains stable.

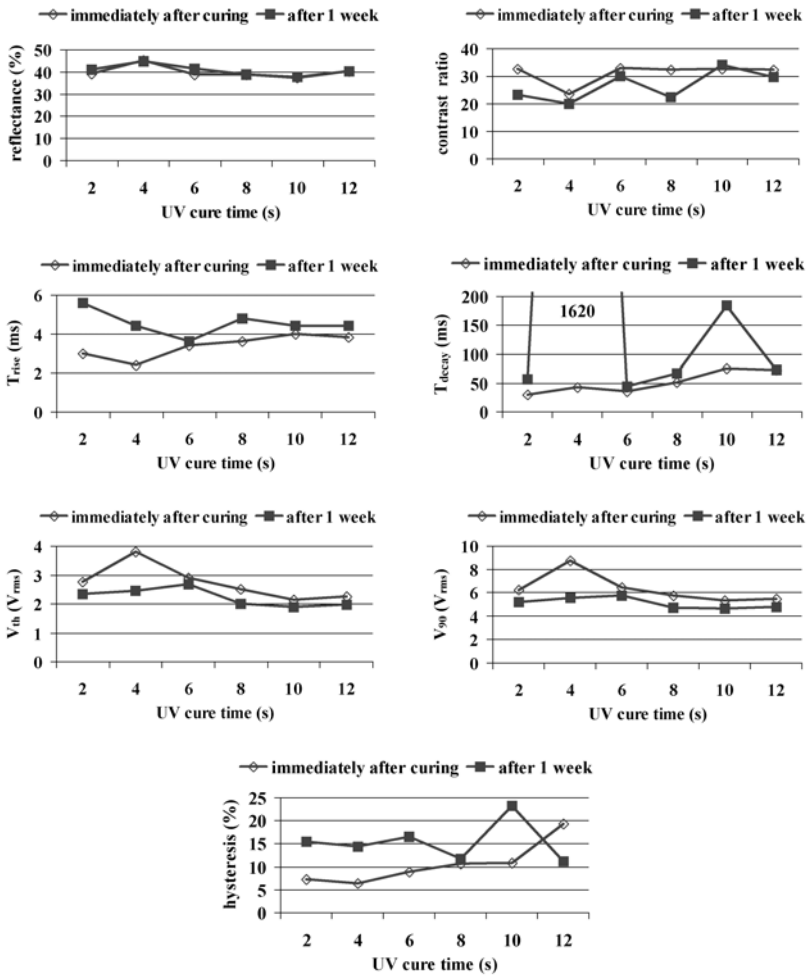

Fig. 3.5: Stability of the electro-optical properties of PDLC for short cure times.

To be certain that the polymerization process has stopped after the UV curing step the curing time has to be long enough. However it is found that the properties of the PDLC deteriorate when the UV curing time surpasses a certain value. This is due to a change in the LC properties. This narrows the process window especially when curing with high UV intensities. The next experiments show the effects of the over curing on the electro-optical

properties of the PDLC and how these effects are linked to a change in LC properties. The PDLC is cured with an UV intensity of 44 $mWcm^{-2}$ at 360nm using a HgXe light source.

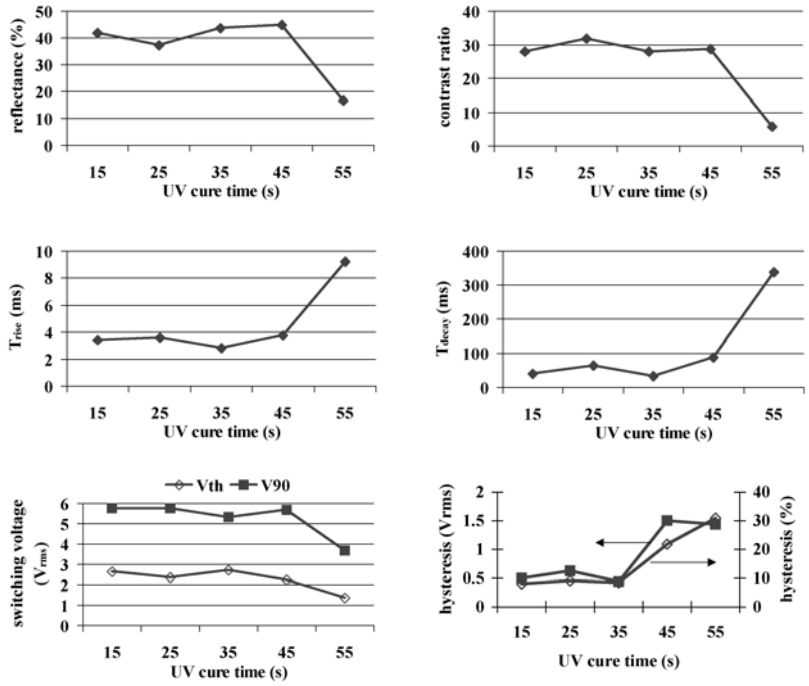

Fig. 3.6: Influence of overcuring on the electro-optical properties of PDLC.

The electro-optical properties of the PDLC are independent of the UV cure time for a cure time between 15s and 45s (Fig. 3.6). When the UV cure time rises to 55s the electro-optical properties change in a dramatic way. In general the properties deteriorate: the reflectance and the contrast ratio are reduced and the switching times are increased. The only advantage is the reduction in switching voltage.

Several analysis on the PDLC displays have been performed to determine the dramatic change in properties. Microscopic observation of the PDLC structure using parallel polarizers and crossed polarizers shows a clear difference between the PDLC cured for 45s or less and the PDLC cured for

55s (Fig. 3.7). The brightness of the pictures taken of the PDLC cured for 55s is less uniform compared to the PDLC cured for 45s or less. This difference is a lot more striking when one compares the pictures that show the regions where there is no scattering of light (Fig. 3.8).

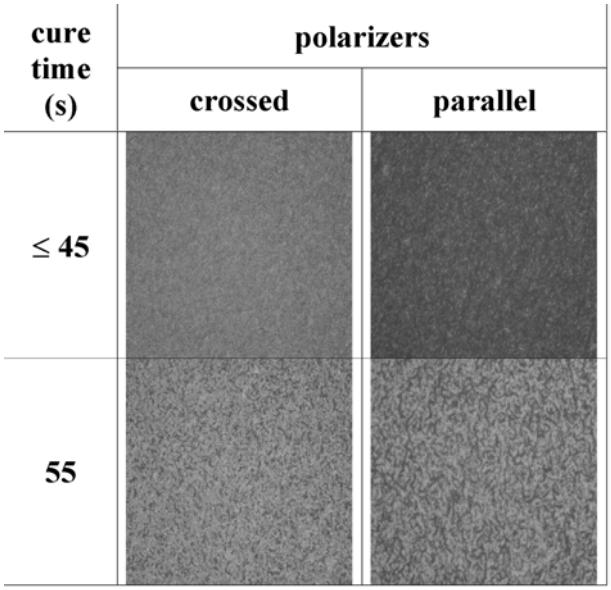

Fig. 3.7: Pictures of a typical PDLC structure with and without overcuring of the PDLC at zero voltage.

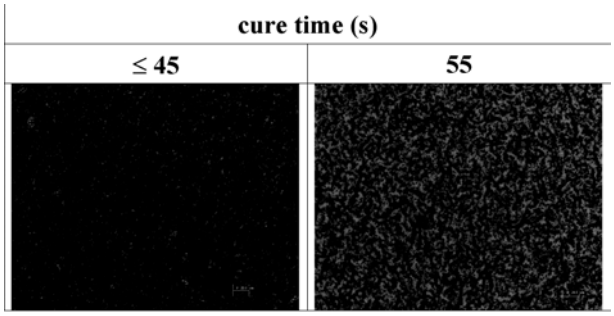

Fig. 3.8: Difference in the concentration of transparent (white) regions in the PDLC between normally cured and overcured PDLC.

These pictures (Fig. 3.8) are calculated based on the pictures taken with parallel and crossed polarizers at zero voltage (Fig. 3.7). The goal of this

calculation is to have pictures that clearly show the regions where incoming light is not polarized. These are the regions where the PDLC is transparent. Transparent PDLC will be white in the pictures taken with parallel polarizers and black in the pictures taken with crossed polarizers. Using Paint Shop Pro © 7.0 these regions can be calculated by subtracting the pictures taken with crossed polarizers from the pictures taken with parallel polarizers. The result is a picture with white regions that coincide with transparent PDLC. Fig. 3.8 shows a much higher concentration of transparent regions for PDLC cured for 55s than for PDLC cured for 45s or less. This explains the strong reduction of the reflectance for over cured PDLC.

The dramatic change in electro-optical properties and the presence of non scattering regions in the PDLC show some similarities with the effects resulting from vertical LC alignment due to cell gap expansion or the properties of the LC droplets near the display electrodes (see paragraph 2.3:

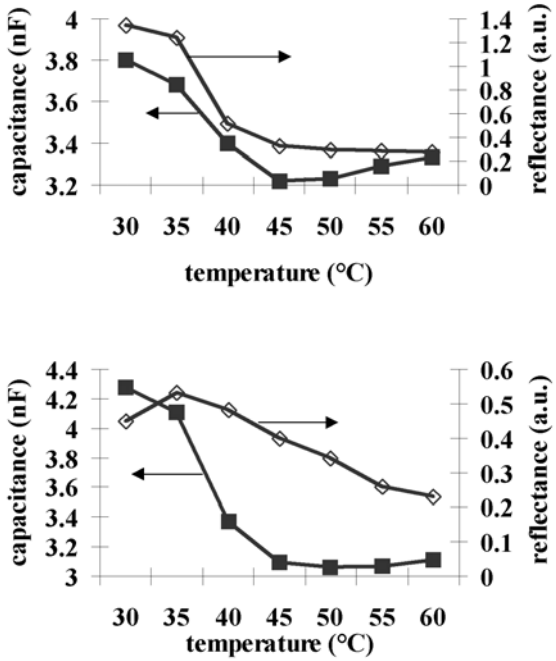

Fig. 3.9: Temperature dependency of the reflectance and capacitance of normally cured PDLC (top) and over cured PDLC (bottom).

"Influence of the cell gap"). Another reason could be an increase in droplet diameter. Cell gap expansion only seems to be possible due to thermal expansion of the polymer during the curing of the PDLC. The temperature of the display rises with about 2°C after 15s and 7°C after 55s of UV curing with an UV intensity of 44mWcm^{-2}. Cell gap measurements on dummy displays filled with the prepolymer PN393 show no change in cell gap within that temperature range that could result in a vertical LC alignment. The capacitance and the reflectance of the displays are measured to check whether the change in electro-optical properties is due to a change in LC alignment.

A change in capacitance means a change in dielectric constant. An abrupt change in capacitance indicates a change in LC orientation. Independent on how long the PDLC has been cured the capacitance shifts to another level between 30°C and 45°C (Fig. 3.9). This means the LC changes orientation in this temperature range and as a consequence the reflectance should also shift in a similar way. This is the case for PDLC UV cured for 45s or less (Fig. 3.9). This is not the case for the PDLC cured for 55s (Fig. 3.9). The abrupt change in capacitance (LC orientation) doesn't result in an abrupt change of the reflectance. The fact that there is no abrupt change in reflectance similar to the change in capacitance (LC orientation) can only be explained by a reduced anisotropy in refractive index of the LC molecules. In conclusion the long UV exposure has damaged the LC molecules.

The change in electro-optical properties due to over curing is not typical for PDLC. Similar materials like PNLC show similar behaviour (paragraph 3 "Characterization of PNLC for reflective displays"). It is believed that this behaviour is also due to damaged LC. Damage to the LC also explains the change in switching time and switching voltage. Both are linked to the anchoring energy between the LC and the polymer [7, 8]. If the LC material changes then so will the anchoring forces between the LC and the polymer

surface. The reduction of the switching voltages and the increase in switching time can both be explained by a reduction of the anchoring energy. The UV cure time has to be long enough to obtain stable PDLC properties. However the LC in the PDLC mixture is damaged when the UV cure time is too long. This results in a deterioration of most of the PDLC properties. The change in PDLC properties as a function of the UV cure time is abrupt and determines the maximum cure time.

2.3 Influence of the cell gap

2.3.1 Results of the experiments

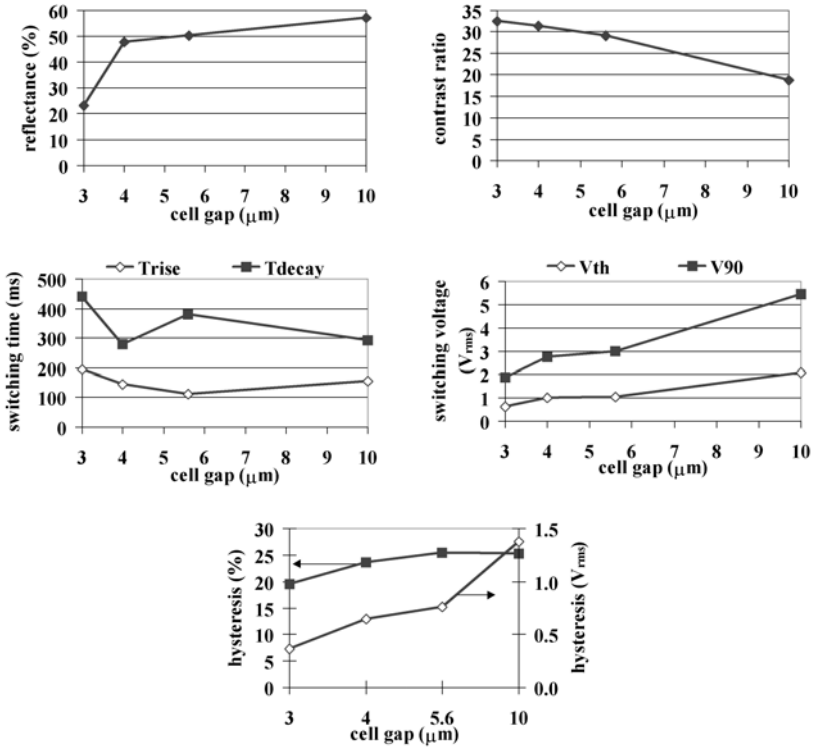

Fig. 3.10: Influence of the cell gap on the electro-optical properties of PDLC.

The PDLC is cured for 180s with an UV-intensity of 12.5mW/cm^2 using a Hg lamp. Fig. 3.10 illustrates the influence of the cell gap reduction on the switching voltages. For a display with 3µm spacers V_{th}=0.6V_{rms} and V_{90}=1.9V_{rms}, for a 10µm display V_{th}=2.1V_{rms} and V_{90}=5.5V_{rms}. The linear relation between the switching voltages, V_{th} and V_{90}, and the cell gap corresponds with the theory that the electric reorientation fields in PDLC films is not determined by the cell gap (Eq. (3.1)). The electric field corresponding with V_{th} and V_{90} is E_{th}≅0.22V/µm and E_{90}≅0.55V/µm respectively for a cell gap ≥ 5.6µm. These values are smaller compared to other PDLC displays [5] where E_{th}≅0.38V/µm and E_{90}≅0.61V/µm for a cell gap ≥ 5µm. For a cell gap of 3µm E_{th} has decreased to a value of 0.2V/µm. The reason for this decrease will be explained further on in this paragraph.

The contrast ratio increases as the cell gap decreases (Fig. 3.10). For a display with a cell gap of 3µm the contrast ratio is 33. This is a good result if we compare this with other reflective displays like reflective TN or STN [10].

The hysteresis determines the number of greyscales the display is able to display [11]. The reduction of the cell gap reduces the hysteresis (Fig. 3.10). The reason for this decrease will be explained further on in this paragraph.

For the measurement of T_{rise} an electric field E_{appl}=2E_{90} is applied. T_{rise} and T_{decay} depend on E_{th} (Eq. (3.2)) and E_{th}≅0.22V/µm for all cell gaps ≥ 5.6µm (Fig. 3.10). So it is no surprise that T_{rise} and T_{decay} do not depend a lot on the cell gap for displays with a cell gap ≥ 5.6µm (Fig. 3.10). The switching times for a 3µm cell gap are longer than for a display with a cell gap ≥ 5.6µm. This can be explained by the smaller E_{th} for displays with a 3µm cell gap. According to Eq. (3.2) and Eq. (3.3) a decrease in E_{th} results in an increase of T_{rise} and T_{decay}.

The reflectance of a 10µm display (57%) drops to 48% for a 4µm display (Fig. 3.10). This linear dependency (the reflectance increases with 1.5%/µm) is also measured in [5] for displays with a cell gap between 5µm and 20µm.

The reflectance of a 4μm display (48%) drops to 23% for a 3μm display. This drop is big compared to the drop in reflectance for a 10μm to a 4μm display. This will be discussed further on in this paragraph.

2.3.2 Discussion

The reduction of the cell gap has a positive influence on the switching voltage, contrast ratio and hysteresis and a negative influence on the reflectance. The cell gap has almost no influence on the switching time for cell gaps ≥ 4μm. The switching voltage and the switching time for cell gaps ≥ 4μm seem to be in line with the theoretical models. The contrast ratio is higher for a smaller cell gap because the reduction of the light intensity of the PDLC in the scattering state is smaller than for the PDLC in the transparent state. The hysteresis is caused by the anchoring energy of the LC molecules at the interface with the polymer matrix, defect structures in the droplets, internal electric fields,... [8] The strong reduction of the hysteresis for a cell gap ≤ 4μm is caused by a change in the alignment of the LC at the interface with the polymer matrix. This can be concluded from the following observations.

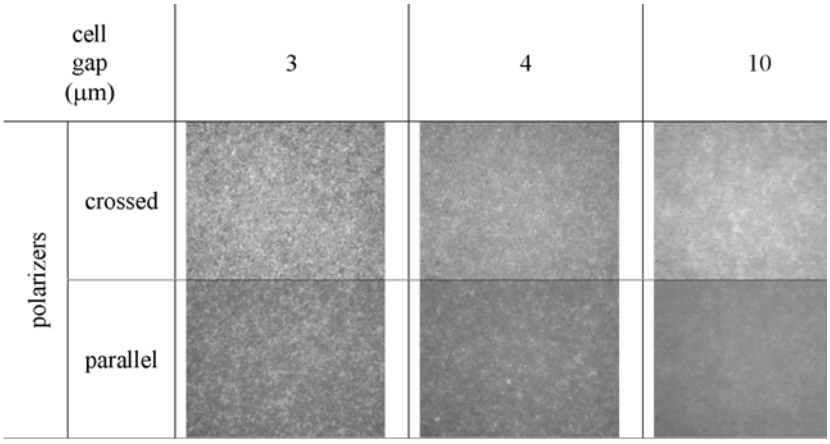

Fig. 3.11: Pictures taken with a microscope using crossed and parallel polarizers show a reduction of the uniformity of reflectance of the PDLC structure for a cell gap of 3μm.

There is a big difference in reflectance between a 4µm display and a 3µm display. Especially if we compare this difference with the difference in reflectance between a 10µm display and a 4µm display. Observation of the PDLC shows a uniform reflectance for 10µm displays (Fig. 3.11). This is not the case for 3µm displays. Bright and dark regions appear all over the PDLC in a 3µm display. Closer observation of the 3µm PDLC shows areas that are dark when viewed with crossed polarizers and bright when viewed with parallel polarizers. This indicates that there are areas in the 3µm PDLC display with little or no scattering of light.

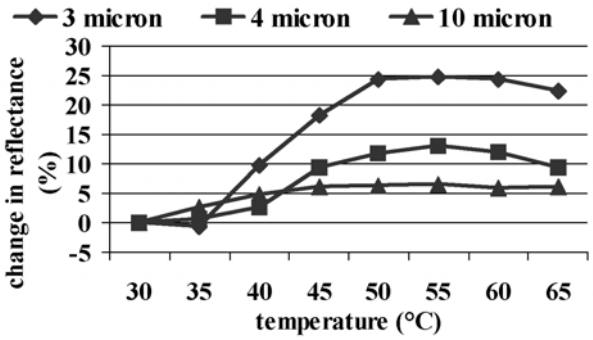

Fig. 3.12: Influence of the temperature on the reflectance of PDLC displays with different cell gaps relative to the reflectance at 30°C.

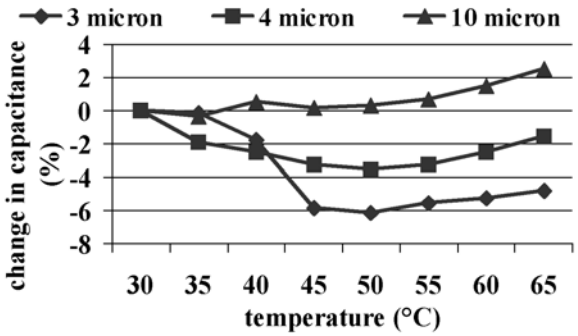

Fig. 3.13: Influence of the temperature on the capacitance of PDLC displays with different cell gaps relative to the capacity at 30°C.

The reflectance (Fig. 3.12) and the capacitance (Fig. 3.13) of the PDLC displays depend on the temperature and the cell gap. There is an increase in reflectance as the temperature rises from room temperature independent of the value of the cell gap. The maximum increase in reflectance is higher for displays with smaller cell gaps. For a 10µm cell gap the reflectance of the display has a maximum increase of 7% compared to the reflectance at 30°C. For a 3µm cell gap the maximum increase is 25%. The temperature dependent behaviour of the capacitance of the PDLC display also differs a lot for the different cell gaps. The capacitance of a 10µm display is slightly reduced at 35°C compared to the capacitance at 30°C and increases slowly for temperatures higher than 35°C. However a 3µm display has an abrupt reduction of the capacitance between 35°C and 45°C. For temperatures higher than 50°C the capacitance slowly increases. This is due to the temperature dependency of the dielectric constant of the PDLC film. Measurements of the cell gap with the set-up described in the paragraph "Measurement of the cell gap in liquid crystal displays" in chapter 2 indicate that the change in capacitance and reflectance is not caused by a change in the cell gap.

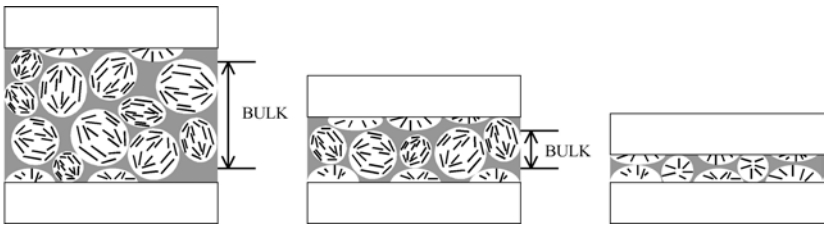

Fig. 3.14: Cross section of a PDLC layer showing the reduction and disappearance of the bulk layer as the cell gap is reduced (from left to right).

The abrupt change in capacitance between 35°C and 45°C for a 3µm display can be explained by a change in the alignment of the LC molecules at the interface with the polymer matrix [12]. The LC molecules at the interface

with the polymer matrix are aligned perpendicular to the polymer matrix at 30°C (Fig. 3.14). These LC molecules align parallel to the polymer matrix for temperatures higher than 45°C. This transition only occurs in the LC droplets at the interface with the ITO and Al layer. In the LC droplets in the interior (bulk) of the PDLC film the LC molecules at the interface with the polymer matrix are aligned parallel to the polymer matrix. The 3μm display has a lot of LC droplets that are in contact with the ITO or Al layer compared to 4μm and especially 10μm displays. First this explains why the drop in capacitance between 35°C and 45°C is larger for a 3μm display than for a 4μm display or even insignificant in the case of a 10μm display. Secondly this explains why the maximum increase in reflectance is relatively large for displays with small cell gaps. The different LC alignment between a 3μm and a 10μm display is also observed in Fig. 3.11. The drastic change in electro-optical properties between a 3μm and a 4μm PDLC display are typical for the explained change in LC alignment [12].

2.3.3 Conclusion

The alignment effect explains the strong reduction in reflectance from a 4μm display to a 3μm display and why the hysteresis, the switching times and the reorientation field deviate from the theoretical model for cell gaps ≤ 4μm. These PDLC characteristics depend on the alignment of the LC molecules at the interface with the polymer matrix. An alignment of the LC perpendicular to the interface with the polymer matrix results in lower hysteresis, higher switching times and a higher reorientation field compared to an alignment parallel to the interface with the polymer matrix.

2.4 Conclusion

The influence of the curing parameters and the cell gap have been analyzed for PDLC mixtures consisting of 20%wt PN393 and 80%wt TL213. In general the PDLC properties can be explained by earlier published work.

Exceptions are the characteristics of PDLC after over curing and the characteristics of PDLC displays with a 3μm cell gap. The reason for this unexpected behaviour is explained in this chapter.

The curing parameters and the display cell gap one chooses for the assembly of a reflective PDLC display depends on the required optical characteristics of the display and the voltage that can be generated by the driver electronics.

A cell gap of 4μm or higher shows good results. The smaller the cell gap the smaller the switching voltage and the higher the contrast ratio and this at only a small expense of the reflectance. A cell gap smaller than 4μm will reduce the switching voltage further more. The downside however is a strong reduction in the reflectance and a strong increase in the switching time due to a different LC alignment and PDLC morphology compared to PDLC displays with a cell gap higher than 4μm.

A wide range in UV curing parameters has only a small influence on the electro-optical properties. This suggests that the PDLC material of Merck is rather robust concerning UV curing parameters. The electro-optical properties do not change much for UV intensities in the range of 20mW/cm^2 to 60mW/cm^2 using a UV energy of 1550mJ/cm^2 using a HgXe light source. The same is concluded for UV cure times in the range of 6s to 45s using an UV intensity of 44mW/cm^2 using a HgXe light source. It is also found that the electro-optical properties depend on the type of light source (Hg or HgXe) used during curing.

3 Characterization of PNLC for reflective displays

3.1 Influence of the cell gap

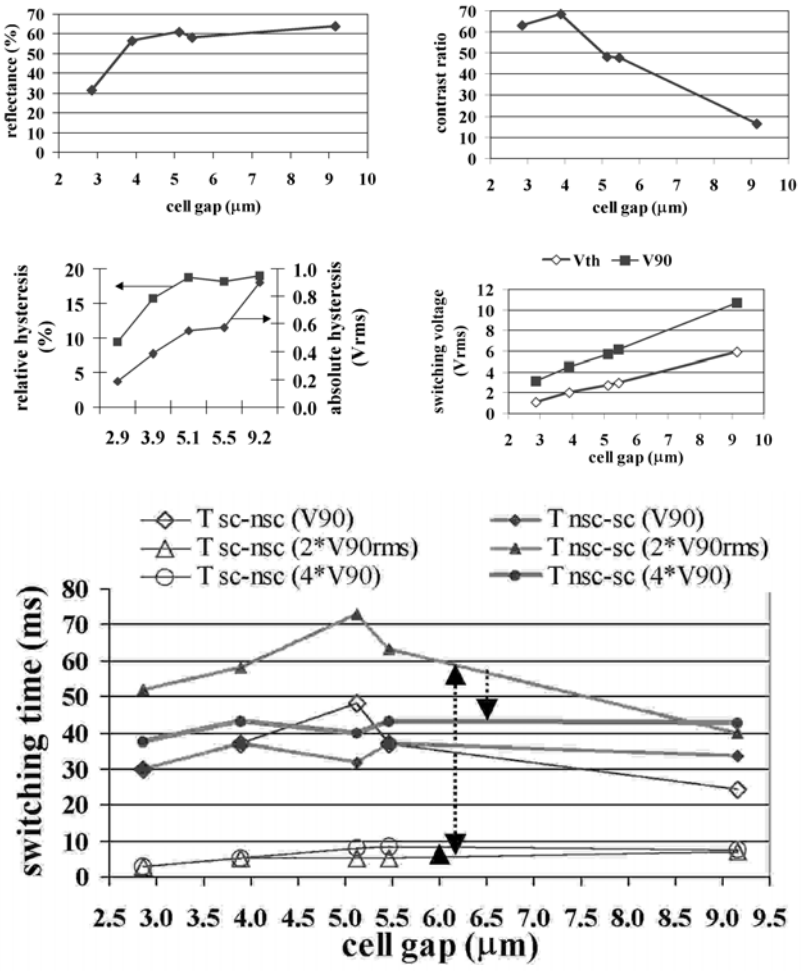

Fig. 3.15: Influence of the cell gap on the electro-optical properties. The arrows indicate the evolution of the switching time as a function of the switching voltage.

The PNLC is cured for 180s with an UV-intensity of 12.5mWcm^{-2} using an UV-filter filtering out all the wavelengths shorter than 345nm. According to the supplier of PNLC, Dainippon Ink & Chemicals, UV below 345nm damages the LC. The illumination source is an Hg lamp. The cell gap of the displays is measured with the set-up described in the paragraph "Measurement of the cell gap in liquid crystal displays" in chapter 2. In general the relationship between the cell gap and the electro-optical characteristics is similar for PDLC and PNLC. The reduction of the cell gap has some advantages.

The first advantage of the cell gap reduction is the reduction of the switching voltages (Fig. 3.15). For a display with a cell gap of 9.2µm, V_{90} = 10.7V$_{rms}$ and V_{th} = 6V$_{rms}$ while for a 2.9µm cell gap, V_{90} = 3.1V$_{rms}$ and V_{th} = 1.1V$_{rms}$. The reorientation electric field E_{th}≈0,53Vµm^{-1} for a cell gap in the 3.9µm to 5.5µm range. For a cell gap of 2.9µm E_{th}≈0,38Vµm^{-1}. Another advantage of reducing the cell gap is the reduction of the hysteresis (Fig. 3.15). Not only the absolute value but also the relative value of the hysteresis is reduced as the cell gap is reduced. A third advantage is that the switching time is shorter for a smaller cell gap (Fig. 3.15). The switching times are to a great extend determined by the applied electric voltage. When a voltage switching between 0V and an rms value of V$_{90rms}$ is applied $T_{rise} \approx T_{decay}$ (= 30ms for a 2.9µm cell gap). When the driving voltage is increased T_{rise} and T_{decay} show different behaviour. When the switching voltage increases to 2V$_{90rms}$, T_{rise} is reduced. In the case of a 2.9µm cell gap T_{rise} is reduced from 30ms to 3ms. The reduction of T_{rise} for a higher applied voltage confirms the theory of Eq. (3.3). A further increase of the switching voltage has no significant effect on T_{rise}. The increase in T_{decay} for a higher applied voltage is surprising. When the switching voltage is doubled from V$_{90rms}$ to 2V$_{90rms}$ T_{decay} will also roughly double except for a cell gap of 9.2µm. In the case of a 2.9µm cell gap T_{decay} rises from 30ms to 52ms. If the switching voltage is doubled from 2V$_{90rms}$ to 4V$_{90rms}$ T_{decay} will decrease instead of increase. In the case of a

2.9µm cell gap T_{decay} decreases from 52ms to 37.5ms. According to the theory of Eq. (3.2) T_{decay} does not depend on the applied electric field. The effect can be explained by defect structures in the PNLC also called a "stuck" disclination (Fig. 3.16) [8]. The theory of Eq. (3.2) does not take this effect into account. LC molecules in the area connecting two LC domains

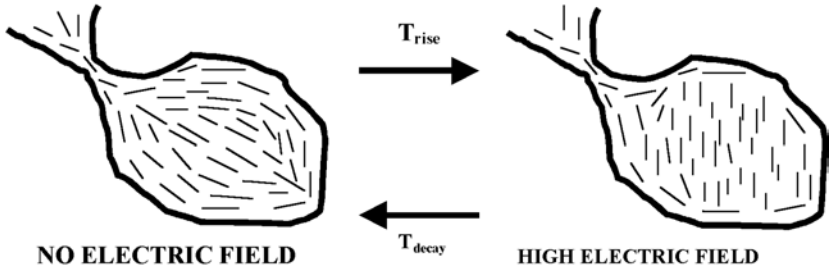

Fig. 3.16: Droplet structure sensitive to stuck disclination.

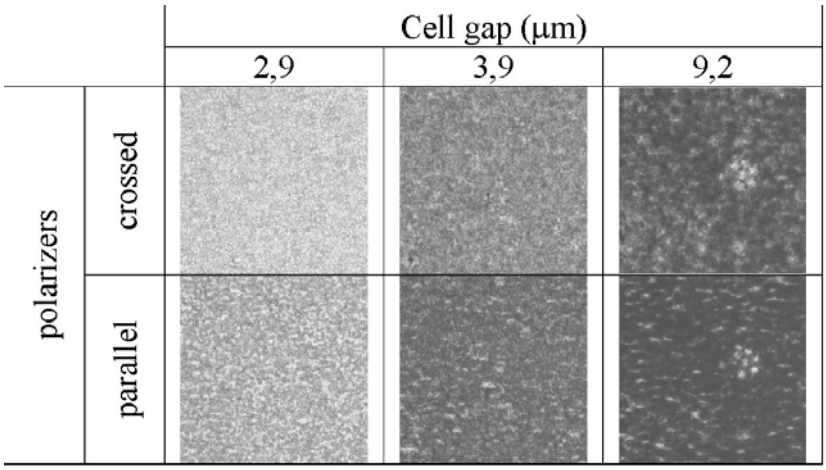

Fig. 3.17: Pictures of a PNLC structure for a 2,9µm, 3,9µm and a 9,2µm cell gap taken with a microscope and crossed and parallel polarizers.

may get trapped in a local energy minimum when applying a high electric field. Upon removal of the electric field some activation energy will be required before the LC molecules relax to the zero field state. This slows down the relaxation process. This phenomenon has been observed in PDLC

films with a high degree of interconnectivity between the different LC "droplets" or domains. PNLC also has a high degree of interconnectivity. Another electro-optical property is the contrast ratio. A contrast ratio of about 69 is achieved for a display with a 3.9μm cell gap. The general trend is that the contrast ratio is reduced as the cell gap increases (Fig. 3.15). The disadvantage of reducing the cell gap is the loss of reflectance (Fig. 3.15). The difference in reflectance between a 9.2μm (64%) and a 3.9μm display (57%) is only 7%. This is rather small compared to the difference of 25% between a 3.9μm (57%) and a 2.9μm display (32%).

Pictures taken with a microscope and crossed and parallel polarizers (Fig. 3.17) show similar differences between a 2.9μm and a 9.2μm PNLC display as PDLC displays with similar cell gap (see previous paragraph 2 "Characterization of PDLC for reflective displays"). Taken into account the abrupt change of the reorientation electric field, reflectance and hysteresis when reducing the cell gap from 3.9μm to 2.9μm there is a similar relation between the cell gap and the electro-optical properties for PDLC and PNLC. The absolute values of the electro-optical properties are different for PDLC and PNLC. The abrupt change in electro-optical properties of PNLC is also explained by the difference in LC alignment near the display electrode and the LC alignment in the bulk of the PNLC layer (see previous paragraph 2 "Characterization of PDLC for reflective displays").

3.2 Influence of the UV cure time

The influence of the UV cure time is analyzed for displays with a 4μm cell gap. The PNLC is cured with an UV-intensity of 12.5mWcm^{-2} using an Hg illumination source. During curing a cut off filter is put on top of the display. This filter filters out all the UV with a wavelength below 360nm.

When varying the cure time from 90s to 540s the switching voltages stay more or less the same between 90s and 360s (Fig. 3.18). For 540s the switching voltages drops from 4.7V$_{rms}$ to 3.7V$_{rms}$ for V_{90} and from 2.1V$_{rms}$ to

$1.4V_{rms}$ for V_{th}. For a cure time of 540s the contrast (Fig. 3.18), the reflectance (Fig. 3.18), the hysteresis (Fig. 3.18) and the switching time (Fig. 3.18) deteriorate. The abrupt change in electro-optical properties for a cure time of 540s coincides with a change in the PNLC structure observed through a microscope using crossed and parallel polarizers (Fig. 3.19). Similar effects are observed when over curing PDLC (see paragraph "Characterization of PDLC for reflective displays"). The same conclusion can be made for PNLC as for PDLC: over curing damages the LC.

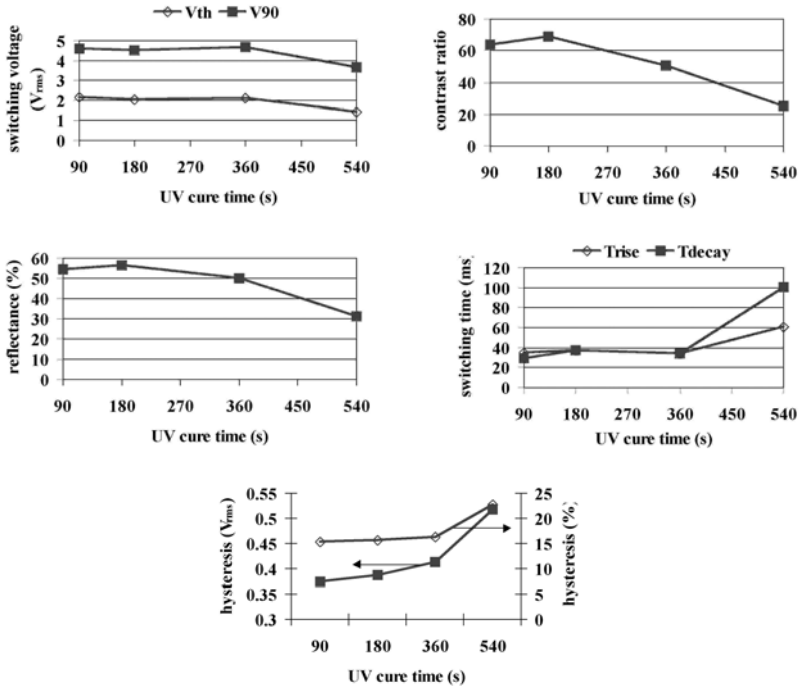

Fig. 3.18: Influence of the UV cure time on the electro-optical properties of PNLC.

For a cure time between 90s and 360s the contrast and the reflectance reach a maximum for 180s (Fig. 3.18). The hysteresis is reduced only slightly for shorter cure times while the switching time stays more or less the same for cure times of 90s to 360s (Fig. 3.18).

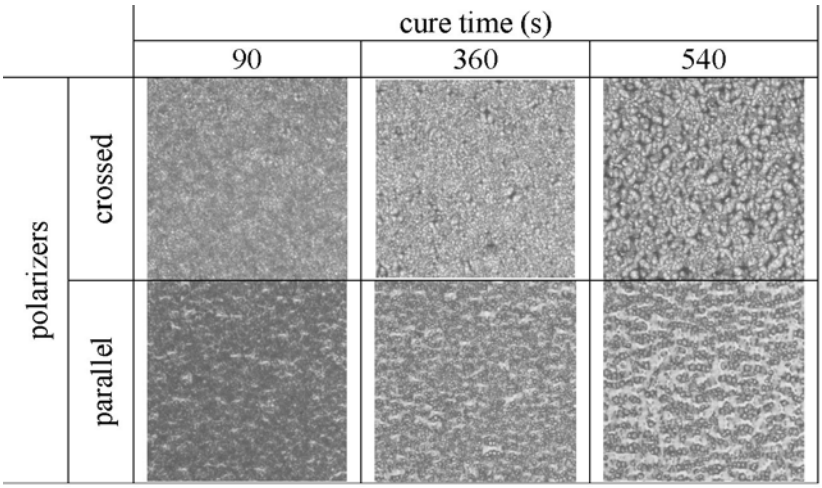

Fig. 3.19: Pictures taken with a microscope and crossed and parallel polarizers showing a different reflectance of the PNLC structure depending on the UV cure time.

3.3 Conclusion

The UV parameters and the cell gap influence in similar ways the electro-optical properties of PDLC and PNLC. Also the abrupt change in electro-optical characteristics caused by a cell gap below 4µm or caused by over curing could be observed both for PDLC and PNLC. The absolute value of the electro-optical properties is very different for PDLC and PNLC. The switching times and the hysteresis are lowest and the reflectance and the contrast are highest for PNLC. The switching voltage is lowest for PDLC.

4 DC effect in reflective PDLC and PNLC displays

4.1 Introduction

The alignment of LC molecules and the scattering properties of PDLC and PNLC are a function of the rms (root mean square) value of the applied voltage. This means that for a voltage with a certain rms value applied to the display the detected light intensity measured with the measurement set-up of Fig. 2.1 should have a constant value. This is not the case when measuring reflective displays. The reflectance of the reflective display is not constant but flickers (see Fig. 3.20). The origin of this flicker is a DC voltage caused

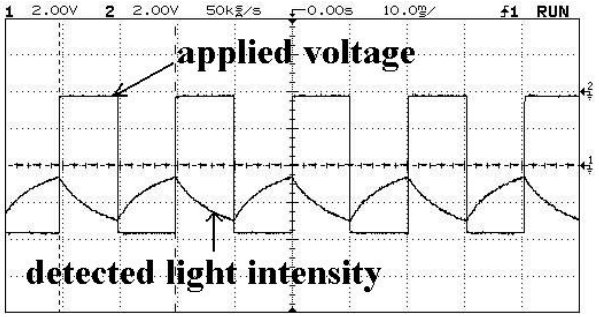

Fig. 3.20: Flicker in the detected light intensity due to a DC voltage typical for reflective displays.

by the difference in work function between the material of the cover glass electrode (Indium Tin Oxide or ITO) and the material of the backplane electrode (Al). When the ITO and the Al electrode are electrically connected with each other a DC voltage will appear across the LC. This occurs when a pixel transistor in the active matrix of the display is selected.

4.2 Measurement of the DC voltage

The DC voltage is measured in two ways. In a first method one adds a DC voltage to the applied square wave voltage of Fig. 3.20. The DC voltage that has to be added to eliminate the flicker in the detected light intensity corresponds with the DC voltage due to the DC effect (see paragraph "Microdisplays" in chapter 1).

In another method the reflectance of the PDLC is measured before the ITO and Al are electronically connected. In this case there is no DC voltage across the PDLC and the reflectance will have its maximum value. As soon as the ITO and Al are connected the DC voltage will be present in the display. This DC voltage is sufficient to align a part of the LC and to reduce the reflectance of the display. The DC voltage caused by the ITO and Al electrode equals the DC voltage one has to apply to the display to obtain the maximum reflectance when the ITO and Al are not connected. The value of the DC voltage varies from display to display. The DC voltage also seems to be time dependent for the same display and vary with the applied voltage.

In general the DC voltage is between 0.25V and 1.1V. The Al electrode has a higher potential than the ITO electrode. No relationship could be found between the UV parameters or cell gap and the DC voltage. There is also no striking difference between reflective PDLC and reflective PNLC displays.

4.3 Discussion

Without the compensation of the DC voltage a good operation of the display is not possible. The DC voltage and the corresponding flicker in the reflectance of the display make the selection of greyscales difficult. In one of my experiments an ITO layer was put on top of the Al layer. After the assembly the display showed no DC voltage. It can be concluded that putting an ITO layer on top of the Al pixel electrodes eliminates the DC voltage. Another solution is an electronic compensation of the DC voltage by the

display electronics [2]. This is not easy due to the time dependent behaviour (drift) of the DC voltage.

Although the different materials (Al and ITO) used for the reflective and cover glass electrode are at the origin of the DC voltage their difference in work function alone cannot explain the value of the DC voltage. The DC voltage would be constant in time if the work function would be the only cause. In literature [13] there are reports that the DC voltage is also caused by a battery effect when Al is in contact with polyimide and by a difference in charge trapping by the ITO and the Al electrode under illumination and driving. These effects explain the time dependent value of the DC voltage. The polyimide is the alignment layer. In PDLC and PNLC there is no alignment layer. However the Al makes contact with the polymer in the PDLC and PNLC. This will also result in a battery effect. The time dependent behaviour (drift) of the DC voltage makes it hard to compensate in an electronic way. However the drift in DC voltage can be eliminated. This requires the coating of the ITO and the Al electrodes with diamond-like-carbon [13].

4.4 Conclusion

At the origin of the DC effect is the difference in work function of the electrode on the cover glass (ITO) and the electrode on the backplane (Al). No relationship could be found between the curing parameters, cell gap, LC material (PDLC or PNLC) and the DC voltage. The DC voltage has to be compensated to allow a good operation of the display. This can be done by putting an ITO layer on top of the Al electrode. An electronic compensation of the DC voltage is also a solution. In this case the DC voltage drift has to be eliminated. This can be done by coating the Al and ITO electrode with diamond-like-carbon.

5 Applicability of reflective PDLC and PNLC displays for direct view applications

5.1 Introduction

The applicability of reflective PNLC and PDLC displays is analyzed. The measurement set-up described in chapter 2.4 is used for this analysis. The applicability of a single polarizer HGH (Heilmeier Guest Host) display is also analyzed. A comparison of both analysis allows a better understanding of the strong and weak points of both display technologies. The reflective single polarizer HGH display is a normally white Guest Host display and is based on the absorption of polarized light [14]. When no voltage is applied the dyes (Guest) and LC (Host) have a homeotropic alignment resulting in a transparent LC layer. Incoming light is reflected in the specular direction by the Al reflector electrode. By applying a voltage the dichroic dyes and LC align perpendicular to the electric field. The incoming light is absorbed by the dyes and the display is dark.

5.2 Results

The measurements in Fig. 3.21 to Fig. 3.23 are the results for the diffuse illumination. Fig. 3.24 contain the results for directed illumination. The definition of the angles is given in chapter 2.4. The contrast ratio equals the

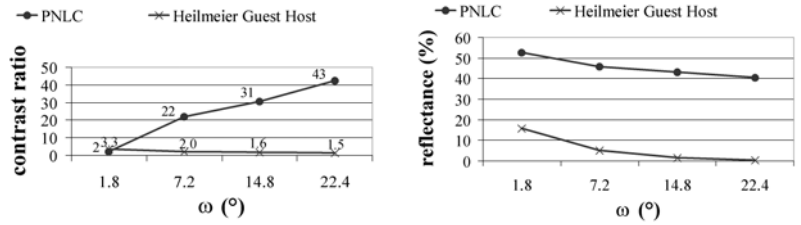

Fig. 3.21: Contrast ratio and reflectance as a function of the dark area ω for diffuse illumination with θ=90°.

ratio of the luminance of the display when no voltage is applied to the luminance of the display when the maximum voltage is applied. The reflectance is the ratio of the zero-voltage display luminance to the luminance of a white standard (Spectralon® Reflectance Standard of Labsphere®) for the same illumination. For a reflective PNLC display (Fig. 3.21) the contrast ratio increases and the reflectance decreases as the dark area ω increases. The higher ω is, the closer the observer is to the display. An ω=22.4° corresponds with the situation of an observer looking at a wrist watch keeping his arm stretched. In the case of the Heilmeier Guest Host both the contrast ratio and the reflectance decrease as the observer comes closer to the display (Fig. 3.21). When the observer is close to the display the contrast of the reflective PNLCD is less sensitive to a change in the inclination θ of the observer (Fig. 3.22). By changing θ contrast inversion

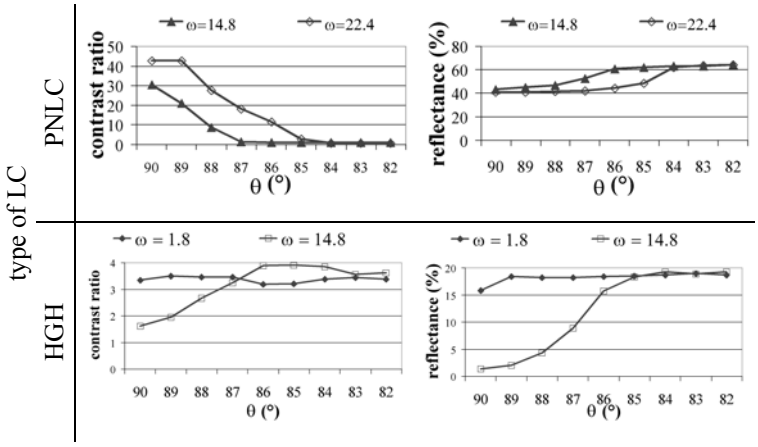

Fig. 3.22: Influence of the angular position of the observer on the contrast ratio and reflectance of a reflective PNLC and single polarizer HGH display under diffuse illumination.

(contrast < 1) may occur. The reason for this contrast inversion is explained further on in this paragraph. The angle φ=90°-θ for which the contrast is 1 is the angle of contrast inversion. This angle depends on the dark area ω (Fig. 3.22 and Fig. 3.23). The smaller φ, the more critical the orientation of the

display to the observer is. This is an important parameter for the ease of use of the display especially in mobile applications where the position of the

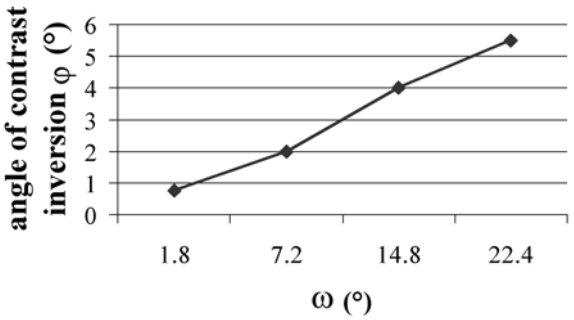

Fig. 3.23: Influence of the dark area ω on the angle of contrast inversion φ for a reflective PNLCD under diffuse illumination.

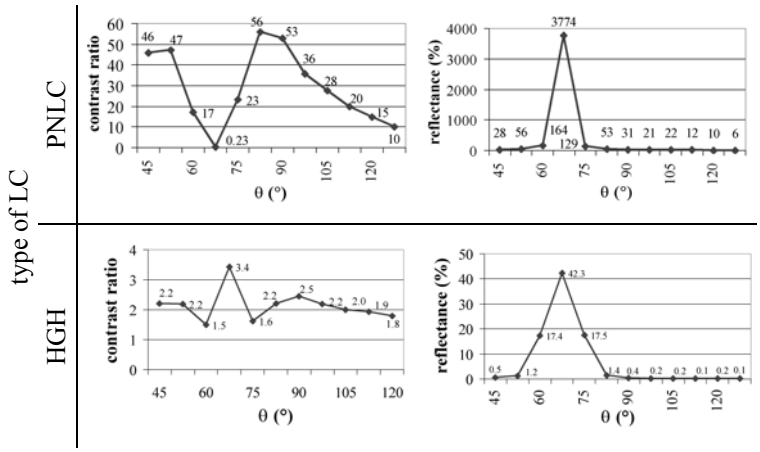

Fig. 3.24: The contrast ratio and reflectance of a reflective PNLC and single polarizer HGH display as a function of the angular position θ keeping θ+β=135°.

display to the observer is not fixed. The single polarizer Heilmeier Guest Host display has no contrast inversion (Fig. 3.22). When the observer is close to the display both the contrast and the reflectance (Fig. 3.22) are considerably larger in the non perpendicular observation direction (θ<90°).

In Fig. 3.24 measurements for directed illumination are shown with $\theta+\beta=135°$ during the measurements. These measurements simulate the situation where the light source and the observer (detector) have a fixed position while the display is tilted (for instance when looking at a wrist watch). For most values of θ the contrast ratio and the reflectance of the reflective PNLCD have acceptable values (Fig. 3.24). For the specular reflection direction ($\theta=\beta=67.5°$) the PNLCD has contrast inversion (Fig. 3.24) and a high reflectance (3774%). The Heilmeier Guest Host has only an acceptable reflectance in a small cone around the specular reflection direction (for $60°<\theta<75°$) (Fig. 3.24). The contrast is more or less independent of θ (Fig. 3.24).

5.3 Discussion

It is demonstrated that the different types of illumination and the position of the observer have a big influence on contrast and reflectance. The different results for reflective PNLCDs and reflective HGH displays can be explained from their optical working principle. The first main difference is that a PNLCD switches between a transparent state and a light scattering state while a HGH display switches between a transparent state and a light absorbing state. This difference explains why contrast inversion is possible in PNLCDs. When the PNLC is in the scattering state the PNLCD will have the highest reflection in the specular direction however a major part of the light will be reflected in the non specular directions (see Fig. 3.24). When the PNLC is in the transparent state almost all the light will be reflected by the Al reflector of the PNLCD in the specular direction. This means that in the specular direction, the scattering state has a lower luminance and in the non specular direction, the scattering state has a higher luminance than the transparent state. For diffuse illumination light specularly reflected on the Al reflector of the PNLCD reaches the detector when $\varphi\geq\omega/4$, resulting in contrast inversion (Fig. 3.22 and Fig. 3.23). Reflective HGH displays don't

have contrast inversion because the light absorbing state can not have a higher luminance than the transparent state. The HGH display has to be tilted so specular reflections could reach the observer when the display is transparent, otherwise the reflectance is very low. This is the case for both diffuse (Fig. 3.22) and directed illumination (Fig. 3.24). The reflectance pattern of the HGH display caused by directed illumination (Fig. 3.24) shows a peak in reflectance in the specular reflection direction with a haze component (Fig. 3.25) [16] for θ=60° and θ=75°. Due to this haze component the change in contrast ratio and reflectance for diffuse illumination as a function of the tilt angle θ of the tilt angle θ is gradual and

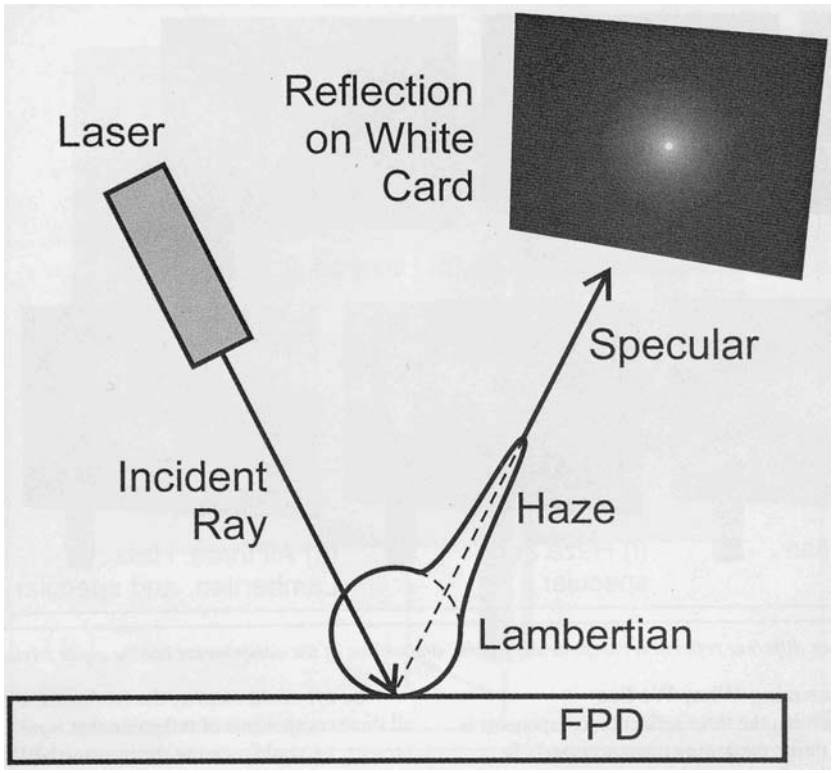

Fig. 3.25: Illustration showing the specular, haze and lambertian component of light reflected by a Flat Panel Display (FPD) on a white card [16].

not abrupt (Fig. 3.22). PNLC also has a haze component (Fig. 3.24) causing a gradual change in contrast ratio and reflectance (Fig. 3.22). For small values of ω a large part of the incoming light is close to the direction perpendicular to the display and a lot of the detected light is haze. For bigger values of ω the haze component will not be detected, only the Lambertian component [14,16] ($\theta \leq 52.5°$ and $\theta \geq 82.5°$ in the measurements of Fig. 3.24). This is why the reflectance for $\theta=90°$ is reduced for bigger values of ω and the contrast ratio is reduced for the HGH display (Fig. 3.21). The contrast ratio is the lowest for small ω's in the case of PNLC. For small ω's the luminance of the dark state of the display is determined by the haze component of the reflections on the cover glass, the transparent PNLC layer and the Al reflector. These reflections do not have a big Lambertian component contrary to the reflections of the scattering PNLC.

The second main difference is that PNLC does not require a polarizer while HGH uses 1 polarizer. Displays with polarizers have the highest reflectance and contrast ratio for perpendicular illumination and perpendicular observation. This is not possible for direct view displays because the observer would be in the illumination path. This is the main reason why the HGH display has a smaller peak reflectance than the PNLCD (Fig. 3.24).

For portable applications the observer is close to the display. Under these conditions reflective PNLCDs have the highest contrast and angle of contrast inversion for diffuse illumination. A situation with contrast inversion can be easily corrected by the observer since the display is mobile. Reflective PNLC displays achieve, high reflectance and contrast for directed non perpendicular illumination. Even in the case of contrast inversion the inverted image still has a contrast of $(0.23)^{-1}=4.3$ (in the case contrast = (light intensity of bright image) / (light intensity of bright image)). Contrary to Heilmeier Guest Host displays the maximum contrast of a reflective PNLC occurs in a non specular reflection direction. This is an advantage for direct view applications. The HGH displays could use special electrodes [17-20] or diffusing layers so the direction with maximum contrast and

reflectance does not coincide with the specular reflection on the cover glass of the display (Fig. 1.6-1.7). If we compare the results of the contrast ratio with other reflective display technologies [10] and we take into account the high reflectance we may conclude that PNLC is a good solution especially for mobile applications. The single polarizer Heilmeier Guest Host display has some acceptable values for the reflectance but the contrast ratio is low.
The results and conclusions for PNLC can be transferred to PDLC displays. Both are based on the same optical principle based on switching between a Lambertian like diffuser and a mirror. The absolute values of the reflectance and the contrast will have to be adapted.

5.4 Conclusion

The reflectance, the contrast ratio and the angle of contrast inversion strongly depend on the type of illumination and the position of the observer to the display. The best case situation for one display technology may be the worst case situation for another. This should be taken into account when evaluating different display technologies.
Reflective PNLC has good values for the contrast and the reflectance for mobile direct view applications. The single polarizer Heilmeier Guest Host display has some acceptable values for the reflectance but the contrast ratio is low.

6 Conclusion on the characterization of PDLC and PNLC for reflective displays

The influence of the UV parameters and of the cell gap on the electro-optical properties of reflective PDLC and PNLC displays are analyzed. The UV intensity of the illumination during curing is not only determined by the UV intensity at 360nm. The experiments show a significant difference in electro-optical properties depending on the light source (Hg or HgXe) used for the curing. The impact of the UV intensity is in line with predictions. The higher the UV intensity is, the smaller the average droplet diameter is. The UV cure time also seems to follow the predictions. A higher UV cure time results in a higher degree of polymerization which is beneficial for the stability of the PDLC and PNLC film. However when the cure time is too high the LC is damaged. This results in a drastic change of the electro-optical properties. A display with a 4μm cell gap has the smallest switching voltage and highest contrast while the reflectance, switching time and hysteresis stay more or less the same compared to displays with a larger cell gap. If the cell gap is smaller than 4μm the reflectance will be reduced dramatically and the switching time will increase dramatically. This is caused by a change in the dominant alignment of the LC. The DC voltage which is typical for reflective displays is caused by the difference in electrode materials for the cover glass (ITO) and the reflector electrode (Al) and their work functions. There is not a clear relation between the UV parameters or the cell gap and the DC voltage. The DC voltage varies from display to display and is time dependent and applied voltage dependent. The reflectance and contrast depends a lot on the type of illumination and the position of the observer. It is shown that the best case situation for scattering displays (PDLC, PNLC) may be the worst case situation for single polarizer displays (HGH display) and vice versa.

References

[1] Bruyneel F., De Smet H., Vanfleteren J., Van Calster A., Fujisawa T., Aizawa M., "Characteristics of PNLC in reflective displays", 2000, in *Proc. of the 20th IDRC*, pp. 217-220

[2] Bruyneel F., De Smet H., Vanfleteren J., Van Calster A., "Cell gap optimization and alignment effects in reflective PDLC microdisplays", 2001, in *Liquid Crystals*, **Vol. 28, No. 8**, pp. 1245

[3] Bruyneel F., De Smet H., Van Calster A., Egelhaaf J., "Comparison of reflective PNLCDs and reflective single polarizer Heilmeier Guest Host displays", 2001, in *Journal of SID*, **Vol. 9 No. 4**, pp. 313-318

[4] Bruyneel F., De Smet H., Van Calster A., Egelhaaf J., "Measurement and evaluation of the applicability of reflective displays for direct view applications", 2000, in *Proc. 7th IDW*, pp. 45-48

[5] Nolan, P., Jolliffe, E., Coates, D., "Film formation parameters affecting the electro-optic properties of low-voltage PDLC films", 1995, *SPIE Proc*., **2408**, 2

[6] Drzaic, P.S., 1995, PDLC film operating voltage. In *Liquid Crystal Dispersions*, edited by H. L. Ong (Singapore: World Scientific Publishing), pp. 235-257

[7] Drzaic, P.S., 1995, Numerical models for PDLC response times. In *Liquid Crystal Dispersions*, edited by H. L. Ong (Singapore: World Scientific Publishing), pp. 264-267

[8] Drzaic, P.S., 1995, Sources of hysteresis. In *Liquid Crystal Dispersions*, edited by H. L. Ong (Singapore: World Scientific Publishing), pp. 271-274

[9] Bruyneel F., De Smet H., Vanfleteren J., Van Calster A., "Method for measuring the cell gap in liquid crystal displays", 2001, in *Optical Engineering*, **Vol. 40 No. 2**, pp. 259

[10] T. Maeda, T. Matsushima, E. Okamoto, H. Wada, O. Okumura, S. Iino "Reflective and transflective color LCDs with double polarizers", Journal of the SID 7/1, pp. 9-15, 1999

[11] De Baets, J., Capon, J., De Cubber, A. M., De Smet, H., Van Calster, A., Vanfleteren, J., Fujisawa, T., Ogawa, H., Aizawa, M., Takatsu, H., 1993, *Proc. 13th IDRC,* pp. 117-120

[12] Fujisawa, T., Nakata, H., Aizawa, M., 1998, IEICE Trans. Electron., **Vol. E81-C No. 11**, pp. 1675-1680

[13] Lu M., Yang K. H., "Reflective Nematic LC Devices for LCOS Applications", 2000, *Conf. Rec. of the 20th IDRC*, pp. 1-7

[14] G.H. Heilmeier, J. A. Castellano, L.A. Zanoni "Guest-Host interactions in nematic liquid crystals", Molecular Crystals and Liquid Crystals, 1969, Vol. 8, pp.293-304

[15] E.F. Kelley, G.R. Jones, T.A. Germer, "Display reflectance model based on the BRDF", Displays, Vol. 19, Issue 1, pp. 27-34, 1998

[16] E. F. Kelly, G. R. Jones, T. A. Germer " The three components of reflection", Information Display, Vol. 14, No. 10, 1998, pp. 24-29

[17] I. Hiyama, O. Itoh, K. Kondo, A. Arimoto "High-performance reflective STN-LCD with a blazed reflector", Journal of the SID 7/1, pp. 49-54, 1999

[18] K. Tsuda, N. Kimura, S. Mizushima, "Development of Reflector for HR-TFTs ", Sharp Technical Journal, No.74, 08/1999, pp.41-45

[19] D.L. Ting, W.-C. Chang, C. Liu, J. Shiu, C. Wen, C. Chao, L. Chuang, C. Chang, "A High-Brightness High-Contrast Reflective LCD with a Micro Slant Reflector (MSR)", SID 99 Digest, 1999, pp.954-957

[20] N. Sugiura, T. Uchida, "Designing Bright Reflective Full-Color LCDs using an optimized Reflector", SID 97 Digest, 1997, pp.1011-1014

CHAPTER 4:
Assembly and filling of PDLC and PNLC microdisplays

1 Introduction

Conventional filling methods apply vacuum during filling. This is to prevent air from getting trapped in the display cell gap. The typical problem with PDLC and PNLC type LCs is that some of the prepolymer components in the PDLC or PNLC mixture are sensitive to evaporation when exposed to vacuum. Experiments showed that droplets of PDLC and PNLC evaporate completely when exposed to vacuum. This is something that should be prevented during the assembly and filling of the display. As a result conventional vacuum filling methods can not be used for PDLC or PNLC. This is also mentioned in the datasheets of Merck.

Three alternative assembly and filling methods have been analyzed and optimized for PDLC and PNLC: a droplet filling method, a vacuum filling method and a capillary filling method [1]. Measurements on test displays indicate that the electro-optical properties of the PDLC and PNLC do not depend on the filling method. From this it is concluded that there is no evaporation of prepolymer components during the assembly and filling of the display.

Two major problems that are typical for microdisplays occur when using these filling methods. The first problem is the filling of the vias in the reflector electrodes with PDLC or PNLC [1]. These vias connect the pixel electrode with the underlying transistors (Fig. 1.9). Another problem is caused by the stability of the cell gap after the curing of the PDLC or PNLC [1,2].

2 Description of the assembly and filling methods

2.1 Droplet filling method

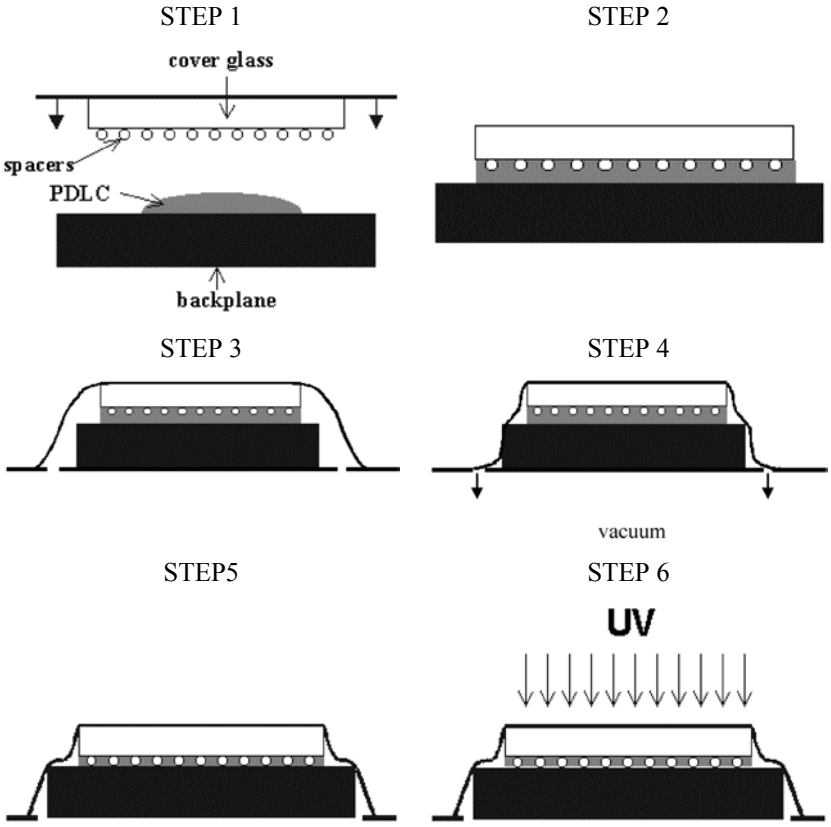

Fig. 4.1: Process flow of the Droplet Filling Method.

The Droplet Filling Method (DFM) is designed to limit the exposure to vacuum of the LC to an absolute minimum. There is only an exposure to vacuum when the display is already filled (STEP 4 to STEP 6 in Fig. 4.1). This filling method takes advantage of an unique feature of PDLC or PNLC: the presence of an acrylate type of prepolymer in the PDLC or PNLC

mixture. Although this prepolymer is essential for the optical principle of the PDLC or PNLC film, it can also be used as an adhesive between the cover glass and the back plane of the display.

The first step in the process flow of the DFM (Fig. 4.1) consists of putting a droplet of PDLC or PNLC on the back plane of the display. Then the cover glass is pressed against the back plane (STEP 2, Fig. 4.1). On the cover glass are spacers with a diameter equal to the desired cell gap. These spacers have been put on the cover glass by spinning. For the spinning the spacers are put in methanol. During and after spinning the methanol evaporates. Due to the evaporation the spacers stick to the cover glass. The forces that keep the spacers on the cover glass are strong so there is no lift off of the spacers during assembly. In order to have a cell gap equal to the spacer diameter we first put a silicone flap on top of the display (STEP 3, Fig. 4.1) and we apply a vacuum in the space under the silicone flap (STEP 4, Fig. 4.1). The difference in pressure between the atmosphere and the vacuum under the silicone flap will result in a force compressing the cell gap to the spacer diameter (STEP 5, Fig. 4.1). The PDLC or PNLC is now ready for UV curing (STEP 6, Fig. 4.1). After the curing of the PDLC or PNLC the silicone flap is removed and the display is sealed.

2.2 Vacuum filling method

When the display is filled with the Vacuum Filling Method (VFM) the back plane and the cover glass are connected to each other with a sealing ring. This sealing ring at the edge of the cover glass has only one opening: the filling opening. Through this filling opening the LC will enter the display once vacuum has been obtained. The LC will enter the cell gap due to capillary forces. Because the filling takes place in vacuum the cell gap will be filled with LC only.

As we have already mentioned some of the prepolymer components in PDLC or PNLC are very sensitive to evaporation in vacuum. Still it is possible to fill displays with PDLC or PNLC using a VFM. This is because

the PDLC or PNLC is in a syringe and not in an open reservoir as with conventional VFMs. By putting PDLC or PNLC in a syringe the exposure time to vacuum is drastically reduced. The PDLC or PNLC is released and put in front of the filling opening once vacuum has been reached. The syringe is emptied by the syringe controller arm (Fig. 4.2). The position of

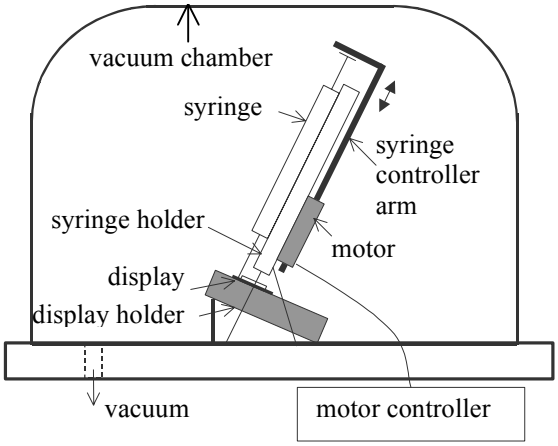

Fig. 4.2: Set-up for the Vacuum Filling Method.

the syringe controller arm is driven by an electric motor. This electric motor can be operated from outside the vacuum chamber. In the case the PDLC or PNLC would be in an open reservoir (this is the case for conventional vacuum filling methods) the LC is exposed to low pressure during the time required to reduce the pressure in the vacuum chamber from atmospheric pressure to vacuum, the time required to fill the display and the time to return from vacuum to atmospheric pressure. When the LC is in a syringe, exposure to low pressure is limited to the time required to fill the display and the time to return from vacuum to atmospheric pressure. This is a drastic reduction of the exposure time to vacuum because the time to reach vacuum is by far the longest.

We have to position the display first on the display holder before we can fill the display. The filling opening is positioned near the tip of the syringe needle. The syringe already contains the PDLC or PNLC. The display holder

has an angle of inclination. By positioning the display with the filling opening facing upward, the gravity will not oppose the filling of the display. After the positioning of the display the vacuum chamber is closed. The pressure in the vacuum chamber is reduced from atmospheric to vacuum. In general good filling results could be obtained with a vacuum pressure of about 2 Tor (≈270 Pa). Once vacuum is obtained in the vacuum chamber the syringe is emptied. Once the filling opening is entirely covered with LC the vacuum is broken. Only LC and no air will be able to enter the display cell gap. When the display is filled the remaining LC in front of the filling opening is removed and the filling opening is sealed using sealing glue. Finally the sealing glue and the PDLC or PNLC are cured in the same process step. The sealing glue is the UV curable NOA 68 and is also an acrylate just like the polymer component in PDLC and PNLC.

2.3 Capillary filling method

The similarity between the capillary filling method and the vacuum filling method is that the LC enters the cell gap due to capillary forces. The difference is that the filling doesn't take place in vacuum when using the Capillary Filling Method (CFM). For the filling of the display the sealing ring of the display needs a second opening opposite to the filling opening. This opening is an exit for the air in the cell gap when the LC enters the cell gap.

The filling of the display starts by putting the LC in front of the filling opening. Once the display is filled sealing glue is put in front of the opening opposite to the filling opening. The remaining LC in front of the filling opening is removed and sealing glue is put in front of the filling opening. Finally the PDLC/PNLC and the sealing glue are cured in the same processing step.

3 Typical problems during the filling and the assembly of PDLC and PNLC microdisplays

3.1 Filling of vias

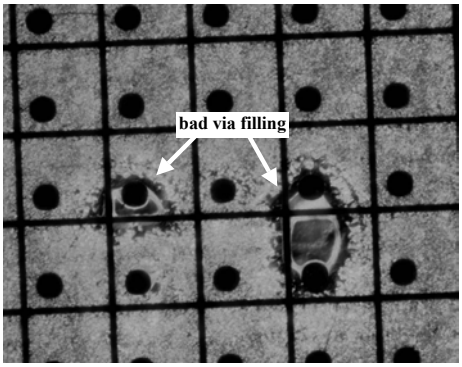

Fig. 4.3: Bad filling of the vias when using the Vacuum Filling Method.

The filling of the vias in the Al reflector electrodes of the microdisplays may cause some problems when using the VFM or the CFM (Fig. 4.3). These vias connect the reflector electrode with the underlying pixel transistors (Fig. 1.9). They are about 15μm in diameter and about 2μm deep. This difference of 2μm between the top of the reflector electrode and the bottom of the via is rather big considering that the display cell gap is only 4μm. The reason for a 4μm cell gap is explained in chapter 3: "Characterization of PDLC and PNLC for reflective displays".

The bad via filling occurs across a line near the filling opening in case of the VFM. A typical example is given in Fig. 4.4. The dark region in the display is the result from bad via filling. The position of the dark region relative to the filling opening is most likely determined by the moment the pressure in

the vacuum chamber returns from vacuum to atmospheric pressure. The initial increase in pressure is abrupt. Due to the pressure difference in the cell

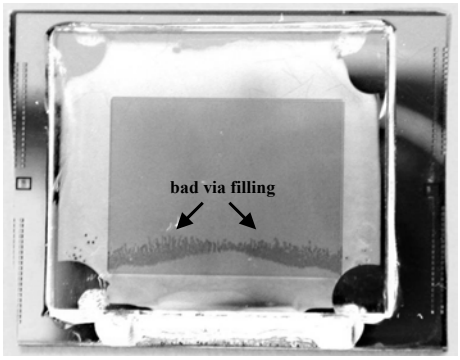

Fig. 4.4: Bad via filling when using the VFM.

gap and in the vacuum chamber the LC is forced in the cell gap. As a result some of the vias are not filled. This problem could be solved by releasing the vacuum after the LC has filled the display or by raising the pressure more gradually. Both solutions are in conflict with the idea that the exposure time to vacuum of PDLC/PNLC should be limited to an absolute minimum. The exact timing of the vacuum release is hard to master. Another solution is to heat the display.

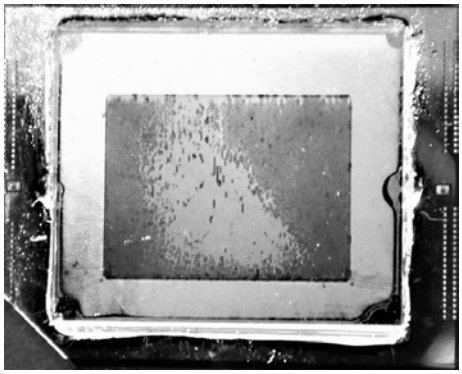

Fig. 4.5: Bad via filling when using the CFM.

The bad via filling occurs across the entire display in case of the CFM (Fig. 4.5). This problem is solved by heating the display and the PDLC/PNLC to

105°C and by filling the display on a hot plate at 105°C. After the filling of the display and putting sealing glue at the openings the filled display is cooled down to room temperature before the PDLC/PNLC can be cured. This takes about 15 minutes. This is necessary because the temperature of the PDLC/PNLC during curing affects the opto-electrical properties [3].
No difference in electro-optical properties could be measured on displays filled at room temperature or displays filled at 105°C or even 120°C. This indicates that the heating of the display does not initiate the polymerization process before UV curing and that the displays have cooled down sufficiently after filling by the time they are being UV cured.

3.2 Cell gap stability

The scattering properties of the cured PDLC are not always stable in time. Sometimes PDLC that used to be scattering immediately after the UV curing turns transparent. In general the transition from the scattering state to the transparent state starts within 24 hours after the curing of the PDLC. This transition is irreversible at room temperature. The transparent PDLC can not

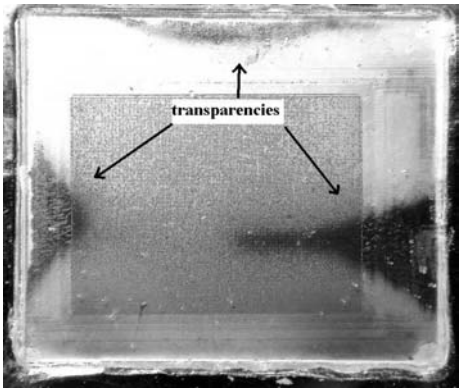

Fig. 4.6: Typical places for transparencies in displays filled with the DFM.

be switched to a scattering state and is therefore useless for displaying information. Some areas in the display are more sensitive to this effect than others depending on the filling method. In the case of the DFM the

transparencies start in the middle of the short edges of the cover glass (Fig. 4.6) and expand in time towards the centre of the display. When using the Vacuum Filling Method (VFM) the transparencies start at the filling opening and expand to the opposite side of the display (Fig. 4.7).

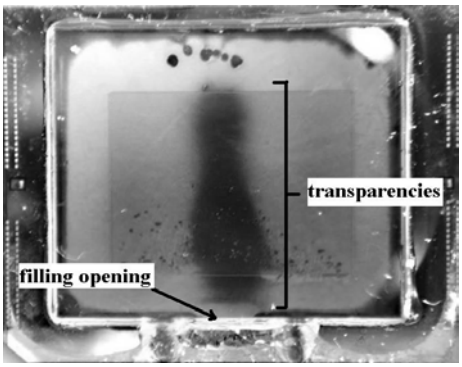

Fig. 4.7: Typical places for transparencies in displays filled with the VFM.

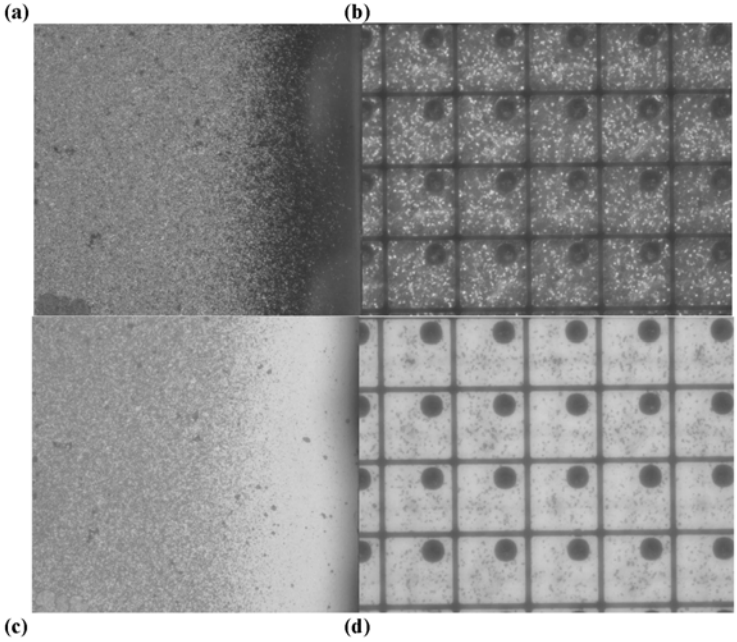

Fig. 4.8: Pictures of the transparent PDLC using crossed ((a) and (b)) and parallel ((c) and (d)) polarizers. The dimensions of the pixels in (b) and (d) are 80μm by 80μm.

Fig. 4.8 contains some pictures of transparencies at the edge (Fig. 4.8a and Fig. 4.8c) and in the centre of the display (Fig. 4.8b and Fig. 4.8d). The display is illuminated by light passing through a linear polarizer. The reflected light is observed with a CCD camera. An analyzer is in front of the CCD camera. The pictures were taken with the polarization direction of the analyzer perpendicular (crossed) (Fig. 4.8a and Fig. 4.8b) or parallel (Fig. 4.8c and Fig. 4.8d) to the polarization direction of the polarizer. The transparent PDLC regions are dark in the pictures taken with crossed polarizers and white in the pictures taken with parallel polarizers. The scattering regions have about the same brightness in the picture with crossed and parallel polarizers. In Fig. 4.8a and Fig. 4.8c one clearly sees the transition from scattering PDLC (left part of the Fig. 4.8a and Fig. 4.8c) to transparent PDLC (right part of Fig. 4.8a and Fig. 4.8c). In Fig. 4.8b and Fig. 4.8d the pixel electrodes and the via (big black dot) connecting the pixel electrode with the underlying pixel transistors are visible. In the picture with crossed polarizers there are white ‘dots’ on a black background and in the pictures taken with parallel polarizers there are dark ‘dots’ on a white background. The concentration of these dots decreases going from a scattering region to a transparent region.

These observations indicate that the transparent regions are caused by a vertical alignment of the LC (alignment perpendicular to the backplane). The vertical alignment of the LC molecules explains why the transparent regions above the Al pixel electrodes are dark when using crossed polarizers and bright when using parallel polarizers. The observed ‘dots’ in the pictures with crossed and parallel polarizers are LC droplets in the PDLC containing LC molecules that did not align vertically. These droplets still scatter the light and are therefore visible in the pictures with crossed and parallel polarizers. The presence of the ‘dots’ indicates that the polymer matrix and the LC are still intact. This is confirmed by the following experiment. The transparent regions in the display return to the scattering state by heating the PDLC to 40°C or more. Another independent experiment confirms the

vertical alignment of the LC. Incident light perpendicular to the backplane of the display reflects the light perpendicular to the backplane. This reflected light has an interference pattern determined by the optical path $n_{gap}d_{gap}$ [4] with d_{gap} the cell gap of the display and n_{gap} the refractive index of the material in the cell gap. In the case the LC is vertically aligned $n_{gap}=n_o$ with n_o the ordinary refractive index of the LC. The interference pattern is measured in a transparent region once without a voltage being applied to the display and once with a voltage of $10V_{rms}$. The voltage of $10V_{rms}$ is sufficient to have the LC vertically aligned. In both cases the same optical path $n_{gap}d_{gap}$=6950nm was measured (Fig. 4.9). For TL213 $n_{gap}=n_o$=1.527 [10] so d_{gap}=4552nm. This is an acceptable value of the cell gap for a display with 4µm spacers. All these experiments indicate that the LC is vertically aligned.

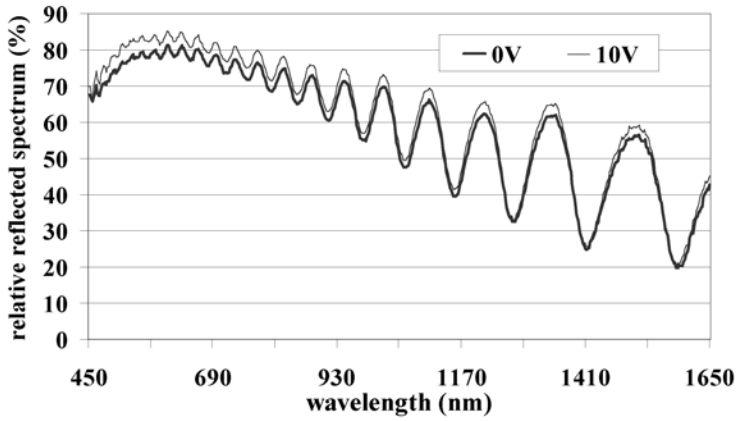

Fig. 4.9: Measurement of the change in refractive index by measuring the interference pattern without an applied voltage (0V) and with an applied voltage of $10V_{rms}$.

The vertical alignment of the LC is caused by the instability of the cell gap after the curing of the PDLC. The cell gap is measured on different spots (Fig. 4.10) of several displays. These displays consist of a cover glass with an ITO layer and a silicon backplane with an Al reflector electrode. The spacers are made of glass. Silicon is chosen as backplane material because,

based on our experience, the chance of transparencies appearing in displays with a silicon backplane is higher than for displays with a glass backplane. Some of the displays are filled using the DFM others using the VFM. The measurement of the cell gap [4] immediately after the curing of the PDLC indicates that the cell gap in some regions of the display (Fig. 4.10) is a lot smaller than the diameter of the spacers (Table 4.1). After some time the cell

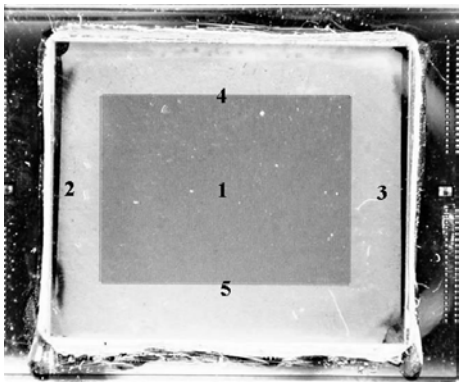

Fig. 4.10: The five positions mentioned in table 1 where the evolution of the display cell gap is measured.

time after	cell gap (μm)				
curing	position 1	position 2	position 3	position 4	position 5
1 hour	3.6	3.3	3.5	3.8	3.6
12 days	3.8	3.4	3.6	3.7	3.6
30 days	3.9	3.7	3.8	3.7	3.6

Table 4.1: Example of a cell gap evolution in a display with a 4μm cell gap filled using the DFM.

gap increases to a value close to the spacer diameter. The positions with the biggest cell gap compression (position 2 and 3) correspond with the positions where the transparencies begin. After 30 days the PDLC in position 1, 2 and 3 is transparent while the PDLC in position 4 and 5 is still scattering. This pattern of regions with transparent and scattering PDLC is

similar to the one in Fig. 4.6. Position 1, 2 and 3 correspond with the positions with a cell gap increase after the curing of the PDLC. In position 4 and 5 the cell gap is stable in time. In another experiment mechanical pressure is applied to compress the cell gap. As a result the transparent PDLC turns to the scattering state. As soon as the mechanical pressure is lifted the transparencies return.

The compression of the cell gap to a value smaller than the spacers' diameter (Table 4.1) is caused by the capillary forces occurring during the filling of the displays. This can also be derived from the fact that a part of the sealing glue penetrates the filled display before curing. The compressed spacers are forcing the cell gap to expand. When the cell gap expands after the curing of

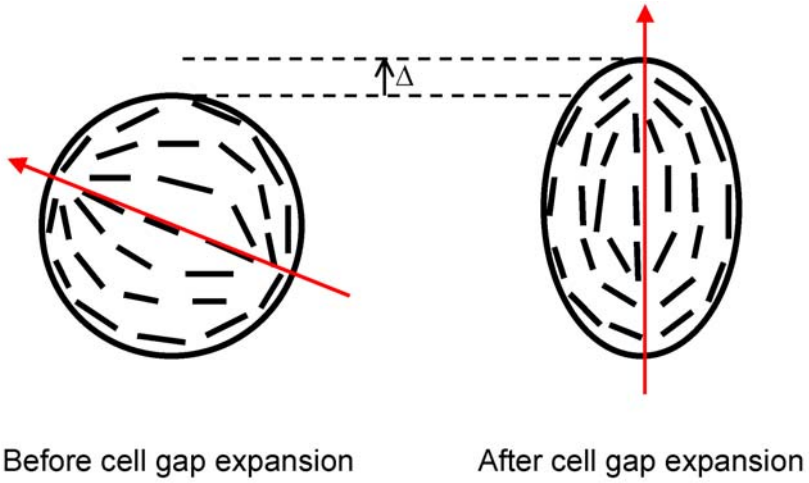

Fig. 4.11: Change of the droplet shape and LC orientation due to a cell gap increase Δ. The arrow indicates the average LC orientation.

the PDLC the ball shaped LC droplets in the cured PDLC will change into ellipsoid shaped LC droplets with a long axis parallel to the direction of the expanding cell gap (Fig. 4.11). The change of the shape causes the LC to align vertically. The alignment of the LC molecules due to the change of shape of the LC droplets also occurs in PDLC based on a PolyVinyl Alcohol (PVA) system [5]. However the alignment of the LC in the PDLC based on a

PVA system is horizontal due to a shrinkage of the cell gap. This is different from the PDLC used in the experiments described in this Ph.D.. The PDLC in this Ph.D. is based on a photo-initiated polymerization induced phase separation system and the alignment of the LC is vertical due to an expansion of the cell gap. The instability of the cell gap as a reason for the transparencies explains many other aspects of the phenomenon. First it explains where the first transparencies occur. This is in the regions with the biggest expansion of the cell gap after the curing of the PDLC. In these regions the capillary forces that occur during the filling of the display are probably the highest. Displays with a silicon backplane, like microdisplays, are more sensitive to the transparencies compared to displays with a glass backplane. Silicon backplanes are less rigid and flat than glass backplanes making the display more sensitive to cell gap compression and expansion.

A first solution is to prevent a strong cell gap compression during the filling by increasing the spacer concentration. The choice of spacer material (glass or plastic) will also have an influence on the compression. Another solution is to wait for curing the PDLC until the cell gap is decompressed and stable. In the CFM a period of 15 minutes is respected between the filling of the display and the curing of the PDLC. This period is sufficient to prevent transparencies caused by the vertical alignment of LC molecules.

4 Conclusion

Three different filling methods have been analyzed and optimized for the filling of microdisplays with PDLC/PNLC. The two main challenges are to prevent the evaporation of prepolymer components in the PDLC/PNLC mixture and to achieve an uniform PDLC/PNLC layer. The filling methods reduced the evaporation of the prepolymer components to the level that it doesn't affect the electro-optical properties of the PDLC/PNLC. Frequent problems for microdisplays are the difficult filling of vias and the stability of the cell gap after the curing of the PDLC/PNLC. These problems are solved for all the filling methods. For the experiments in this PhD the method that was the easiest to control and had the highest yield is the capillary filling method. Because the encountered problems are display dependent the other filling methods may have better results for other displays (larger active matrix area, smaller vias, larger cell gap, glass backplane instead of silicon backplane,…). It was beyond the scope of this PhD to confirm this due to the large variety of displays.

References

[1] Bruyneel F., De Smet H., Vanfleteren J., Van Calster A., "Assembly of Reflective PDLC Microdisplays", 2001, *Proc. of SID'01*, pp. 442-445

[2] Bruyneel F., De Smet H., Vanfleteren J., Van Calster A., "Cell gap optimization and alignment effects in reflective PDLC microdisplays", 2001, in *Liquid Crystals*, **Vol. 28, No. 8**, pp. 1245

[3] Nolan, P., Jolliffe, E., Coates, D., "Film formation parameters affecting the electro-optic properties of low-voltage PDLC films", 1995, *SPIE Proc*., **2408**, 2

[4] Bruyneel, F., De Smet, H., Vanfleteren, J., Van Calster, A., 2001, Optical Engineering, **Vol. 40 No. 2**, pp. 259-267

[5] Drzaic, P.S., 1995, Polyvinyl alcohol systems. In *Liquid Crystal Dispersions*, edited by H. L. Ong (Singapore: World Scientific Publishing), pp. 23-28

CHAPTER 5:
Field oriented addressing for color sequential displays

1 Introduction

In chapter 3 it is demonstrated that the electro-optical properties of the PDLC and PNLC film can be changed using different polymer and LC material or by changing the cell gap or the UV-parameters (intensity and energy). The problem is that the different electro-optical properties can not be changed independently. For instance the UV parameters for minimum switching voltage coincide with the parameters for maximum switching time (Eq.(3.2) and Eq. (3.3)). A parameter that affects only the switching time without affecting the switching voltage would be interesting. PDLC with short switching time and low switching voltage would then be possible. By using field oriented addressing one can reduce the switching time without increasing the switching voltage. In most LCDs the optical response of the LC (and the display) is determined by the magnitude of the electric field. When using field oriented addressing the optical response of the LC is not only determined by the magnitude of the electric field but also by the orientation of the electric field. That's why it is called field oriented addressing. Measurements on PDLC displays using field oriented addressing indicate that the switching times can be reduced to levels compatible with color sequential displays.

2 Principle of field oriented addressing

2.1 Introduction

To make PDLC color sequential compatible the rise time T_{rise}, the time to switch from scattering to transparent PDLC, and the decay time T_{decay}, the time to switch from transparent to scattering PDLC, have to be small (T_{rise} + T_{decay} in the order of 10ms or smaller). Switching times are reduced by an optimization of the UV parameters and the selection of the appropriate LC and polymer (see chapter "Characterization of PDLC and PNLC for reflective displays"). A disadvantage of this procedure is that the optimization of the switching times often leads to a deterioration of the other electro-optical properties like contrast ratio, reflectance and especially the switching voltage. T_{rise} can also be reduced by increasing the applied electric field E_{appl} since $T_{rise} \cong \frac{\gamma}{\varepsilon_0 \Delta\varepsilon\left(E_{appl}^2 - E_{th}^2\right)}$ (Eq. (3.3)). This is not the case for T_{decay} since $T_{decay} \cong \frac{2\gamma}{\varepsilon_0 \Delta\varepsilon E_{th}^2}$ (Eq. (3.2)). T_{decay} is not determined by the applied electric field but by the elastic forces in the LC and at the polymer-LC-interface. T_{decay} can be an order of magnitude bigger than T_{rise}. To make PDLC color sequential compatible it is important to reduce T_{decay}.

In this chapter a method is presented to improve the switching times in an electronic way and not by changing the characteristics of the PDLC. This method is based on changing the orientation of the electric field in the PDLC. The orientation can be switched between vertical and horizontal (Field Oriented Addressing or FOA).

2.2 Operating principle of field oriented addressing

In classic addressing methods the scattering state of PDLC is obtained by a random orientation of the LC molecules when no electric field is applied (Fig. 5.1). The random orientation of the LC molecules corresponds with the orientation of minimum free energy. Incoming light experiences a difference

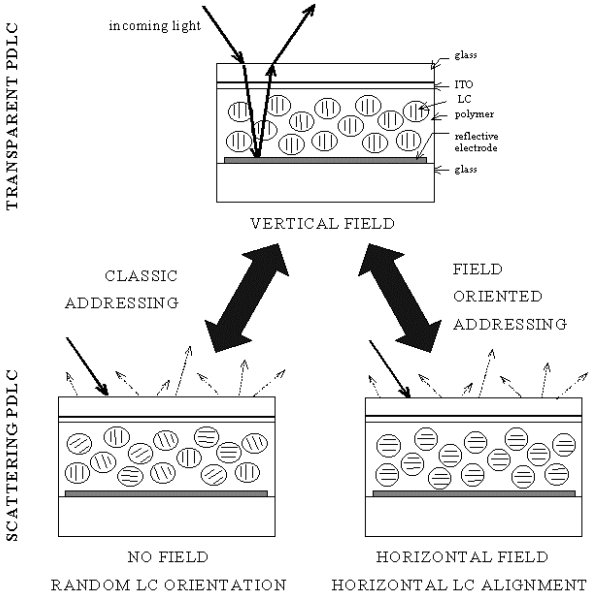

Fig. 5.1: Comparison of the principle of classic addressing and field oriented addressing.

in refractive index between the polymer matrix and the LC molecules. This will result in scattering PDLC. There a 3 types of scattering. Type 1 is due to a difference in refractive index between the polymer and the LC. Type 2 is due to changes in LC orientation within a droplet. Type 3 is due to changes in average refractive index in neighbouring droplets. The LC molecules are forced to align vertically by applying a vertical electric field. Incoming light will experience no difference in refractive index between the LC molecules

and the polymer so the PDLC will appear transparent. Only the transition of the scattering state to the transparent state requires an electric field. This explains why only T_{rise} depends on the applied electric field and T_{decay} does not.

For the classic addressing method the orientation of the LC molecules is only determined by the magnitude of the electric field. For FOA the orientation of the LC molecules is also determined by the orientation of the electric field. The orientation of the electric field in FOA can be switched between vertical and horizontal. In the case of a horizontal electrical field incoming light will experience a difference in refractive index between the polymer matrix and the horizontally oriented LC molecules (Fig. 5.1). Because both the transparent and the scattering state are determined by an electric field not only T_{rise} but also T_{decay} will depend on E_{appl}. In this way T_{decay} can be reduced by changing the electric field and not only by changing the characteristics of PDLC.

2.3 Implementation of the principle

The main challenge for implementing the principle of FOA is how to obtain both a vertical and a horizontal electric field in the cell gap of the display. For a perfect vertical and horizontal electric field a total of four electrodes are needed: two electrodes in horizontal planes for the vertical electric field and two electrodes in vertical planes for the horizontal electric field. This is a complex pixel electrode structure that is not straightforward from a technological point of view.

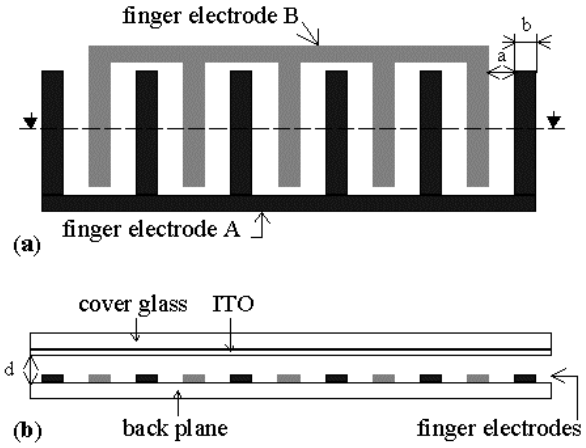

Fig. 5.2: Top view (a) and cross section (b) of the displays used for field oriented addressing.

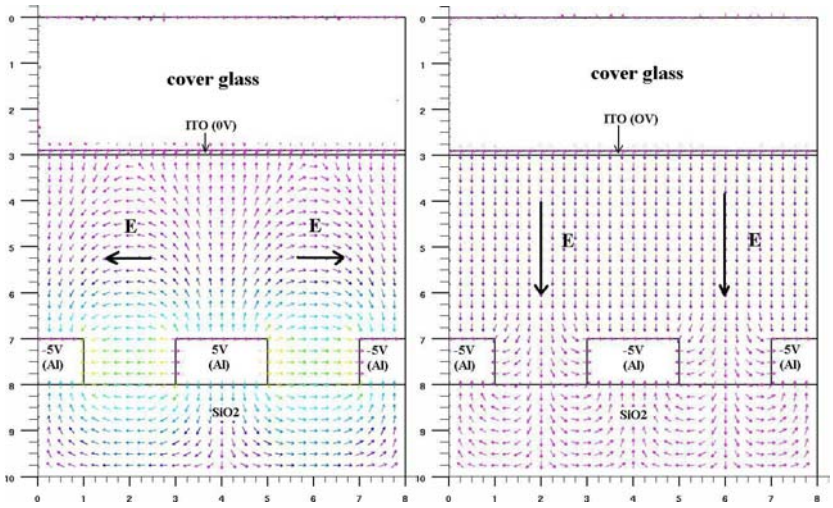

Fig. 5.3: Simulation of the horizontal electric field (left) and vertical electric field (right). The brighter the field lines the stronger the electric field.

For the displays in this Ph.D. an alternative pixel electrode layout is used with only 3 electrodes for every pixel (Fig. 5.2). Each pixel has 2 finger electrodes on the backplane of the display and 1 transparent ITO (Indium Tin Oxide) electrode on the cover glass. This last electrode is a common

electrode for all the pixels of the display. Finger electrodes are also used in In Plane Switching (IPS) [1] and Fringe Field Switching (FFS) [2] to obtain a horizontal electric field. Contrary to IPS and FFS there is still an ITO electrode on the cover glass. This electrode is required to obtain a vertical electric field.

A horizontal electric field is generated when the finger electrodes have the opposite electrical potential symmetrical to the potential of the ITO electrode (Fig. 5.3). A vertical electric field is obtained when finger electrode A and B have the same potential different from the ITO electrode. A disadvantage of the simplification of the pixel electrodes is the reduced uniformity of the vertical and horizontal electric field. Simulations indicate that the horizontal electric field will be strong between the finger electrodes and weak near the ITO electrode (Fig. 5.3). The vertical electric field is rather uniform. Above the finger electrodes there will be always a vertical electric field.

3 Characteristics of PDLC using field oriented addressing

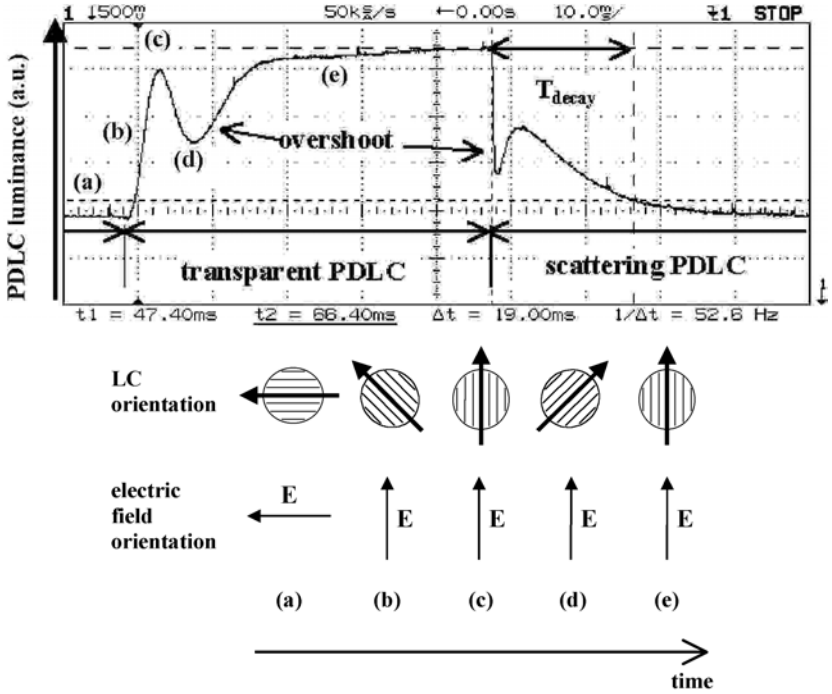

Fig. 5.4: Detected luminance when switching the PDLC between the scattering and transparent state for a display with a=3.3µm, b= 2.7µm and d=4µm (display 1). The overshoot in optical response is explained by an overshoot in LC orientation.

The principle of field oriented addressing is evaluated with PDLC. The displays have a cell gap d = 3µm or d = 4µm. Al finger electrodes are patterned on a glass back plane. The displays are measured in transmissive mode. Displays with different values for both spacing a and thickness b of the finger electrodes (Fig. 5.2) have been assembled. This allows an evaluation of the influence of the reduced uniformity of the vertical and

horizontal electric field (compared to the ideal case) on the display characteristics. Displays with a high *a/b* have a more uniform horizontal and a less uniform vertical electric field compared to displays with a low *a/b*. The optical response of the PDLC is measured by applying a square wave of $25V_{ptp}$ ($\approx 2*V_{90}$). When the phase of the square waves applied to the finger electrodes is the same then the PDLC is transparent (vertical electric field). Scattering PDLC (horizontal electric field) is obtained when the square waves are in opposite phase.

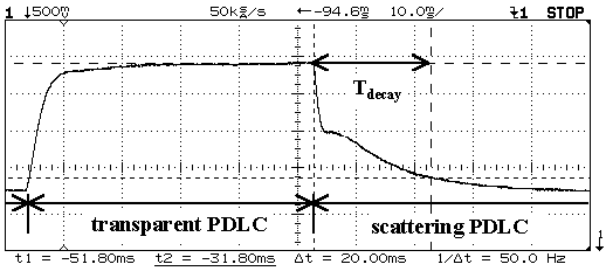

Fig. 5.5: Detected luminance when switching the PDLC between the scattering and transparent state for a display with a=8.5µm, b=2.5µm and d= 4µm (display 2).

The optical response of the PDLC when switching between the transparent state and the scattering state depends on the ratio *a*/*d*. For *a*≈*d* there is an overshoot in the optical response (Fig. 5.4), for *a*≈2*d* there is no overshoot (Fig. 5.5). For *a*≈*d* the horizontal electrical field will be a lot stronger than for *a*≈2*d*. This means that the difference in the aligning energy of the vertical and the horizontal electric field is larger for *a*≈*d* than for *a*≈2*d*.

An explanation for the measured optical overshoot is given by an overshoot of the LC orientation (Fig. 5.4). When the orientation of the electric field switches from horizontal to vertical the orientation of the LC molecules will initially also switch from horizontal to vertical ((a) to (c) in Fig. 5.4). When the difference between the aligning energy of the horizontal and vertical electric field is high enough the LC molecules will overshoot the orientation

of minimum free energy ((c) to (d) in Fig. 5.4). Once in state (d) of Fig. 5.4 the influence of the switching between horizontal and vertical electric field has expired. The LC molecules will align to the orientation of minimum free energy ((d) to (e) in Fig. 5.4).

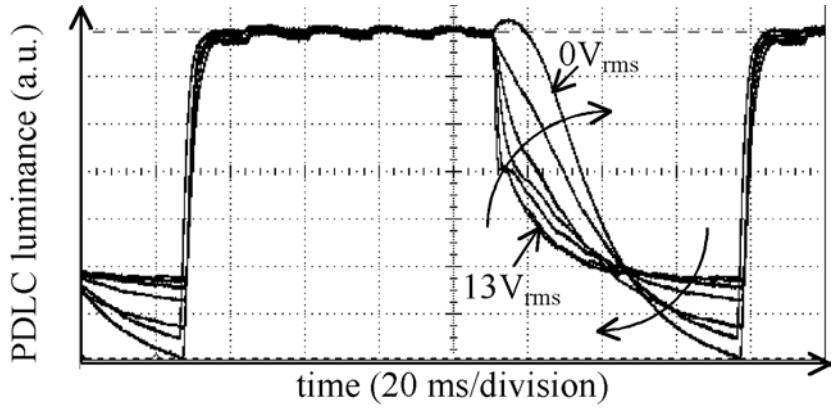

Fig. 5.6: Influence of the magnitude of the horizontal electric field when switching from transparent to scattering PDLC.

	T_{decay} (ms)	
Applied voltage (V_{rms})	**display 1**	**display 2**
0	46	49
3,5	42	46
6,75	35	32
10	20	24
13,25	13	19

Table 5.1: T_{decay} for display 1 (a≈3.3µm, b≈2.7µm) and display 2 (a≈8.5µm, b≈2.5µm) as a function of the applied voltage for the horizontal electric field.

T_{decay} depends on the magnitude of the applied voltage and the geometry of the pixel electrode (values for a, b and d) (Fig. 5.6). This could be expected since both determine the orientation and the magnitude of the horizontal electric field. The reduction of the horizontal electric field results in an

increase of T_{decay} (Table 5.1). This indicates that in the formula for T_{decay} (Eq. (3.2)), E_{appl} should be introduced similarly to the formula of T_{rise} (Eq. (3.3)). This behaviour was predicted by the principle of the FOA method. The reduction of the horizontal electric field results in an increase of the contrast ratio (Table 5.2). It seems that the PDLC is less scattering when the LC molecules are horizontally aligned than when they are randomly aligned (Fig. 5.6). The scattering due to the difference in refractive index between the polymer and the LC is higher. However the scattering due to changes in

	Contrast ratio	
Applied voltage (V_{rms})	**display 1**	**display 2**
0	2,9	2,9
3	2,9	2,6
6	2,6	1,9
9	2,3	1,7
12,5	2,0	1,6

Table 5.2: Contrast ratio for electrode 1 (a≈3.3µm, b≈2.7µm) and electrode 2 (a≈8.5µm, b≈2.5µm) as a function of the applied voltage for the horizontal electric field.

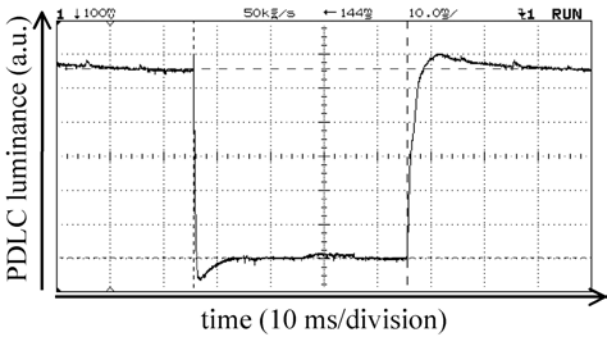

Fig. 5.7: For a display with a=3µm, b=1µm and d=3µm and an applied square wave voltage of 8.5V_{rms}, T_{rise}=2.56ms and T_{decay}=0.64ms with a contrast of 2.7.

LC orientation within a droplet and due to changes in average refractive index in neighbouring droplets decreases. The measurements indicate that the total scattering is less for horizontally aligned LC than for the LC alignment with no electric field. The contrast ratio and T_{decay} without a horizontal field measured for display 1 is 2,9 and 55ms respectively and for display 2: 3,2 and 48,2ms respectively.

So far the best switching times have been achieved for a display with a=3μm, b=1μm and d=3μm (Fig. 5.7). When applying a square wave voltage of 8.5V_{rms}, T_{rise} equals 2.56ms and T_{decay} equals 0.64ms with a contrast of 2.7. The required addressing voltage of 8.5V_{rms} is considerably smaller compared to the 100V_{rms} required for color sequential PDLC displays using classic addressing [3,4]. A contrast of 2.7 is of the same magnitude as other color sequential PDLC displays [4]. The contrast of PDLC-like displays depends a lot on the position of the observer and the light source (see chapter 3.5) and the display mode (transmissive, reflective with an absorber or reflective with a reflector). The measured displays are transmissive and have just been designed to evaluate the influence of FOA on the PDLC switching time. A contrast of 2.9 is measured on these transmissive displays using classic addressing. It has been demonstrated that reflective PDLC displays with a reflector electrode and a similar PDLC layer allow contrasts of more than 30 in the non-specular reflection direction. This shows that there is still room for improvement concerning the contrast when using FOA.

4 Conclusion

So far there are only reports on obtaining only the transparent state or only the scattering state of PDLC in an electronic way but not both in the same display at the same time. In this chapter we report on a method that selects both the scattering state and the transparent state of the PDLC in an electronic way. As a consequence T_{decay} does not only depend on the material parameters of the PDLC but also on the applied electric voltage. An increase of the applied voltage will reduce T_{decay} in a similar way as T_{rise}. The switching time T_{decay} could be reduced by a factor 4 for an applied voltage of about 2 times V_{90}. The contrast ratio of the field oriented addressing method is about 2/3 of the contrast ratio with the classic addressing method. Values of 0.64ms for T_{decay} and 2.56ms for T_{rise} have already been measured using FOA. The required voltage of $8.5V_{rms}$ is considerably smaller than the $100V_{rms}$ of other color sequential PDLC displays. The contrast ratio is of the same magnitude as other color sequential PDLC displays. There is still improvement possible by optimizing the curing parameters, using other PDLC mixtures, using PDLC in the reflective mode instead of the transmissive mode.

References

[1] C. C. Bowley et al., “Improved IPS-Mode Response Times through Polymer Network Stabilized”, 1998, *Proc. of Asia Display 98*, pp. 847-850

[2] S. H. Lee et al., “High-Transmittance, Wide-Viewing-Angle Nematic Liquid Crystal Display Controlled by Fringe-Field Switching”, 1998, *Proc. of Asia Display 98*, pp. 371-374

[3] Nakadaira A., Date M., Koshiishi Y., Tanaka H., Uehira K., “PDLC on Light Guide for Large-Area Displays”, 2000, *Conference Record of 20th IDRC*, pp. 300-303

[4] Nakadaira A., Date M., Tanaka H., “High-pixel-density module using PNLC on light guide for high-definition large-area displays”, 2001, *Proc. of Asia Display/IDW '01*, pp. 1299-1302

CHAPTER 6:
Color displays using color filters

1 Introduction

A commonly used technology to obtain transmissive color LCDs is the use of color filters. When adapting this technology to reflective displays some specific aspects of reflective displays and PDLC or PNLC have to be taken into account. This makes the implementation of color filters in reflective displays not so straightforward.

One of the main problems with reflective displays is to have a high brightness for different types of illumination. Reflective displays should be designed to use incoming light in an effective way. This is contradictive with the principle of color filters. Color filters are based on the absorption of a part of the color spectrum. The higher the color selectivity the more light is absorbed by the color filter. The absorbed light can not be recuperated for displaying the information. This results in a reduction of the brightness of the display. When using color filters for reflective displays one has to choose between color selectivity and display brightness.

Another problem is due to the UV light needed for the curing of the PDLC and PNLC. The color filters do not only absorb visible light but also UV light. However UV light is needed for the curing of the PDLC or PNLC. This may be a problem since the color filters are already on the cover glass of the display during the curing of the PDLC or PNLC. First of all the color filters may absorb too much UV light so the curing of the PDLC or PNLC can not be done or only with high UV intensity illumination sources. The use of high intensity light sources is to be avoided because a large part of the UV will be absorbed by the color filter resulting in the heating of the display during curing. This changes the temperature during the curing of the PDLC or PNLC and this may have an effect on the electro-optical properties [1].

Another problem would be that the UV transmission is not the same for all three base color filters. This may result in unbalanced electro-optical properties for the three base colors red, green and blue.
The brightness and the color spectrum of the display is to a great extend linked to the used color filter materials. The thickness of the color filters is optimized with respect to the overall brightness of the display and to match the UV transmission of the three base color filters.
Color pictures of Fig. 6.3 and Fig. 6.5 to 6.7 can be found in Appendix A.

2 Optimizing the color filters

The ultimate goal of the color filter optimization is to obtain displays with a high reflectivity, a high color purity and a good match in UV transmission for the different colors. Although all three goals are important during the first round of evaluation only the UV transmission for the 3 base colors are taken into account. If there is no UV transmission or not a good match between the different colors then it will be very hard to cure the PDLC or PNLC. In this case the color filter materials would have to be applied on the silicon backplane of the microdisplay and not on the cover glass. This approach has some disadvantages. First of all the color purity is reduced because the PDLC or PNLC layer is on top of the color filter layer. A part of the light will be scattered towards the observer before it has been filtered. If the color filters are on the silicon backplane then they are on top of the Al reflector electrode. This means part of the voltage will be across the color filter and not across the PDLC or PNLC layer. Higher voltages would then have to be applied to obtain the same electrical field across the PDLC or PNLC layer. Another disadvantage lays in the processing of color filters on a silicon backplane. Color filters are applied on a substrate by spinning. The spinning has a border effect. The border effect is a reduction of the homogeneity of the color filter thickness and therefore also a change in color spectrum near the edge of the substrate. For this reason the color filters are

preferably processed on a large substrate so the border effect is relatively small compared to the entire substrate. The microdisplays in our lab are on 2" square wafers. Problems with the border effect on these wafers are more likely to happen than when the color filters are processed on 4" cover glass substrates. Of course the cost of silicon backplanes is considerably higher than of cover glasses. For this reason it is also more interesting to process the color filters on glass substrates and not on the silicon backplanes.

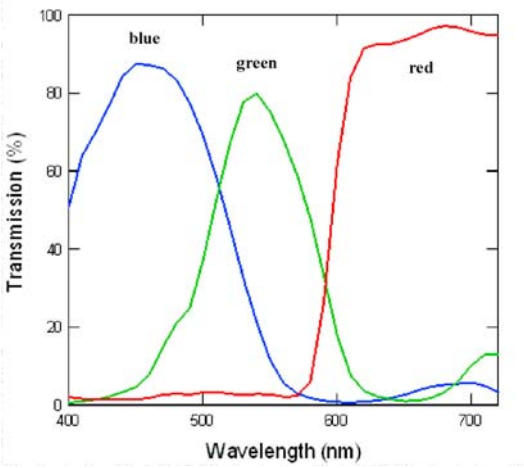

Fig. 6.1: Transmission spectrum of the Brewer Science color filters.

Different color filter materials have been tested. The products of Brewer Science showed a high color purity (Fig. 6.1). These color filter materials are aimed at LCD or CCD applications. The problem with these color filter materials is that they have a rather low UV transmissivity which differs a lot

filter thickness	UV transmission (%) red	green	blue
minimum	27	3	13
maximum	9	1	5

Table 6.1: Measured UV transmission at 365nm of Brewer Science color filters.

for each color (Table 6.1). The UV transmissivity is measured using an UV detector with a peak sensitivity at about 365nm. The best ratio between the UV transmissivity of the red color filter to the green color filter is about 3/1. In this case the red color filter has the highest thickness and the green filter

spinning speed (rpm)	filter thickness (nm)			UV transmission (%)		
	red	green	blue	red	green	blue
750	1000	860	785	31	36	18
1700	670	560	485	45	50	32
2500	510	445	410	51	56	38

Table 6.2: Measured thickness and UV transmission at 365nm of Arch Chemicals color filters for reflective displays as a function of the spinning speed.

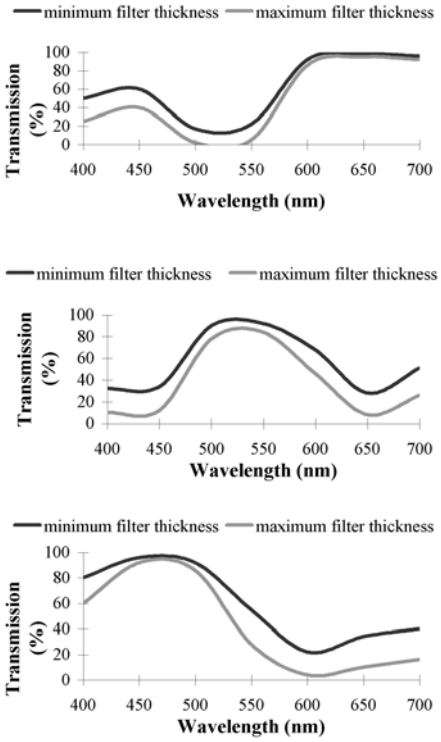

Fig. 6.2: Arch Chemicals' datasheets of the transmission spectrum of the red (top), green (middle) and blue (bottom) color filters for reflective LCDs for different filter thickness.

the smallest and the UV transmissivity is rather low (3% to 9%). Better results concerning UV transmissivity can be obtained with the color filter materials of Arch Chemicals (Table 6.2). These color filter materials have been especially developed for reflective displays. One can clearly see a peak in the transmissivity of each color in their respective spectrum (Fig. 6.2). However the transmissivity is also rather high in the rest of the spectrum. The result is a higher display reflectance and a reduction of the color purity.

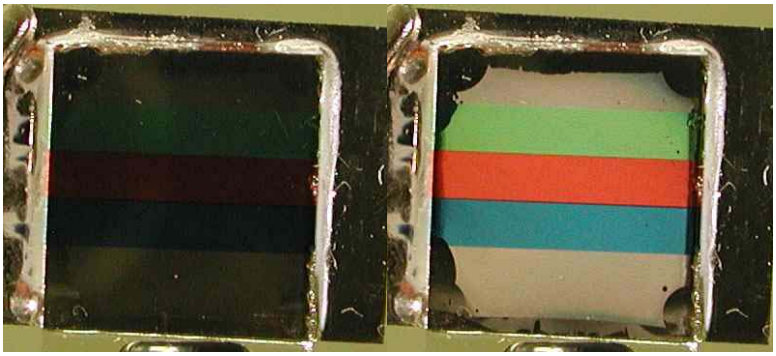

Fig. 6.3: A monopixel reflective PDLC color display switched ON (left) and OFF (right).

The color filter materials are spun at different spinning speeds. This spinning speed has to be between 750rpm and 2500rpm (Table 6.2). The red, green and blue color filter have a spinning speed of 1700rpm, 1700rpm and 2500rpm respectively. The corresponding UV transmissivity for red, green and blue is 45%, 50% and 38% respectively. Using these parameters cover glasses are processed for reflective monopixel displays (Fig. 6.3). These displays allow an easy characterization of the PDLC under the color filters (Fig. 6.4). The PDLC is cured with a UV intensity of 80mWcm^{-2} for different cure times. Due to the match in UV transmissivity for the red and green color filters the PDLC characteristics should also be the same for the red and green color filters. The PDLC for the blue color filter should have slightly higher switching times and lower switching voltages than the red and green.

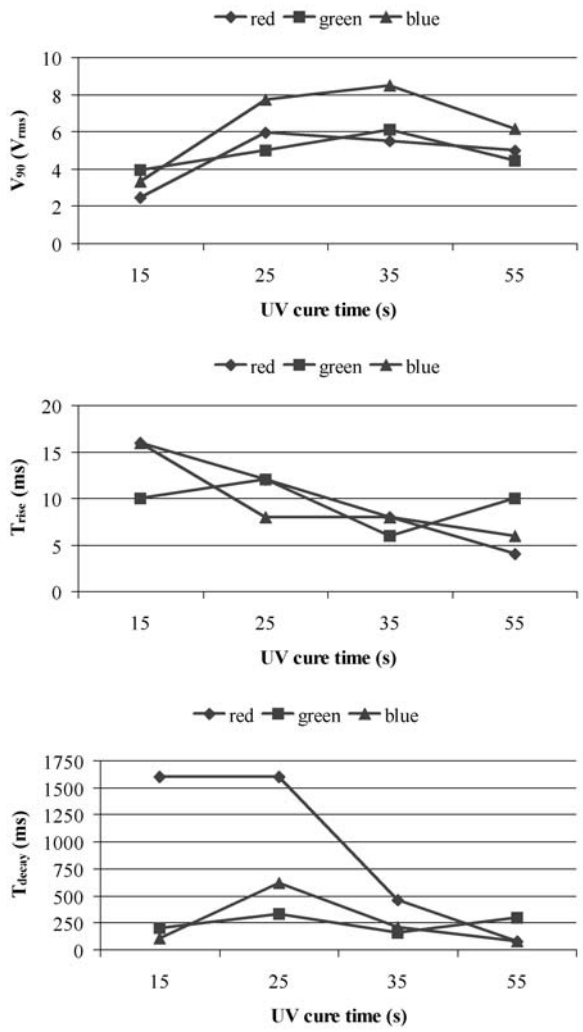

Fig. 6.4: The switching voltage V_{90}, rise time T_{rise} and decay time T_{decay} of the PDLC under different color filters for different cure times.

3 Results

The properties of the PDLC for the red and green color filter are more or less the same for the switching voltage V_{90} and switching time T_{rise}. There is a

big difference in T_{decay} for small curing times (≤25s). The switching voltage is higher and the switching times are smaller for the PDLC under the blue color filter than for the PDLC under the red and green color filter. This is different from what is expected based on the measured UV transmissivity. Another aspect is the behaviour of the electro-optical properties as a function of the cure time. In the case there is no color filter on top of the PDLC the switching voltage and switching time is independent on the cure time (see chapter 3.2.2.3). In the case there is a color filter on top of the PDLC the switching time and voltage vary a lot. Only PDLC under the green color filter has a behaviour that is similar to PDLC that is not under a color filter.

It has already been demonstrated that the curing of the PDLC, and therefore also the electro-optical properties, is not determined by the UV intensity at a wavelength of 360nm alone (see chapter 3.2.2.1). The whole spectrum plays a role in the ultimate electro-optical properties. Especially in the case there are color filters on top of the PDLC the spectrum of the light during curing will vary a lot from color filter to color filter. To be able to compare the different displays it is important that the thickness and transmission spectrum of the color filter are homogenous. This could also explain some of the differences in electro-optical properties.

4 Discussion

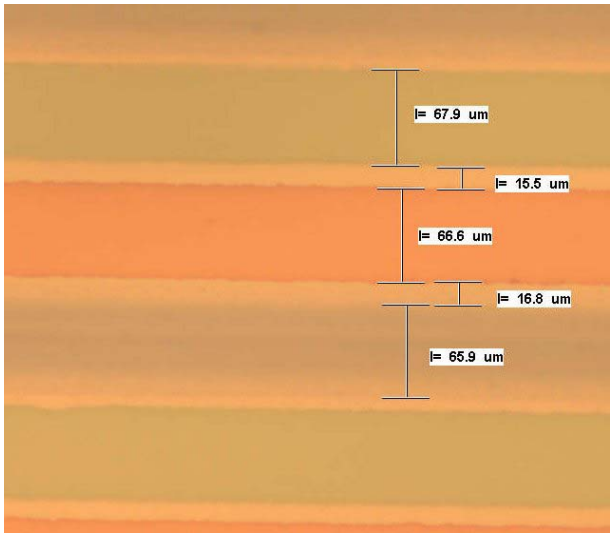

Fig. 6.5: The red, green and blue color filters used for the assembly of the color microdisplay are arranged in stripes.

For the assembly of the color microdisplays the red, green and blue color filters are arranged in stripes (Fig. 6.5). The color filters are on the cover glass and the same process parameters are used as for the monopixel color display (Fig. 6.3). There is no planarization layer on top of the color filters. The difference in filter thickness will result in an inhomogeneous cell gap. The maximum difference in filter thickness is about 250nm (Table 6.2) in case the same process parameters are used as for the monopixel color display. This variation in cell gap thickness has almost no impact on the electro-optical properties of PDLC. It also doesn't result in any problems for the processing of the ITO layer on the color filters. Between the color filters there is a gap with no filter material or black matrix. This inter filter gap has

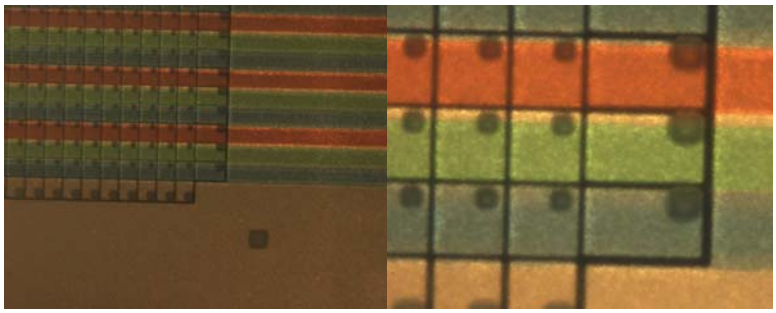

Fig. 6.6: Pictures taken with a microscope to illustrate the accuracy of the color filter alignment in a color microdisplay (close-up on the right).

a width of 15µm while the color stripes have a width of 65µm (Fig. 6.5). Due to this relatively large gap between the color filters a larger error in the alignment of the color filters on the cover glass to the pixels on the backplane of the display is allowed. Fig. 6.6 illustrates the accuracy of alignment of the color filers to the pixels on the backplane. The display has already been filled with PDLC and the PDLC is cured. The pixels are 75µm by 75µm with an inter pixel gap of 5µm. Because the inter filter gap is transmissive to all wavelengths the part of the inter filter gap that is on top of

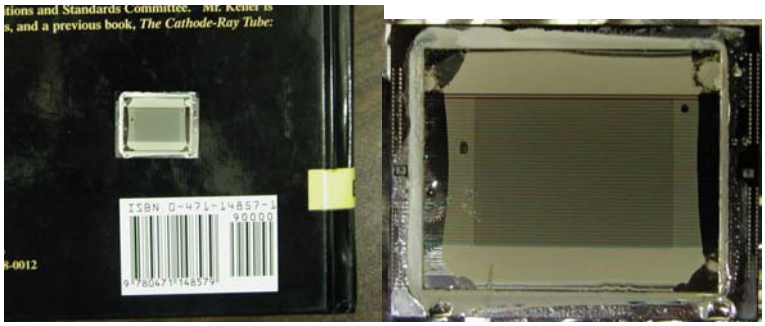

Fig. 6.7: Pictures of the color microdisplay.

a pixel will reflect all light. This will improve the overall reflectance of the color microdisplay. A picture of a color microdisplay is shown in Fig. 6.7. The reflectance of the color microdisplay is 22.5% using the measurement set-up of chapter 2.2. This is a high reflectance compared with other

reflective display technologies. In the European project HELICOS (finished in August 2000) aimed at handheld colour reflective displays, one of the targets was to have a reflectivity of 15%. The reflectivity of the color PDLC microdisplay is 50% higher than the target in the HELICOS project.

5 Conclusion

A full color PDLC microdisplay using color filters has been demonstrated. Color filters especially developed for reflective displays are used. These filters absorb less light. The process parameters are optimized so each of the 3 color filters (red, green and blue) has about the same UV transmissivity. The result is a reflective display with a high reflectance of 22.5%.

References

[1] Nolan, P., Jolliffe, E., Coates, D., “Film formation parameters affecting the electro-optic properties of low-voltage PDLC films”, 1995, *SPIE Proc.*, **2408**, 2

CHAPTER 7:
Personal viewer

1 Introduction

An optical system is required for the eye to resolve all the information on high resolution microdisplays. For portable applications this optical system is called a personal viewer. The personal viewer produces an enlarged virtual image of the information on the display. A design is made of a personal viewer using only standard lenses and mirrors. The personal viewer is built to demonstrate the possibilities of PDLC and PNLC microdisplays in these portable applications.

2 Design rules

Two parameters are taken into consideration for the design of the personal viewer. The first parameter is the distance between the observer and the image produced by the personal viewer. This distance has to be large enough so the eye can focus on the image without causing pain to the eyes. This distance varies from person to person and depends of the age of the person. In general a value of 25cm is taken for this distance [1,2]. The second parameter is the required magnification of the personal viewer. This magnification is determined by the field of view of the eye. The human eye is able to do observations in a polar angle of 100° [1]. Of this 100° only 10° to 15° is sharp to the observer. Because the observer scans the environment during observation the viewing angle with sharp images rises to 20° to 40°. This is the viewing angle the personal viewer should have.

Besides these optical design rules some practical design rules have to be taken into consideration as well. The personal viewer should have minimal dimensions and weight since these optical systems are intended for portable

applications. Another important aspect is the price of the system. For this reason only standard lenses and mirrors are used.

3 Design of the personal viewer

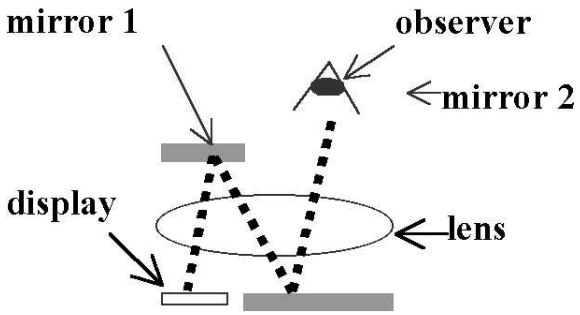

Fig. 7.1: Principle of the personal viewer.

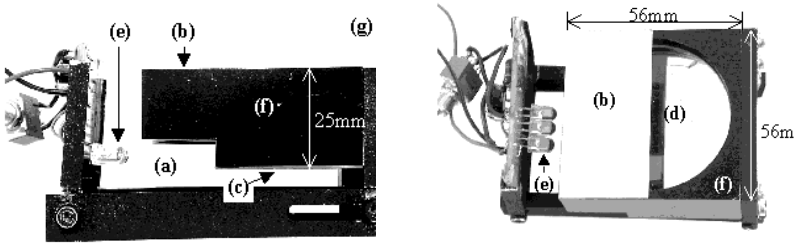

SIDE VIEW TOP VIEW

Fig. 7.2: Pictures of the personal viewer with an indication of the position of the display (a), mirror 1 (b), mirror 2 (c), the lens (d), the diodes for the illumination of the display (e), the lens holder (f) and the position of the observer (g).

A design of a personal viewer is made using only 2 mirrors and 1 lens (Fig. 7.1). By using mirrors the same lens is used more than once to magnify the information on the display. Due to the mirrors the optical path is folded reducing the thickness of the personal viewer. Because only 1 lens is used the weight of the personal viewer will also be limited.

Some simulations are made with the simulation software ZEMAX-SE™. This software tool allows a first selection of candidate standard lenses. It is also possible to determine the critical parameters in the optical system. This is important information for the construction of the personal viewer. The mirrors and the microdisplay are perpendicular to the optical axis of the lens. The distance of the mirrors and the microdisplay to the optical axis is critical. The position of these components is important to limit the aberrations in the virtual image and to be able to view the entire virtual image.

4 Prototype

The results of the ZEMAX™ simulations are used to build a temporary optical set-up. The temporary optical set-up consists of posts that are fixed on translational and rotational stages. The different components of the personal viewer (lens, mirrors, microdisplay) can be fixed on these posts. The translational and rotational stages give the different components a high degree of freedom of movement while it is still possible to put the components in fixed positions. This temporary optical set-up serves as some kind of pre-prototype of the personal viewer. It is used for evaluating the results of the simulations by an observer. In this way it is possible to get some feedback on the ease of use of the personal viewer and how to improve it.

The ease of use of a personal viewer is determined by 3 parameters [12]. The first parameter is the far point of the personal viewer. The far point is the largest distance from the eye of the observer to the personal viewer where the entire virtual image is still visible to the observer. The far point is preferably as large as possible. Otherwise the personal viewer can only be used at small distance from the observer. The second parameter is the required viewing angle to see the entire virtual image. The viewing angle is preferably between 20° and 40°. The third parameter is the distance the eye

of an observer is allowed to move across the optical axis without loosing sight of the entire virtual image. If this parameter is small then the head is not allowed to move a lot without loosing sight of the entire image. Besides the ease of use the thickness of the personal viewer, the magnification by the personal viewer and the aberrations in the virtual image have to be taken into account when evaluating the different personal viewers.

For the realisation of the personal viewer (Fig. 7.2) a standard achromatic lens is used with a diameter of 50mm and an effective focal length of 100mm. The thickness of the personal viewer is 30mm. An advantage of PDLC and PNLC is that perpendicular illumination of the display is not required to obtain good contrast and brightness. On the contrary a non-perpendicular illumination is even preferred for PDLC and PNLC (see chapter 3.5: “Applicability of reflective PDLC and PNLC displays for direct view applications”). This simplifies the illumination system considerably compared to reflective microdisplays using polarizing liquid crystals. White LEDs are used as light source.

5 Conclusion

A personal viewer system consisting of 1 standard lens and 2 mirrors has been analyzed. The analysis is based on simulations using ZEMAX and observations of the microdisplay through the personal viewer. This has resulted in the realisation of a personal viewer to demonstrate the possibilities of reflective PDLC and PNLC microdisplays in personal viewer applications.

References

[1] Hildebrand Alfred P., Kintz Gregory P., “Twice folded compound magnified virtual image electronic display”, US Patent 5684497, issued Nov. 4, 1997

[2] Bruce H. Walker, “Optical engineering fundamentals”, ISBN 0-8194-2764-0, The Society of Photo-Optical Instrumentation Engineers, pp. 181, 1998

CHAPTER 8:
Conclusions concerning the innovative aspects of this Ph.D.

A large part of this Ph.D. focuses on the analysis and characterization of PDLC and PNLC for reflective displays with a reflector. Three different measurement set-ups have been developed and built for these purposes. One measurement set-up is used for characterizing the electro-optical properties of reflective PDLC and PNLC displays. A second measurement set-up allows the measurement of the cell gap in liquid crystal displays with an error margin of less than 2%. This set-up is very flexible concerning the requirements for the liquid crystal display. The cell gap can be measured before or after the filling of the LCD. The LCD can be transmissive or reflective. The electro-optical principle of the LC can be based on polarized light or light scattering. A third measurement set-up analyzes the applicability of different types of reflective displays for direct view applications. This measurement set-up uses a completely different approach compared to similar measurement set-ups used for transmissive or emissive displays. The principle of this measurement set-up has been implemented in commercial measurement set-ups for reflective displays and is used as a reference in a new standard on the measurement of reflective displays.

An extensive characterization of PDLC and PNLC for reflective displays with a reflector has been made. So far PDLC and PNLC are mainly used in transmissive displays and reflective displays with an absorber. In general the electro-optical behaviour of the PDLC and PNLC in reflective displays with a reflector can be explained with previously published theory. However there are two exceptions. One is the characteristics due to overcuring and the other

is the characteristics for a cell gap smaller than 4μm. The origin of these deviations from theory has been determined.

Three alternative filling methods have been optimized for PDLC and PNLC filling. Besides the problems with the exposure of PDLC and PNLC to vacuum there were also problems with via filling and the stability of the cell gap after curing. One has to bear in mind that the cell gap of these displays is only 4μm. This is small compared to other PDLC and PNLC displays described in literature. In the end these problems have been solved for all three filling methods.

A new principle has been devised for addressing liquid crystal. The conventional addressing method changes the optical properties of the LCD by changing the magnitude of the electric field. Using this new principle not only the magnitude but also the orientation of the electric field is changed for addressing the liquid crystal. This principle is called field oriented addressing. Using field oriented addressing it is possible to switch PDLC between a transparent and a scattering state in an electronic way. The advantage of field oriented addressing is that it is possible to reduce the switching times to levels compatible with color sequential addressing using low switching voltages compared to switching voltages of other color sequential PDLC displays.

Color PDLC displays have been demonstrated using color filters. The UV transmission has been matched for the three color filters. This is done by choosing the appropriate color filter material and changing the filter thickness. Also the UV parameters during curing have been optimized to match the electro-optical properties of the PDLC under the three color filters.

CHAPTER 9:
What's next?

This Ph.D. research has solved some of the problems concerning "Introduction of color in reflective PDLC and PNLC microdisplays". Of course not all problems could be solved and some new problems are encountered. In this chapter an overview of some of these problems is given.

Although quite some work has been spent in the characterization of PDLC and PNLC for reflective displays this work is still unfinished. Further research is required to reduce the hysteresis in PDLC and PNLC and to eliminate the DC voltage in reflective displays.

It has been demonstrated that field oriented addressing is able to reduce the switching times considerably using low switching voltages. However the contrast needs further improvement. It would be interesting to analyze field oriented addressing for reflective displays. Contrast measurements on PDLC and PNLC in reflective displays and transmissive displays show that reflective displays have a better contrast. So far the same PDLC is used as for displays using the classic addressing. First of all the UV curing parameters could be optimized for field oriented addressing. Other PDLC mixtures could also be analyzed. These mixtures should be more scattering when the LC molecules are horizontally aligned. This could be achieved by increasing the internal scattering in the LC or by having more LC-polymer-interfaces. So far field oriented addressing is used to switch between a horizontal and a vertical electric field. It would also be interesting to know how the PDLC behaves when field oriented addressing is not only used to switch between a horizontal and a vertical orientation of the electric field but also between the intermediate orientations. These intermediate orientations could be used to select grey scales.

It has been demonstrated that it is possible to have full color reflective PDLC displays using color filters. It would be interesting to have color filters with a

better UV transmission for these applications. This would make it easier to match the characteristics of the PDLC cured under the different color filters. High power UV illuminations sources would no longer be required.

A lot of patents concerning personal viewers deal with the perpendicular illumination of the display in the personal viewer. Perpendicular illumination is important for displays using polarizers. However PDLC and PNLC does not require perpendicular illumination to have a good contrast. This ought to simplify the design of the personal viewer. So far not much work is performed in the design of personal viewers for PDLC and PNLC displays.